Miscellaneous Paper GL-94-30
August 1994

US Army Corps
of Engineers
Waterways Experiment
Station

Proceedings, First North American Workshop on Modeling the Mechanics of Off-Road Mobility

5-6 May 1994

by Roger W. Meier, David A. Horner

Prepared for U.S. Army Research Office

Miscellaneous Paper GL-94-30
August 1994

Proceedings, First North American Workshop on Modeling the Mechanics of Off-Road Mobility

5-6 May 1994

by Roger W. Meier, David A. Horner

U.S. Army Corps of Engineers
Waterways Experiment Station
3909 Halls Ferry Road
Vicksburg, MS 39180-6199

Prepared for U.S. Army Research Office
Research Triangle Park, NC 27709-2211

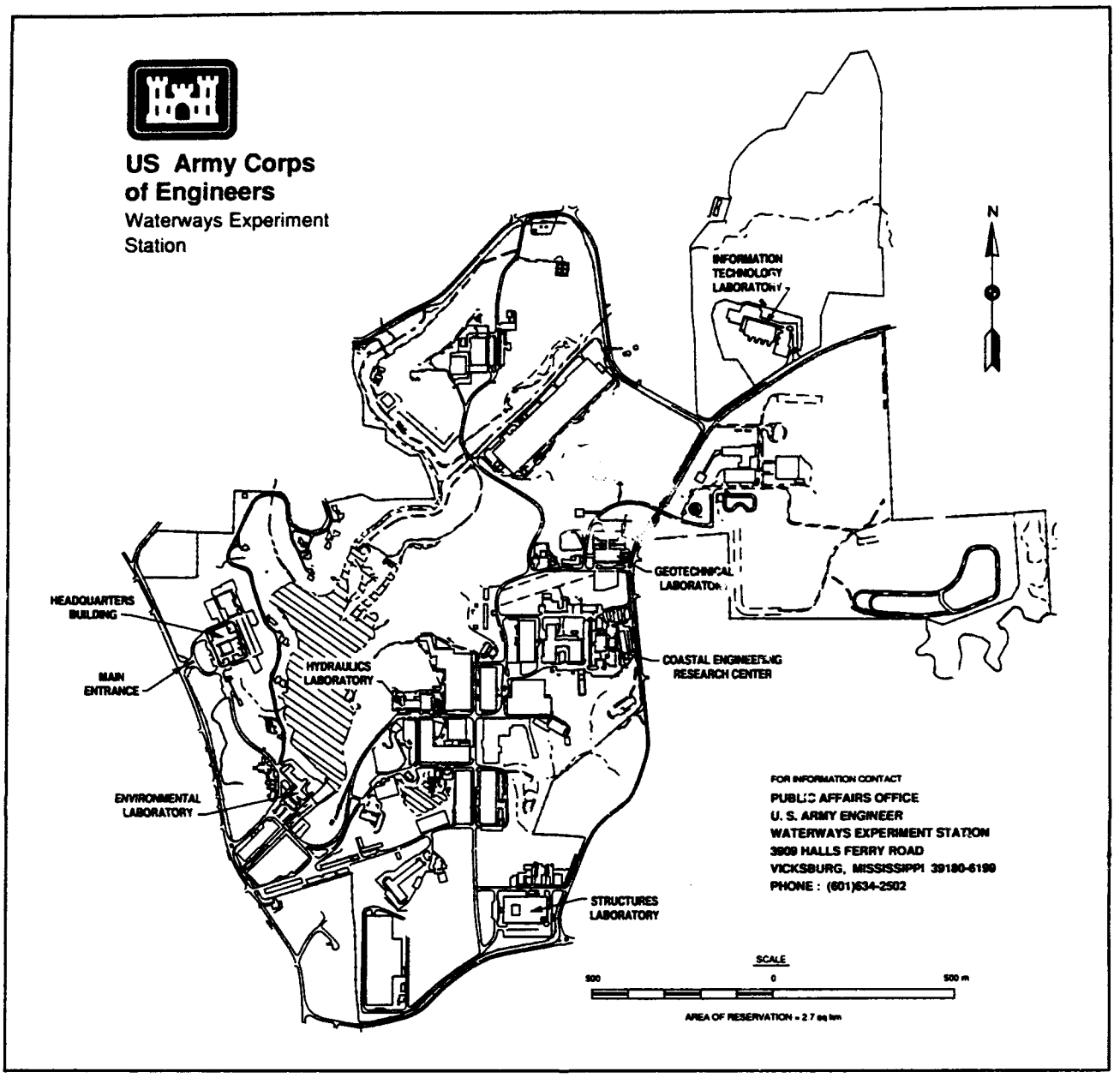

Waterways Experiment Station Cataloging-in-Publication Data

Meier, Roger W.
Proceedings, First North American Workshop on Modeling the Mechanics of Off-road Mobility, 5-6 May 1994 / by Roger W. Meier, David A. Horner ; prepared for U.S. Army Research Office.
151 p. : ill. ; 28 cm. -- (Miscellaneous paper ; GL-94-30)
Includes bibliographic references.
1. Vehicles, Military -- Performance -- Congresses. 2. Vehicles, Military -- Off road operation -- Evaluation -- Congresses. 3. Vehicles, Military -- Dynamics -- Mathematical models. I. Horner, David A. II. United States. Army. Corps of Engineers. III. U.S. Army Engineer Waterways Experiment Station. IV. Geotechnical Laboratory (U.S.) V. United States. Army Research Office. VI. North American Workshop on Modeling the Mechanics of Off-road Mobility (1st : 1994 : Vicksburg, Mississippi) VII. Title. VIII. Series: Miscellaneous paper (U.S. Army Engineer Waterways Experiment Station) ; GL-94-30.
TA7 W34m no.GL-94-30

Contents

Preface

The First North American Workshop on Modeling the Mechanics of Off-Road Mobility was held 5 and 6 May 1994 at the U.S. Army Engineer Waterways Experiment Station (WES) in Vicksburg, Mississippi. The workshop was sponsored by the U.S. Army Research Office under the Terrestrial Science Program of the Engineering and Environmental Sciences Division.

The idea for this workshop originated with Mr. David A. Horner, Mobility Systems Division (MSD), Geotechnical Laboratory (GL). The workshop was subsequently organized by Mr. Roger W. Meier, MSD, under the general supervision of Mr. Newell R. Murphy, Chief, MSD, and Dr. William F. Marcuson, III, Chief, GL. This report, which documents the proceedings of the workshop, was edited by Messrs. Meier and Horner with the assistance of Mr. Jody Priddy, MSD. Mr. Meier wrote the introduction and workshop summary in Chapter 1. Ms. Sally Shoop, U.S. Army Cold Regions Research and Engineering Laboratory, provided the synopsis of the plenary discussions in Chapter 2.

The workshop organizers wish to thank Drs. Peter Haff, Duke University, Shrini Upadhyaya, University of California at Davis, and Paul Corcoran, Caterpillar, Inc., for serving as working group chairmen and providing us with synopses of their group's discussions.

Dr. Robert W. Whalin was Director of WES during the preparation and publication of this report. COL Bruce K. Howard, EN, was Commander.

1 Introduction

Background

In the current atmosphere of belt-tightening and streamlining, the Army needs a means of assessing the mobility performance capabilities of candidate next-generation vehicles without first spending tens of millions of dollars building vehicle prototypes. Shortcomings and design flaws that compromise mobility performance must be identified *before* they are incorporated into the prototypes at Army expense.

The task of evaluating the mobility performance of vehicles in currently accomplished in part with the NATO Reference Mobility Model (NRMM).[1] NRMM uses a collection of algorithms, numerics, and empirical relationships to forecast maximum steady-state vehicle speed as a function of driver, vehicle, weather, and terrain characteristics. The empirical relationships embody more than 40 years of vehicle mobility research, testing, and evaluation. Efforts to improve NRMM and expand its empirical database continue to this day.

There are, however, advances in vehicle design on the horizon that will produce vehicles that operate outside the limits of NRMM's empirical database. Many of these concepts—such as central tire inflation systems, rubber belt traction elements, active suspensions, and weight-saving reactive armor—are already appearing in production and demonstration vehicles. Other concepts—such as lightweight-composites and appliqué armor, zero-ground pressure running gear, and electric drive technologies—are just around the corner.[2] In many cases, the performance characteristics of these vehicles simply cannot be described within the bounds of the existing NRMM database. Expanding NRMM's empirical database to include these advanced vehicles would involve extensive mobility field tests on prototype vehicles. This is exactly the type of expense that the Army can no longer afford.

---

[1] Richard Ahlvin and Peter Haley. 1992. "NATO Mobility Model Edition II, NRMM II User's Guide," Technical Report GL-92-19. U.S. Army Engineer Waterways Experiment Station. Vicksburg. MS.

[2] Board on Army Science and Technology. 1992. "STAR 21: Strategic Technologies for the Army of the Twenty-First Century. Mobility Systems." National Academy Press. Washington. DC.

To accurately access future vehicle performance characteristics in the absence of costly prototyping and field testing, the Army must develop an ability to perform *virtual* mobility testing—the simulation of vehicle mobility performance in the computer. This will require advances in the numerical modeling of vehicle dynamics and vehicle-terrain interaction and in the characterization of the terrain for modeling purposes.

In order to 1) assess the current state of the art in vehicle mobility modeling, 2) identify the most promising areas of current research, and 3) determine the most profitable directions for future research, the Mobility Systems Division of the U.S. Army Engineer Waterways Experiment Station (WES) invited recognized leaders in the field of vehicle mobility modeling from throughout the United States and Canada to participate in a two-day workshop on "Modeling the Mechanics of Off-Road Mobility." This report documents the proceedings of that workshop.

Workshop Summary

Prior to the workshop, participants were asked to provide a brief (3-4 page) technical note or extended abstract describing their current mobility modeling research efforts. These submissions, which are reproduced in this report, were assembled into a workshop preprint volume that was provided to all of the participants when they arrived at the workshop site. The technical notes were used by the workshop organizer to determine the interests of each participant in order to assign them to individual working groups. The preprint volume also served to "introduce" participants to one another. Because the participants came from a wide variety of organizations and had a wide variety of backgrounds, not all of them knew each other or were familiar with each other's research work. It was hoped that the preprint would help initiate off-line discussions between researchers that might lead to fruitful collaborations.

The workshop began with a brief welcome by the Commander and the Director of WES and opening remarks by the workshop organizer. These were followed by two keynote speeches, which are included here. The first speech, by Prof. J. Y. Wong from Carleton University in Ontario, Canada, addressed the state-of-the-art in the analytical modeling of steady-state off-road mobility for wheeled and tracked vehicles. The second, by Dr. Shrini Upadhyaya from the University of California at Davis, described his recent research into the backcalculation of in situ soil properties from field test results using response surface methodologies.

The afternoon was spent in a group discussion trying to determine which of the existing mobility modeling paradigms did and did not work so we could better determine the areas where additional research was needed. A synopsis of that session, presented in the next chapter, has been provided by the session chairperson, Ms. Sally Shoop from the U.S. Army Cold Regions Research and

Engineering Laboratory (CRREL). During that group discussion, the lack of any standardization of in situ tests for ascertaining vehicle mobility was noted. A small working group broke off from the main group to address that issue. Mr. George Mason from WES has submitted a synopsis of those discussions. That synopsis is paraphrased here:

> Any standardized test for determining in situ soil properties must account for 1) soil layering and heterogeneity, 2) the effects of changes in moisture content over depth, 3) the loss of strength that results from remolding, 4) the effects of organic matter such as grass and roots, and 5) the critical depth at which soil shear properties will dictate mobility. It must also permit the backcalculation of unique soil properties, unlike tests such as the military cone penetration test which can produce the same test results for many different combinations of soil strengths and compressibilities.
>
> A standardized test should 1) be able to measure changes in strength with depth at 5 cm increments, 2) produce shearing patterns that correlate in some way with the width of loaded area of interest (e.g., of a track pad or a tire contact patch), 3) include a definition of the remoldability of the soil, 4) be capable of rapid measurements in low soil strengths, and 5) be transportable to the field.

The plenary session was concluded by recommending that the remainder of the workshop be devoted to the identification of specific research needs and the facilitation of possible cooperative research between the participants.

To that end, the participants were broken up into three working groups of equal size the next morning. Each group was asked to return two hours later with an enumerated list of the five biggest knowledge gaps in vehicle mobility modeling. They were also asked to address the question: "If those gaps were to be filled tomorrow, what would it buy us?" The participants were assigned to the different working groups based on perceived similarities in their needs and interests. For example, one group contained most of the researchers mainly interested in ride dynamics. Another group was composed of the researchers primarily concerned with the mechanics of vehicle/terrain interaction.

In all, 17 different knowledge gaps were identified (two of the groups submitted lists with more than five knowledge gaps and several gaps were identified by more than one group):

- need to determine where the existing modeling techniques *don't* work
- need to relate soil mechanics properties to intrinsic soil properties
- need data on the spatial and temporal variability of soils

- need better ways of coping with inhomogeneity
- need better ways to measure and evaluate soil properties in situ
- need valid, repeatable (standard) characterization of the real world
- need to instrument the soil without affecting its structure
- need to measure and understand dynamic soil properties
- need to measure soil adhesion and understand its role in mobility
- need to estimate changes in soil resulting from vehicle traffic
- need an adequate effective stress theory for multi-phase media
- need to understand the mechanics of continuous (large strain) failure
- need to better understand the correlation between slip and sinkage
- need to predict interface stresses during acceleration and braking
- need to determine the 3-D response of terrain to vehicle steering
- need a good model for RAMD prediction
- need numerical models or lookup tables to speed model execution

If those knowledge gaps were filled, the following could be accomplished:

- real time simulation of vehicle mobility
- validation of existing and new mechanisms and models
- accurate modeling of vehicle agility/maneuverability
- the ability to predict, design for, and control soil compaction
- the ability to predict the effects of tread and grouser design
- prediction of site-specific vehicle mobility (e.g., virtual test course)
- prediction of vehicle failure and estimates of reliability
- enhanced mobility-based design and procurement

There are far fewer "knowledge uses" than there are knowledge gaps because many of the participants had very similar needs and desires and some

of those needs could only be met if several knowledge gaps were filled. It is somewhat surprising that there were almost as many knowledge gaps (17) as there were participants (22) despite the similarity in their knowledge needs. Perhaps that is a strong indication that there is still much work to be done in understanding and modeling the mechanics of off-road mobility.

Despite the lack of consensus as to our most pressing research needs, the workshop was successful in that it served to let everyone working in the field know where they stand as a group. The current state of the art was illustrated, ongoing research was brought to light and discussed, and knowledge gaps that need to be filled through future research were identified. This was especially important for the several participants, invited at the behest of ARO, whose backgrounds were outside the realm of vehicle mobility modeling. Those researchers proposed some inventive new approaches to mobility modeling. Several of those approaches are currently being investigated and will probably lead to research contracts or cooperative research agreements. If nothing else were to come of this workshop, that alone will have made it worthwhile.

At the end of the workshop, there was unanimous agreement that the workshop should become a recurring event. ARO has agreed, in principle, to sponsor a recurring workshop. The Mobility Systems Division of WES has agreed to host it again. That "Second North American Workshop on Modeling the Mechanics of Off-Road Mobility" is tentatively scheduled for August 1995.

2 Plenary Discussions

This plenary session was loosely structured with the broad objectives of concentrating on identifying the knowledge gaps in the current state of modeling vehicle-terrain interaction. Because we were of very diverse backgrounds, and with a wide variety of applications for such modeling, the discussion began by grouping the applications as those dealing with prediction and improvement of *performance* (such as vehicle, tire, track, compactor, and agricultural tools), and those dealing with the resulting *soil deformation* (such as compaction, mass flow, and terrain damage).

The discussion then focused on the general needs of vehicle-terrain models, as follows:

- The need to relate remotely-sensed mapped parameters to soil parameters and vehicle performance models.
- The need to use FEM (or other sophisticated tools) to generate lookup tables for bigger, virtual reality type models which must run in real time.
- The need for a common or standard measurement device, and/or a "standard" piece of ground to validate soil devices and models. The general consensus was for coming up with a "standard" shear device.
- It was generally agreed that although the vehicle input needed for such models is well defined and understood, the soils characterization and modeling has a long way to go.

At this point, a small group split off to discuss the device standardization issue. The remaining participants discussed the following issues regarding the specific capabilities that are lacking to do the above. Some of this discussion continued the second day.

- The 3-D contact between the driving element and the soil is not often known but must be used as input for rigorous numerical modeling. (However, using contact mechanics, it is the material properties that must be well known and the contact is calculated.)

- Is it valid to apply the traditional Janosi's shear equation and Bekker's sinkage equation for the case of a 3-D soil-tire contact surface? Janosi's equation assumes horizontal shear and Bekker's sinkage assumes vertical (or normal to the loaded surface) deformation. However, the stresses and deformations involved in soil-tire contact on deformable terrain are not necessarily vertical and horizontal. As Bekker's equation assumes that the pressure is hydrostatic the direction is not critical, however, the asymmetry of the pressure distribution beneath the wheel causes problems. Janosi's equation is based on the shear and normal forces on the wheel being vertical and tangential and was intended to be used with the sum of the forces on the wheel.

- Soil energy absorption terms needed for vehicle dynamics simulations are lacking.

- A good description and understanding of slip-sinkage is needed.

- Description, numerical formulation and modeling methodology for dealing with the rate effects associated with dynamic loading of very wet and saturated soils.

- Problems associated with modeling large deformations are encountered in FEM. The use of Eulerian FEM codes was discussed, as were Discrete Elements and particle theory along with their large computational requirements.

- The ability to describe and model heterogeneous material (such as boulders and roots) is needed.

- The ability to handle the effects of multiple vehicles, loading and unloading, repetitive loads is needed.

- A good (constitutive) model for soil under dynamic loads is needed.

- Money is needed.

A good deal of the remaining discussion centered around tight budgets and where to get the funding to develop and implement these projects. Some funding is available from the Army Research Office (ARO) and some is available from government laboratories through their respective Broad Agency Announcements (BAA). Other sources mentioned were ARPA (Advanced Research Projects Agency), AFOSR (Air Force Office of Scientific Research), and CPAR (Construction Productivity Advancement Program). The formation of a consortium to integrate the defense and commercial industrial bases is of increasing importance and is sponsored through the US Government's Technology Reinvestment Project for Dual Use Technologies. CRDA's (Cooperative Research and Development Agreements) can be used to facilitate cooperative research between the government and private industry while

protecting the interests of both. The research of the future will need to include collaboration between industry, government and academia in order to get the highest return on shrinking research dollars.

Appendix A
Keynote Lectures

Analytical Modeling Keynote Lecture

Computer Simulation Models for Evaluating the Performance and Design of Tracked and Wheeled Vehicles

J.Y. Wong[1]

Summary

A series of computer simulation models for performance and design evaluation of tracked vehicles and off-road wheeled vehicles have emerged in the past decade. In contrast with empirical models developed earlier, they are based on detailed studies of the mechanics of vehicle-terrain interaction, and take into account all major vehicle design features and terrain characteristics. Thus, they provide a comprehensive and realistic tool for the vehicle engineer to optimize vehicle design and for the procurement manager to evaluate competing vehicle candidates. These models have been gaining increasingly wide acceptance in industry and governmental agencies. For instance, the model NTVPM for tracked vehicles with relatively short track pitch has been successfully used to assist vehicle manufacturers in the development of a new generation of high-mobility military vehicles and governmental agencies in the evaluation of vehicle candidates in Europe, North America and Asia.

Introduction

In the past two decades, a variety of computer simulation models (computer-aided methods) for evaluating the mobility of off-road vehicles have emerged. In the early 1970s, to support decision making processes related to the procurement and deployment of military vehicles, an empirical model known as the U.S. Army Mobility Model (AMC-71) was developed. In the mid-1970s, the second generation of this model called AMM-75 was made available (Jurkat, Nuttall, and Haley, 1975). This version of the model forms the basis for the subsequent development of the NATO Reference Mobility Model (NRMM). NRMM has the capability, among others, to predict the tractive performance of off-road vehicles over unprepared terrain using empirical relationships. This capability is, however, limited to the prediction of vehicle performance over two types of terrain, namely, fine- and coarse- grained soils.

To assist the development and design engineer to optimize the design of off-road vehicles and the procurement manager to select the appropriate vehicle candidates for a given mission and operating environment, a series of computer simulation models have been developed under the auspices of Vehicle Systems Development Corporation of Canada, since the 1980s. In contrast with empirical models developed earlier, these models are based on detailed studies of the physical nature of vehicle-terrain interaction and the principles of applied mechanics. They take into account all major design features of the vehicle and the

---

[1] Department of Mechanical and Aerospace Engineering, Carleton University and Vehicle Systems Development Corporation, Ottawa, Canada.

basic characteristics of the terrain.

For performance and design evaluation of vehicle with flexible tracks, such as rubber-belt tracks or link tracks with relatively short track pitch, commonly found in military fighting and logistics vehicles, a model known as NTVPM has been developed (Wong, 1986, 1989, 1992a and b, and 1993; Wong and Preston-Thomas, 1986a and 1988). This model is based on the assumption that this type of track can be idealized as a flexible belt. It has been successfully used to assist manufacturers in the development of new military vehicles and governmental agencies in the evaluation of vehicle candidates in Europe, North America and Asia. For instance, this model has been employed to assist Hagglunds Vehicle AB of Sweden in the development of a new generation of high-mobility fighting vehicles (CV 90), in the examination of the approach to the further improvement of the performance of the all-terrain carrier BV 206, and in the evaluation of competing designs for a proposed main battle tank. Recently, it has been used in the selection of an optimum configuration for a new, high-mobility armoured personnel carrier for a Spanish vehicle manufacturer and in the assessment of the effects of design modifications on the mobility of a fighting vehicle over tropical terrain for an Asian firm. It has also been employed in the evaluation of the effects of design changes on the cross-country mobility of Canada's main battle tank, Leopard C1, for the Canadian Department of National Defence and in the assessment of the mobility of a variety of container handling equipment used by the U.S. Marine Corps.

For tracked vehicles with rigid links having relatively long track pitch, commonly used in agriculture and construction industry, a model known as RTVPM has recently been developed (Gao and Wong, 1993 and 1994; Wong and Gao, 1994). In this model, the track is considered to be a system of rigid links connected through frictionless pins. The basic features of this model have been verified with available field test data.

For performance and design evaluation of off-road wheeled vehicles, a model known as NWVPM has been developed (Wong and Preston-Thomas, 1986b). It can be employed in the evaluation of the overall performance and design of off-road wheeled vehicles, as well as in the selection of tires for cross-country operations. It has been used in the assessment of the effects of different types of tire on the mobility of 6 x 6 and 8 x 8 armoured wheeled vehicles for the Canadian Department of National Defence and in the evaluation of the mobility of container handling wheeled vehicles used by the U.S. Marine Corps.

In this paper, the basic features and capabilities of these computer simulation models will be presented. Experimental validations of these models with field test data will be described. The applications of these models to parametric analysis of vehicle performance and to the optimization of vehicle design will be demonstrated.

Computer Simulation Model NTVPM for Vehicles with Flexible Tracks

For high-speed tracked vehicles, such as military fighting and logistics vehicles and off-road transport vehicles, rubber tracks or link tracks with relatively short track pitch are commonly used. This kind of short-pitch track system typically has a ratio of roadwheel diameter to track pitch in the range from 4 to 6, a ratio of roadwheel spacing to track pitch in

the range of 4 to 7, and a ratio of sprocket pitch diameter to track pitch usually of the order of 4. The rubber-belt track and the short-pitch link track will be referred to as "flexible track" in this paper and they may be idealized as a flexible belt in the analysis of track-terrain interaction.

The computer simulation model NTVPM has been developed for performance and design evaluation of tracked vehicles with flexible tracks, under the auspices of Vehicle Systems Development Corporation. The model is intended to provide the vehicle designer with a comprehensive and realistic computer-aided method to optimize vehicle design, and to provide the procurement manager with a reliable method to evaluate vehicle candidates. To meet these objectives, the latest version of the model, known as NTVPM-86, takes into account all major vehicle design parameters, including sprung weight, unsprung weight, location of the centre of gravity, number of roadwheels, location of roadwheels, roadwheel dimensions and spacing, locations of sprocket and idlers, supporting roller arrangements, track dimensions and geometry, initial track tension, belly (hull) shape, and angles of approach and departure of the track system. The longitudinal elasticity of rubber-belt tracks or of link tracks with rubber bushings are taken into consideration. The track longitudinal elasticity affects the tension distribution in the track and as a result influences the performance of the vehicle to a certain extent over marginal terrain. The characteristics of the independent suspension of the roadwheels are fully taken into account in the model. Torsion bar suspensions, hydro-pneumatic suspensions with non-linear load-deflection characteristics, and others can be accommodated in the model. Suspensions characteristics have a significant effect on vehicle mobility over soft ground. On highly compressible terrain, such as deep snow, track sinkage may be greater than the ground clearance of the vehicle. If this occurs, the belly (hull) of the vehicle will be in contact with the terrain surface and will support part of the vehicle weight. This will reduce the load carried by the tracks and will adversely affect the traction of the vehicle over terrain that exhibits frictional behaviour. Furthermore, belly contact will give rise to an additional drag component - the belly drag. The problem of belly contact is of importance to vehicle mobility over marginal terrain, and the characteristics of belly-terrain interaction have been taken into consideration in the model. Terrain characteristics, including the pressure-sinkage relation, shear strength, rubber-terrain shearing (for rubber tracks or tracks with rubber pads) and belly-terrain shearing characteristics, and responses to repetitive normal and shear loadings, are taken into account in the model.

Basic Approach to the Development of the Model

In developing the model, the track is assumed to be a flexible belt with known longitudinal elasticity. The track-roadwheel system used in the analysis is schematically shown in Fig. 1. When a tracked vehicle travels over a deformable terrain, the load applied through the track system causes the terrain to deform. The track segments between roadwheels take up load, and as a result they deflect and have a form of a curve. The actual length of the track in contact with the terrain between the front and rear roadwheels increases in comparison with that when the track rests on a firm ground. This causes a reduction in the sag of the top run of the track and a change in track tension distribution. It should also be pointed out that an element of the terrain beneath the track is first subject to the load applied by the leading roadwheel. When the leading roadwheel has passed, the load on the terrain

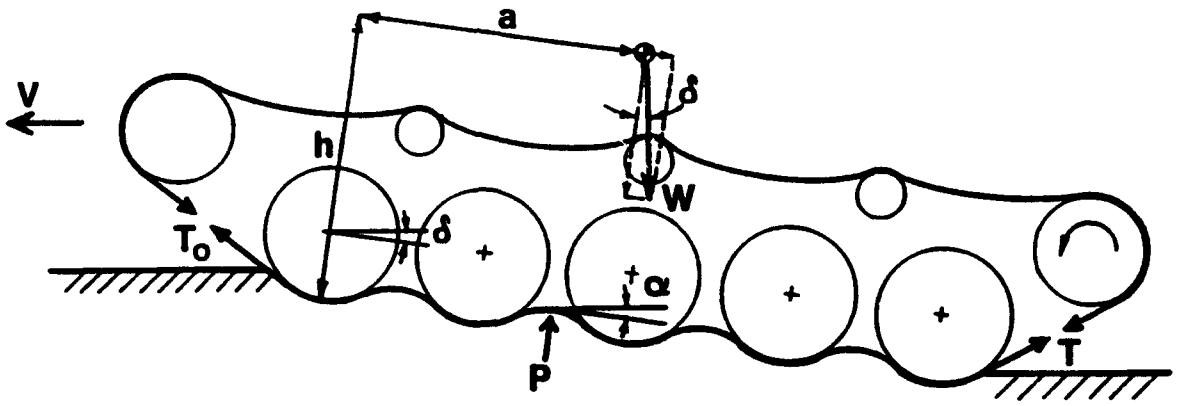

FLEXIBLE TRACK

Figure 1. A flexible track model

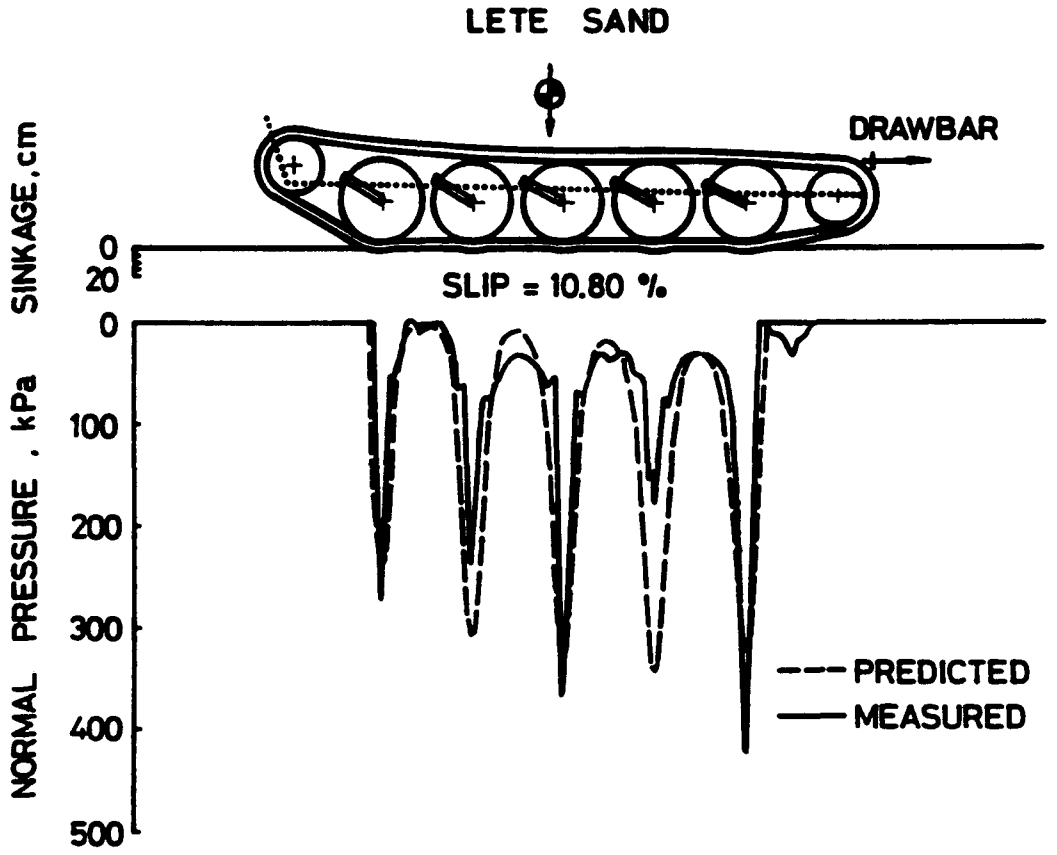

Figure 2. Comparison of the measured and predicted pressure distribution under an M113A1 on a sandy terrain

element is relieved. Load is reapplied as the second roadwheel rolls over it. A terrain element under the track is thus subject to repetitive loading. The loading-unloading-reloading cycle continues until the rear roadwheel of the track system has passed over it. To predict the normal and shear stress distributions under a moving tracked vehicle, the pressure-sinkage relation, shearing characteristics, and responses to repetitive normal and shear loadings of the terrain are taken into consideration.

Based on an understanding of the physical nature of the problem, the mechanics of track-terrain interaction is analyzed in detail. A set of equations for the equilibrium of the forces and moments acting on the track system are derived. They establish the relationship between the shape of the deflected track in contact with the terrain and vehicle design parameters and terrain characteristics. The solutions to this set of equations define the sinkages of the roadwheels, the inclination of the vehicle, the track tension distribution, and the track shape in contact with the ground. From these, the normal and shear stress distributions on the track-terrain interface, and the track motion resistance, belly drag (if the vehicle belly is in contact with the terrain), thrust, drawbar pull, and tractive efficiency of the vehicle as functions of track slip can be determined. For further details of the model, please refer to the references (Wong, 1989 and 1993).

Experimental Validation

The model can be used to predict the performance of single unit and two-unit articulated tracked vehicles over unprepared terrain. Its basic features have been validated with field test data obtaining using various test vehicles, including M113A1, BV202 and BV206, over a variety of unprepared terrains, including mineral terrain, organic terrain (muskeg) and snow-covered terrain. Figures 2 - 4 show a comparison of the measured and predicted normal pressure distributions under the track pad of an armoured personnel carrier M113A1 over a sandy terrain, a muskeg, and a snow-covered terrain, respectively. A comparison of the measured and predicted drawbar performance of an M113A1 over the three types of terrain is shown in Figs. 5 - 7, respectively. Figure 8 shows a comparison between the measured and predicted drawbar performance of a two-unit, articulated tracked vehicle BV 206, over an undisturbed snow. Reasonably close agreements between the measured and predicted normal pressure distributions and drawbar performance obtained using NTVPM-86 confirm the validity of the basic features of the model.

Applications to Parametric Analysis and Design Optimization

NTVPM-86 can be employed to assess the effects of vehicle design parameters on vehicle mobility and the influence of terrain conditions on vehicle performance. The model can also be used in design optimization for a given mission and operating environment.

Figure 9 shows the effects of the number of roadwheels and the initial track tension on the drawbar pull to weight ratio (drawbar pull coefficient) of a reference vehicle with design parameters similar to that of the M113A1 over a deep snow, predicted using the simulation model (Wong and Preston-Thomas, 1986a). It can be seen that both the number of roadwheels and the initial track tension have significant effects on vehicle mobility over soft

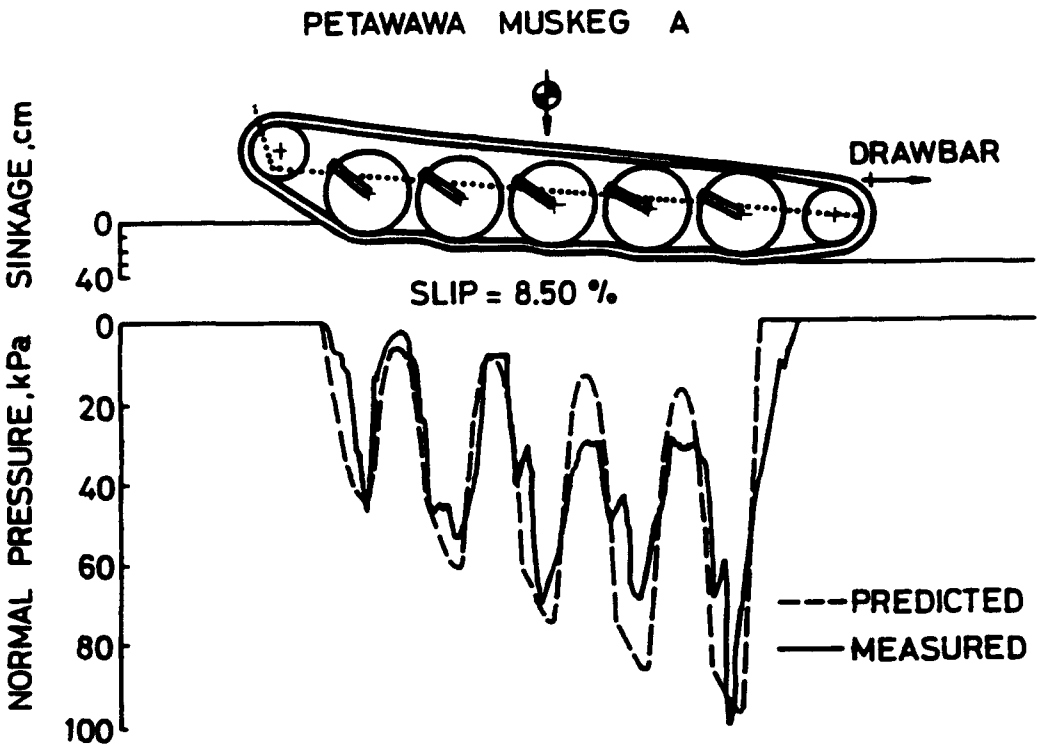

Figure 3. Comparison of the measured and predicted pressure distribution under an M113A1 on a muskeg

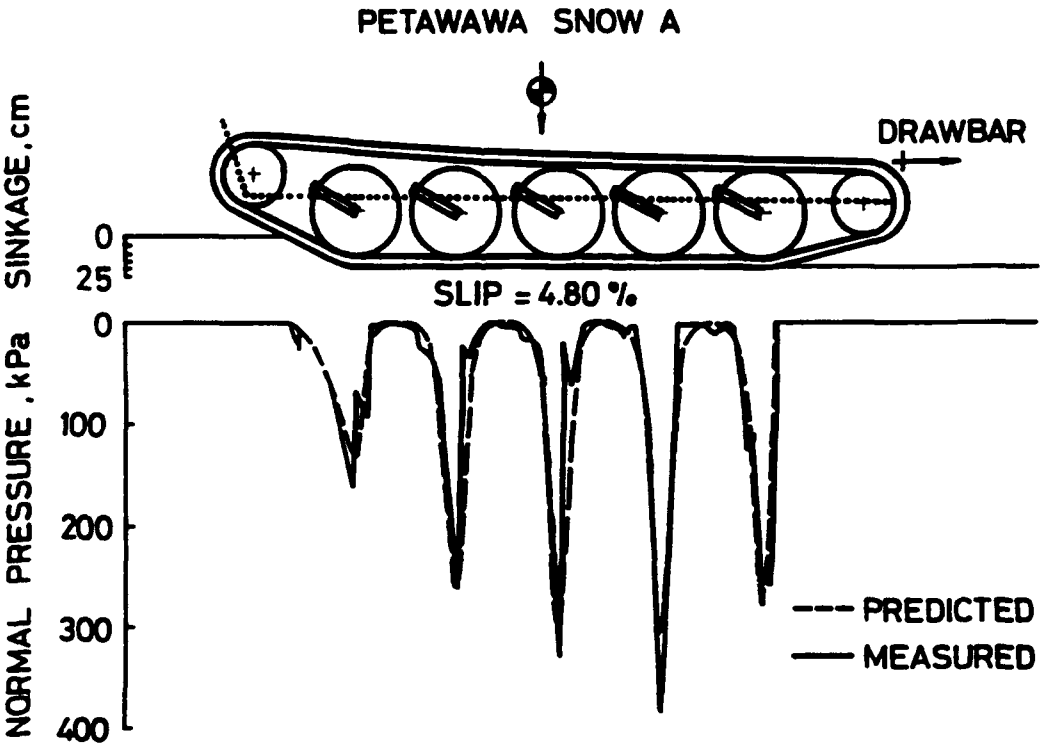

Figure 4. Comparison of the measured and predicted pressure distribution under an M113A1 on a snow

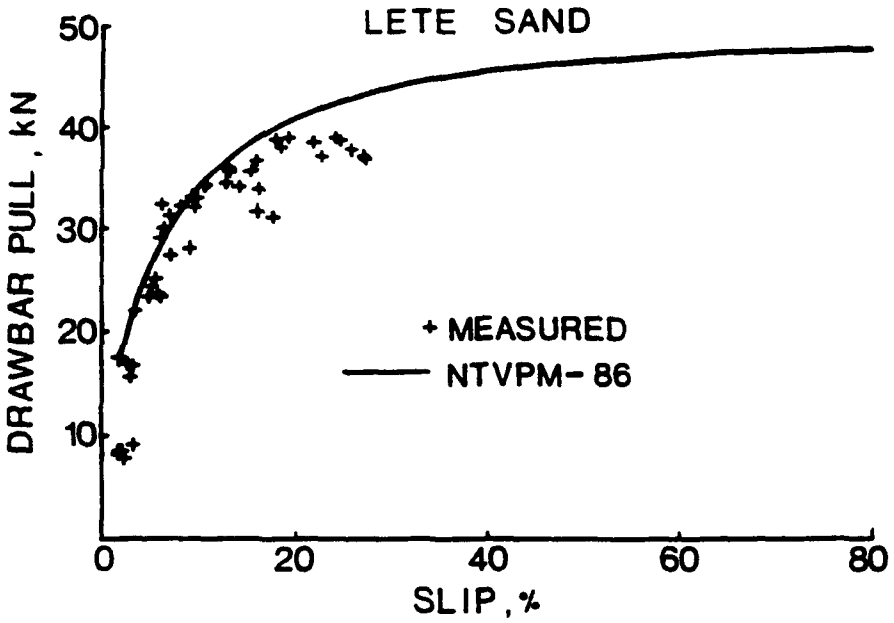

Figure 5. Comparison of the measured and predicted drawbar performance of an M113A1 on a sandy terrain

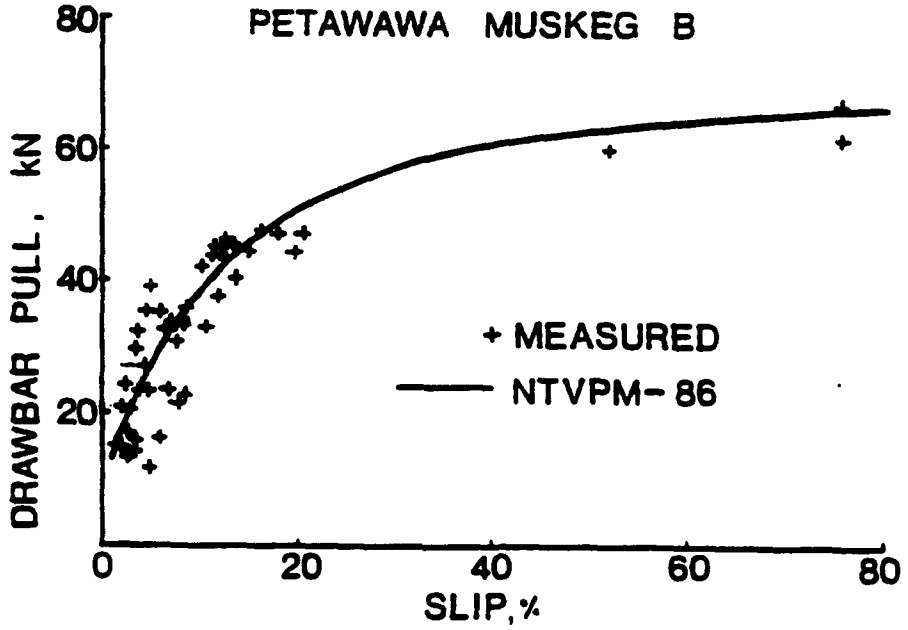

Figure 6. Comparison of the measured and predicted drawbar performance of an M113A1 on a muskeg

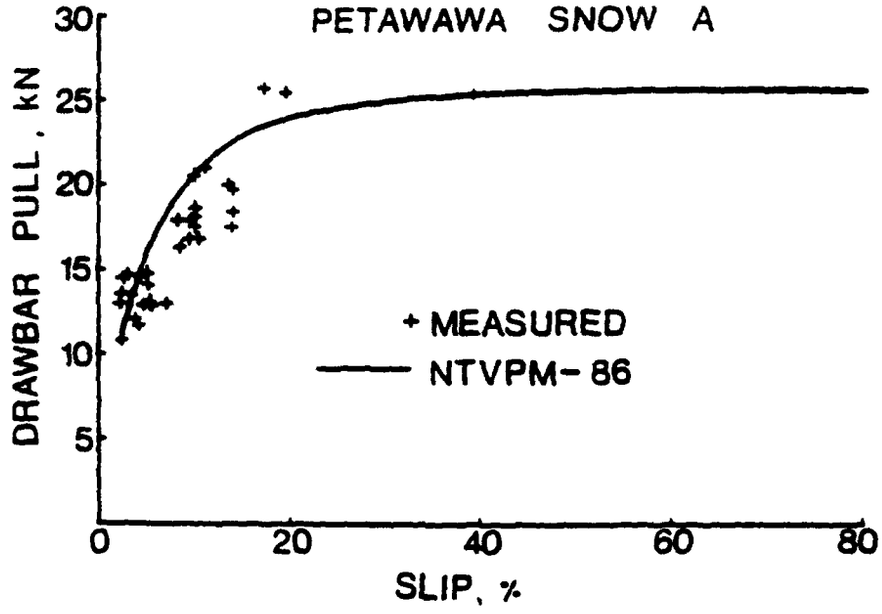

Figure 7. Comparison of the measured and predicted drawbar performance of an M113A1 on a snow

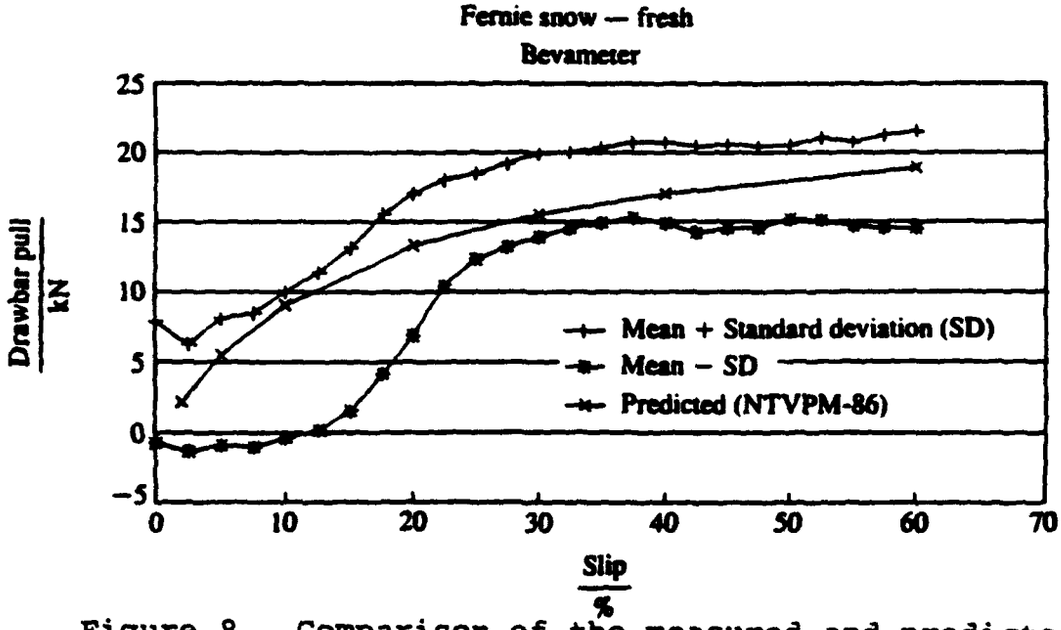

Figure 8. Comparison of the measured and predicted drawbar performance of a BV 206 on a snow

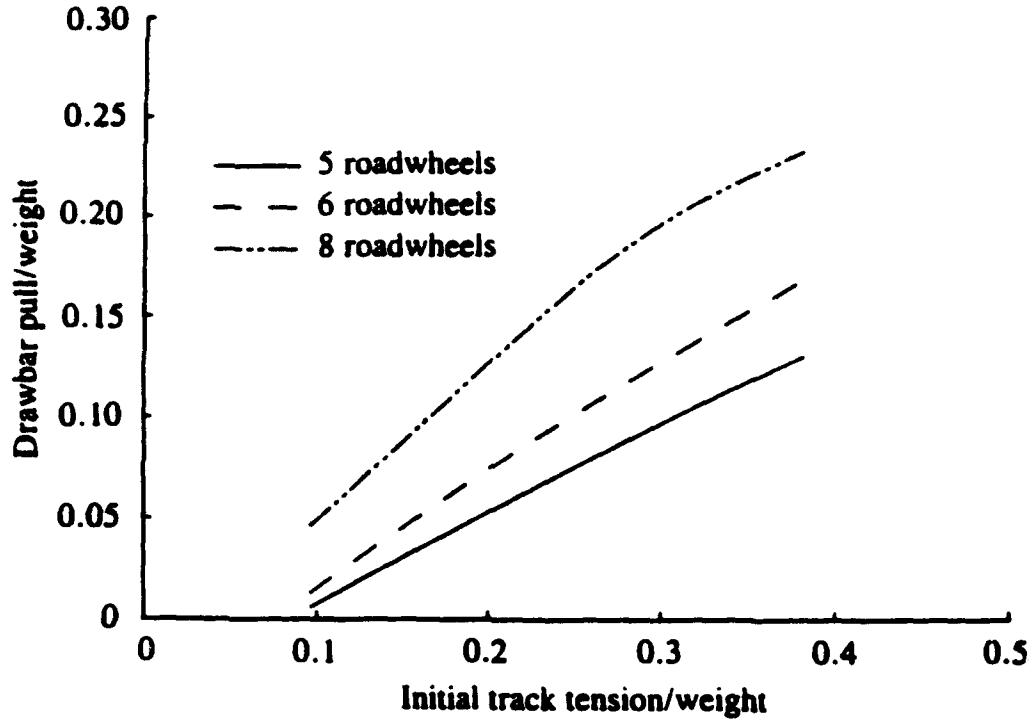

Figure 9. Effects of the number of roadwheels and initial track tension on vehicle performance on a snow

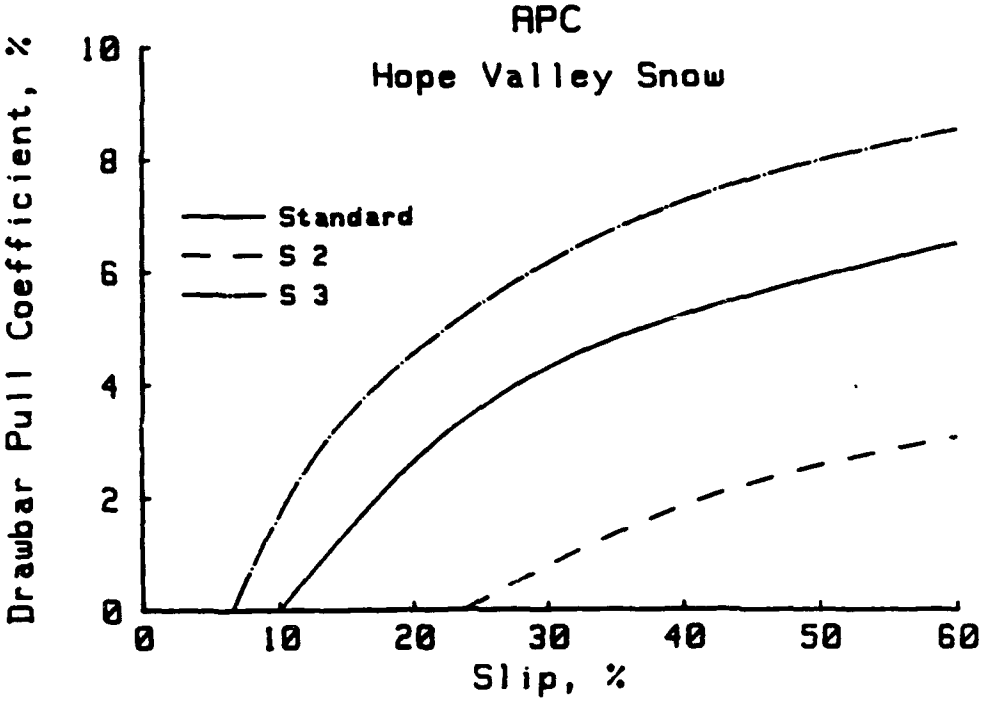

Figure 10. Effects of suspension characteristics on vehicle performance on a snow

ground. For a given (or existing) vehicle, its mobility over marginal terrain can be greatly improved by increasing the initial track tension. This research finding obtained using NTVPM-86 has led to the development of the central initial track tension regulating system controlled by the driver. Over normal terrain, the driver can set the track tension at the regular level. However, when traversing marginal terrain is anticipated, the driver can readily increase the track tension to an appropriate level to improve vehicle mobility. The central track tension regulating system is analogous to the central tire inflation system for off-road wheeled vehicles. A central initial track tension regulating system has been developed and installed on a new generation of high-mobility armoured vehicles currently in production in Sweden.

Figure 10 shows the effects of suspension characteristics on the mobility over deep snow of the reference vehicle noted above. The parameters of the three suspension configurations examined are given in Table 1. The basic difference between them is in the settings of the initial torsion arm angles under no load conditions. The standard configuration is similar to that of the M113A1 with the initial torsion arm angle set at 43° for all roadwheel stations, as shown in Table 1. For suspension configuration S2, the initial torsion arm angle is set in a decreasing order from 51.6° at the front (first) roadwheel station to 34.4° at the rear (fifth) roadwheel station, while maintaining an angle of 43° for the torsion arm at the middle (third) roadwheel station. This setting results in a nose-up attitude for the vehicle body. In deep snow, this causes the load supported by the vehicle belly and the associated belly drag to increase and vehicle performance to decrease, as shown in Fig. 10. For suspension S3, the initial torsion arm angle is set in an increasing order from 34.4° at the front (first) roadwheel station to 51.6° at the rear (fifth) roadwheel station, while maintaining an angle of 43° for the middle (third) roadwheel station. This setting results in a nose-down attitude for the vehicle body. In a deep snow, this causes a reduction in the belly load and belly drag and hence an improvement in performance, in comparison with the standard configuration and configuration S2, as shown in Fig. 10.

Table 1. Torsion Arm Settings for the Standard Suspension and Suspensions S2 and S3

Roadwheel Station	Initial Torsion Arm Angles Under No Load (below the horizontal), degrees		
	Suspension Configuration		
	Standard	S2	S3
1	43	51.5	34.4
2	43	47.3	38.7
3	43	43	43
4	43	38.7	47.3
5	43	34.4	51.6

The model NTVPM-86 can also be used for design optimization of tracked vehicles with flexible tracks. Figure 11 shows the drawbar performance over deep snow of four

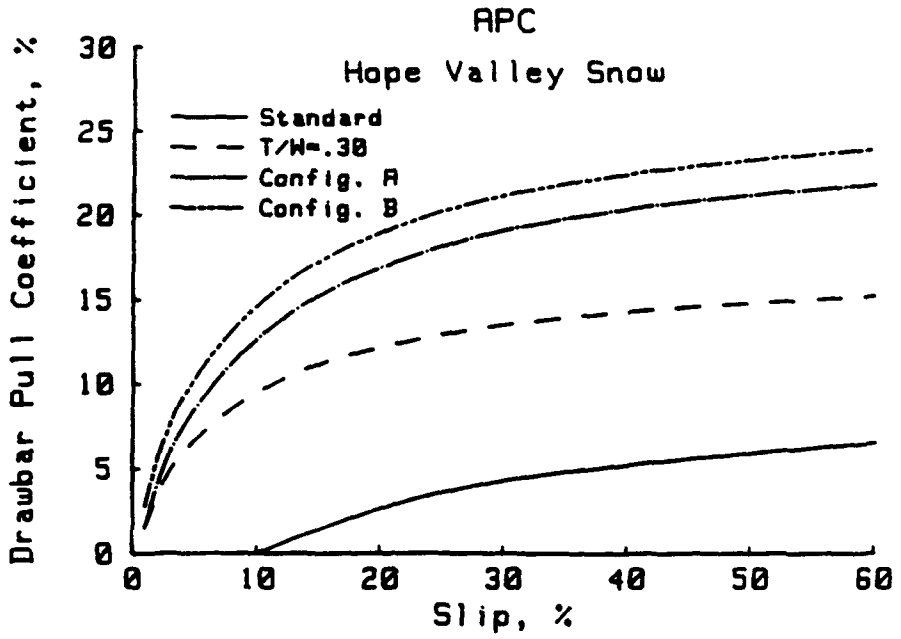

Figure 11. Comparison of the performance of various vehicle configurations on a snow

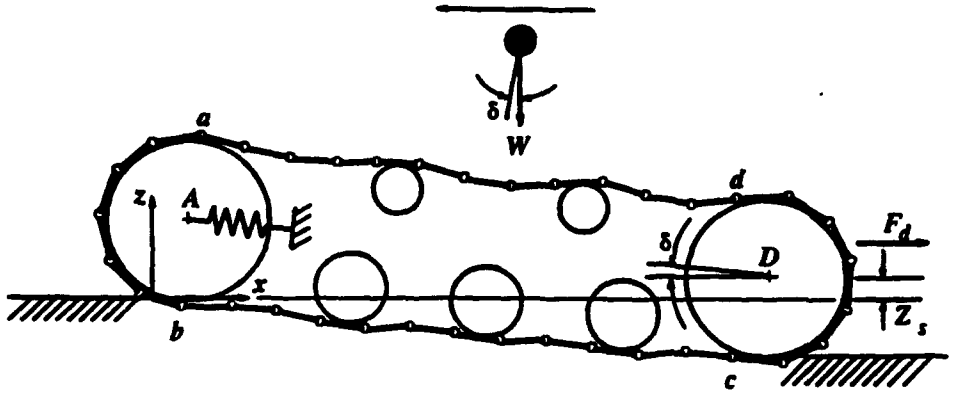

RIGID LINK TRACK

Figure 12. A rigid link track model

vehicle configurations, Configurations A and B, the standard configuration with parameters similar to that of the M113A1, and a vehicle configuration similar to the standard one but with an initial track tension to vehicle weight ratio of 0.3. Configuration A has the suspension configuration S3 described in Table 1, an initial track tension to vehicle weight ratio of 0.25, a track width of 75 cm and a ground clearance of 52 cm. Configuration B has the suspension configuration S3, an initial track tension to vehicle weight ratio of 0.3, a track width of 100 cm and a ground clearance of 57 cm. It is shown that Configurations A and B exhibit superior tractive performance in deep snow over the standard configuration. This indicates that NTVPM-86 can be an extremely useful tool for the design engineer to evaluate competing vehicle designs and to select the optimum configuration for given operating requirements.

Computer Simulation Model RTVPM for Vehicles with Rigid Link Tracks

For low-speed tracked vehicles, such as those used in agriculture and construction industry, rigid link tracks with relatively long track pitch are commonly used. This type of track system has a ratio of roadwheel diameter to track pitch as low as 1.2 and a ratio of roadwheel spacing to track pitch typically 1.5.

The computer simulation model RTVPM has been developed for performance and design evaluation of tracked vehicles wth rigid link tracks. This model takes into account all major design parameters of the vehicle, including vehicle weight, location of the centre of gravity, number of roadwheels, location of roadwheels, roadwheel dimensions and spacing, locations of sprocket and idlers, supporting roller arrangements, track dimensions and geometry, initial track tension, and drawbar hitch location. As the track links are considered to be rigid, the track is assumed to be inextensible. For most low-speed tracked vehicles, the roadwheels are not sprung, and hence considered to be rigidly connected to the track frame. Terrain parameters used in this model are the same as those used in NTVPM.

Basic Approach to the Development of the Model

The model RTVPM treats the track as a system of rigid links connected with frictionless pin, as shown in Fig. 12. As noted previously, the roadwheels, supporting rollers, and sprocket are assumed to be rigidly attached to the vehicle frame. The centre of the front idler is, however, assumed to be mounted on a pre-compressed spring.

In the analysis, the track system is divided into four sections: the upper run of the track supported by rollers; the lower run of the track in contact with the roadwheels and the terrain; the section in contact with the idler; and the section in contact with the sprocket. By considering the equilibrium of various sections of the track system, the interaction between the lower run of the track and the terrain, and the compatibility conditions for various track sections, a set of equations can be formulated. The solutions to this set of equations determine the sinkage and inclination of the track system, the normal and shear stress distributions on the track-terrain interface, and the track motion resistance, thrust, drawbar pull, and tractive efficiency of the vehicle as functions of track slip. Figure 13 shows the predicted normal pressure distribution under a tracked vehicle with seven roadwheels on a

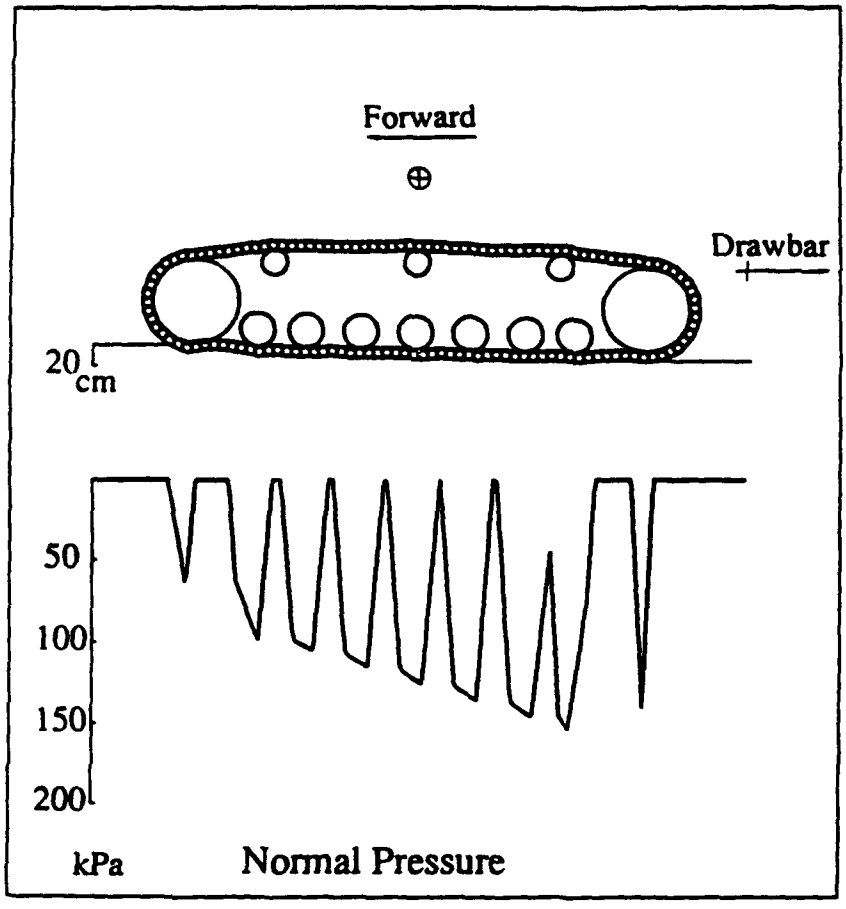

Figure 13. The normal pressure distribution under a tractor with rigid links predicted using RTVPM on a clayed soil

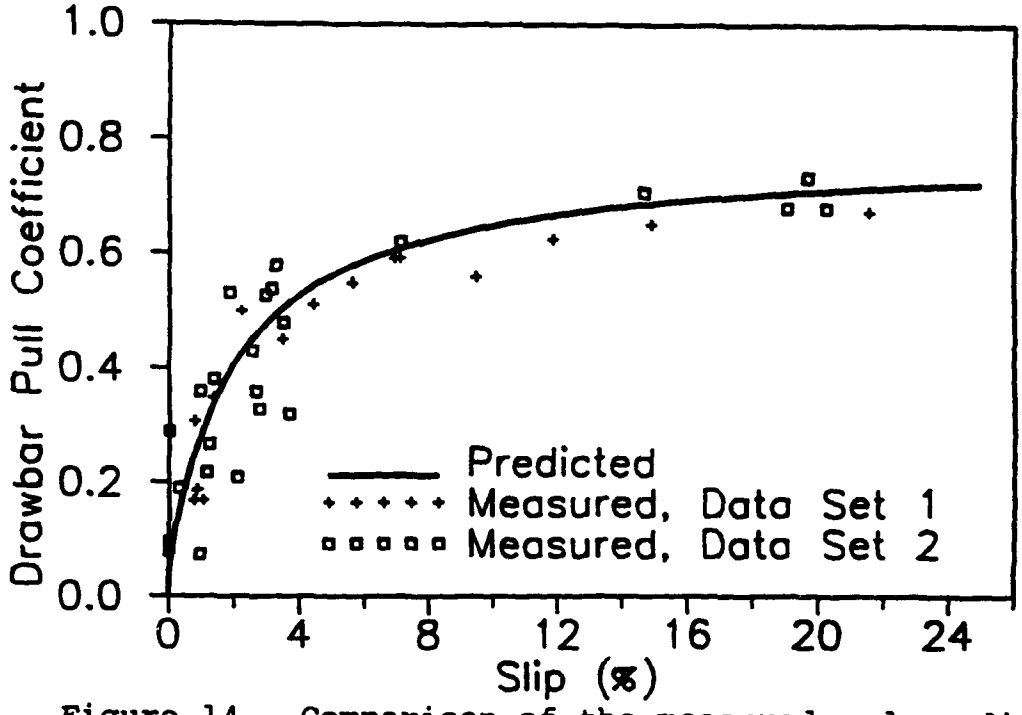

Figure 14. Comparison of the measured and predicted drawbar performance of a tractor on a sandy loam

clayey soil (Wong and Gao, 1994). The detailed description of the model may be found in the references (Gao and Wong, 1993 and 1994).

Experimental Validation

The basic features of RTVPM have been validated with available field test data. Figures 14 and 15 show a comparison of the measured and predicted drawbar pull coefficient and tractive efficiency as functions of track slip, respectively, for a heavy tracked vehicle used in construction industry. The vehicle has a total weight of 329 kN. It has eight roadwheels of diameter 26 cm on each of the two tracks and the average spacing between roadwheels is 34 cm. The track pitch is 21.6 cm and the track width is 50.8 cm. The terrain is a dry, disked sandy loam, with an angle of shearing resistance of 40.1° and a cohesion of 0.55 kPa. The measured data shown in figures are provided by Caterpillar Inc., Peoria, Illinois, U.S.A.

It can be seen that the tractive performance of the vehicle predicted using RTVPM is very close to the measured one. This suggests that the model is capable of providing realistic predictions of vehicle performance in the field. It would be desirable, however, to further validate the model over a wider range of terrain conditions.

Applications to Parametric Analysis and Design Optimization

The applications of RTVPM to design evaluation and parametric study of vehicles with rigid link tracks will be demonstrated through examples.

Figure 16 shows the effects of the track pitch on the drawbar performance on a clayey soil of a reference vehicle with a total weight of 372.4 kN, predicted using RTVPM (Wong and Gao, 1994). The vehicle has seven roadwheels on each track, a track pitch of 21.6 cm, an initial track tension of 22.30 kN, and a centre of gravity at the mid-point of the track contact length. It can be seen that within the range studied, the longer the track pitch, the higher the tractive performance will be. This is primarily due to the fact that with a longer track pitch, the normal pressure distribution under the track becomes more favourable. It should be noted, however, that with a longer track pitch, the fluctuation in speed and the vibrations of the track system may increase. Consequently, there is a practical limit to the track pitch for a given vehicle configuration.

Figure 17 shows the effects of the number of roadwheels on the drawbar performance of the reference vehicle on the clayey soil. It can be seen that increasing the number of roadwheels enhances the tractive performance of the vehicle. The improvement in tractive performance with a larger number of roadwheels is due to a more uniform normal pressure distribution.

The model can also be used for design optimization of tracked vehicles with rigid link tracks. Figure 18 shows a comparison of the drawbar performance of the reference vehicle and an optimized configuration (Configuration A) on the clayey soil. Configuration A has nine roadwheels on each track, a track pitch of 23 cm, an initial track tension of 89.20 kN,

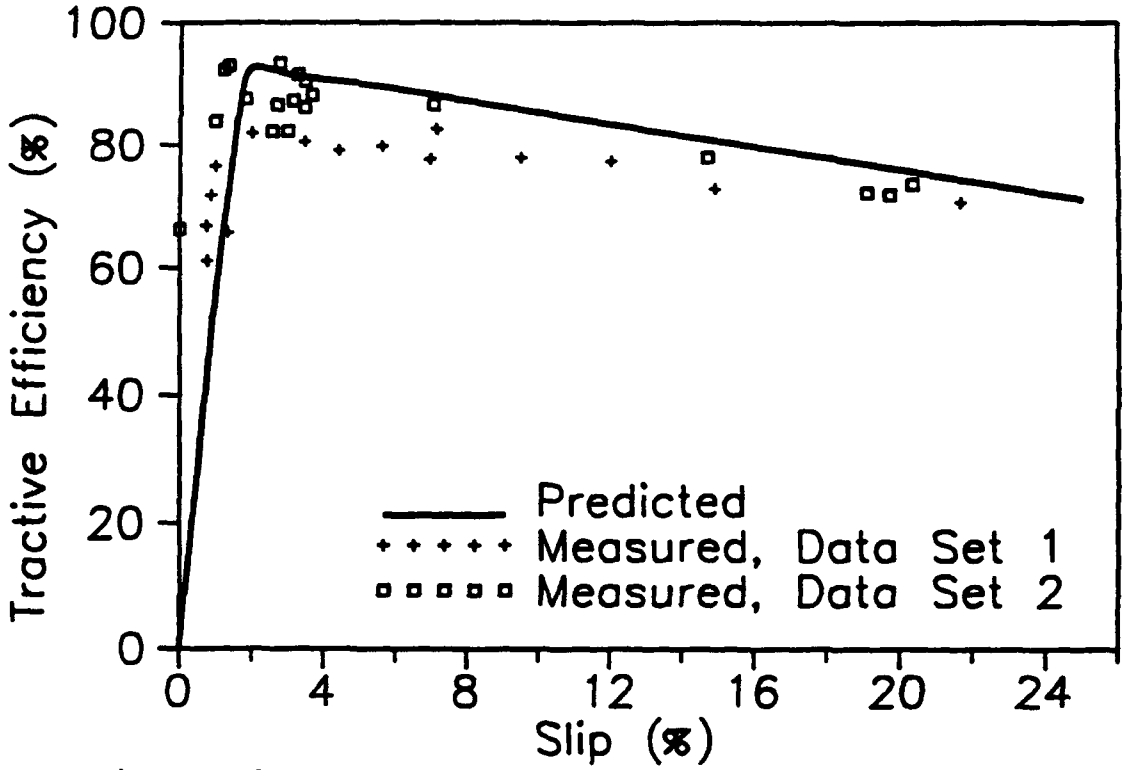

Figure 15. Comparison of the measured and predicted tractive efficiency of a tractor on a sandy loam

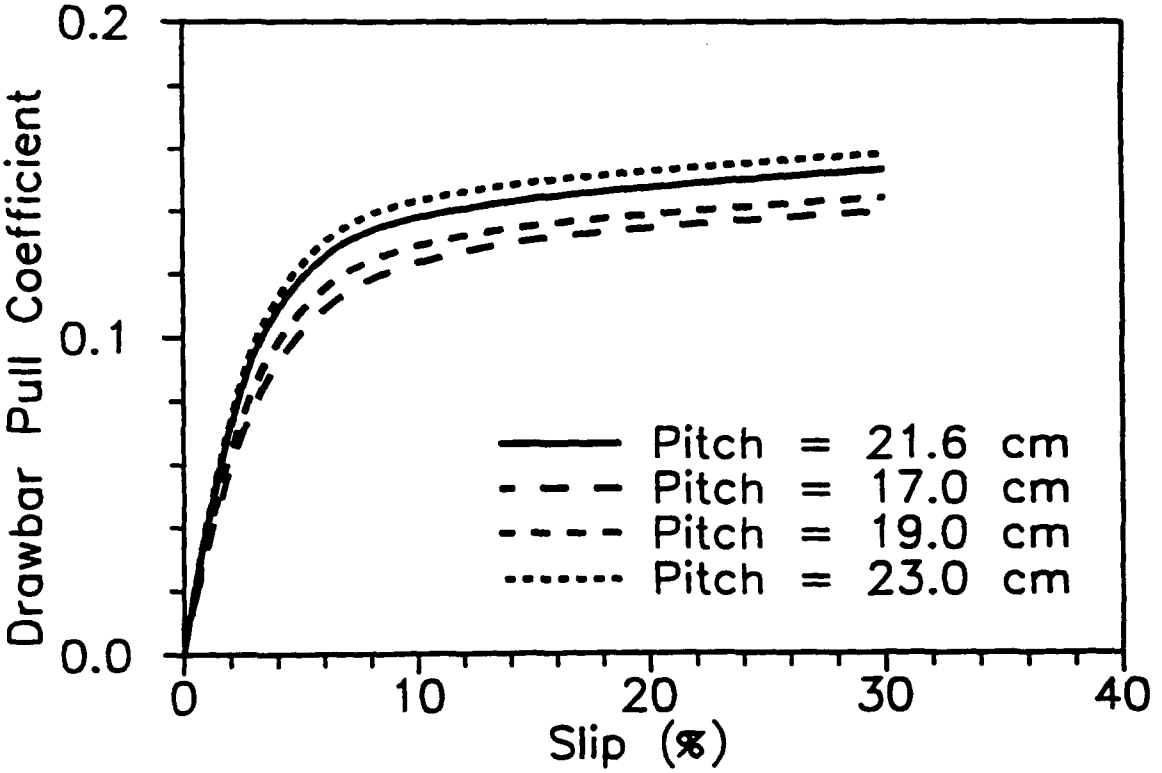

Figure 16. Effects of track pitch on the performance of a tractor on a clayey soil

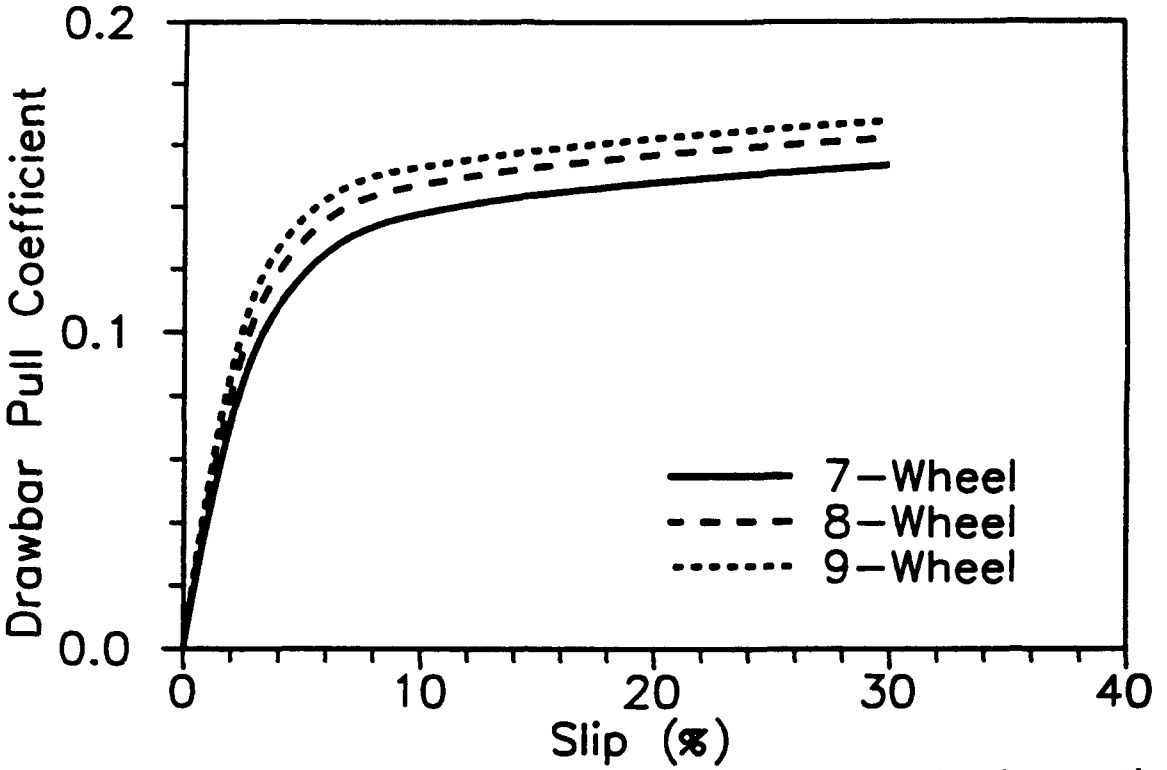

Figure 17. Effects of the number of roadwheels on the performance of a tractor on a clayey soil

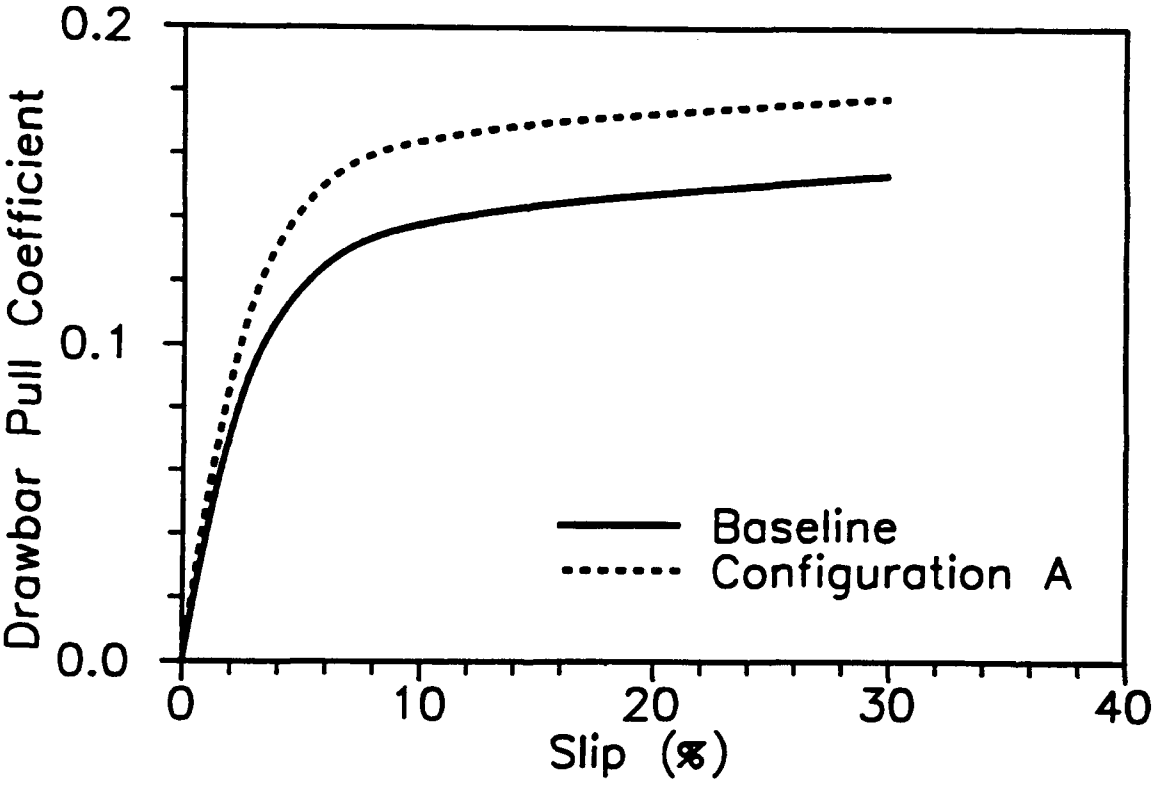

Figure 18. Comparison of the performance of different tractor configurations on a clayey soil

and a centre of gravity at 40 cm ahead of the mid-point of the track contact length. It shows that RTVPM can be a useful tool for the vehicle designer to select the optimum vehicle configuration and design parameters.

Computer Simulation Model NWVPM for Off-Road Wheeled Vehicles

NWVPM has been developed for the evaluation of the overall performance and design of off-road wheeled vehicles over unprepared terrain, as well as for the selection of tires for cross-country operations. The model takes into account all major design parameters of the vehicle as well as the tire. The vehicle design parameters considered include: vehicle weight, axle load, axle spacing, location of the centre of gravity, axle suspension stiffness, function of the axle (driven or non-driven), axle clearance, track of the axle, belly (hull) shape, and drawbar hitch location. The tire parameters considered include: outside diameter, tread width, section height, lug area/carcass area, lug height, lug width, inflation pressure, average ground contact pressure, and tire construction (radial or bias). Terrain parameters used in the model are the same as those used in NTVPM and RTVPM.

Basic Approach to the Development of the Model

The model NWVPM consists of two sub-models, one is the tire sub-model and the other is the vehicle sub-model.

The tire sub-model used is that developed by Wong (Wong, 1989 and 1993). Based on the dimensions of the tire, the inflation pressure and carcass stiffness (or alternatively the average contact pressure on a hard surface), the normal load, and terrain characteristics, the operating mode of the tire ("rigid" or "elastic") is first predicted. Based on a detailed analysis of the mechanics of tire-terrain interaction, a set of equations for the equilibrium of the tire can then be established. The solutions to this set of equations determine the normal and shear stress distributions on the tire-terrain interface, the motion resistance, (including the internal resistance of the tire), thrust, and sinkage of the tire. A schematic of the tire sub-model used is shown in Fig. 19.

The tire sub-model is incorporated into the vehicle sub-model to provide a complete framework for performance and design evaluation of off-road wheeled vehicles. The vehicle sub-model takes into account the dynamic inter-axle load transfer and the suspension stiffness of the axles. Any number of axles can be accommodated. When the track of the front (preceding) axle is the same as that of the rear (following) axle, the tires on the rear axle run in the ruts formed by the tires on the front axle. Terrain properties in the rut will be different from those in the virgin state. To take into account this "multipass" effect, the responses of the terrain to repetitive normal and shear loadings are taken into consideration in the model. In addition, both single and dual tires can be accommodated. The output of the model includes the load, sinkage, motion resistance and thrust of the axles, and the drawbar pull and tractive efficiency of the vehicle as functions of wheel slip.

The basic features of the model have been verified with available field test data. Figures 20 and 21 show a comparison of the measured and predicted drawbar performance of a tractor obtained using NWVPM on a plowed and stubble field, respectively.

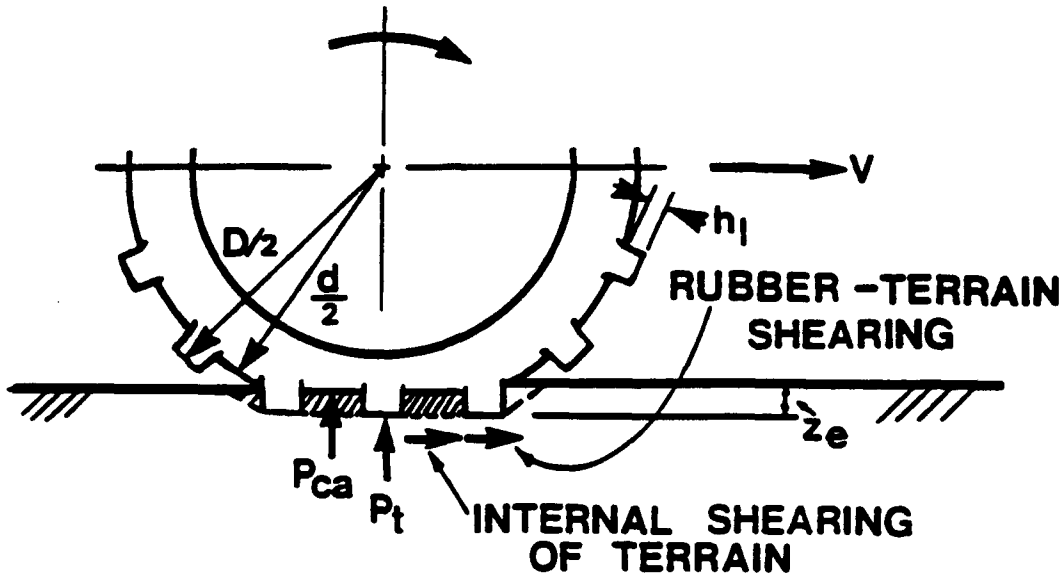

Figure 19. A tire model

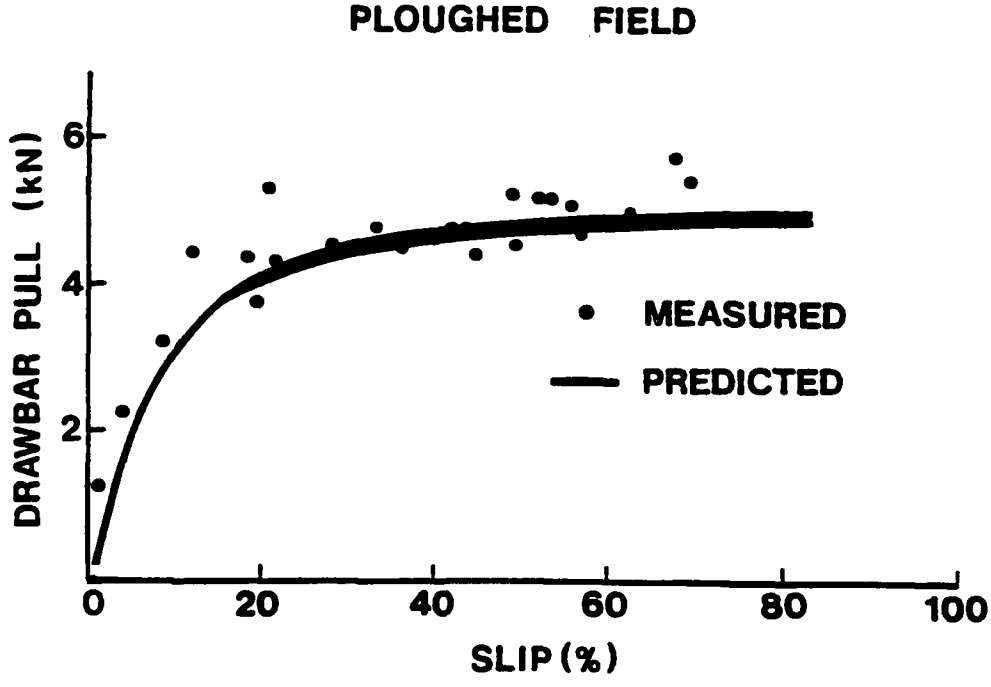

Figure 20. Comparison of the measured and predicted performance of a wheeled tractor on a plowed field

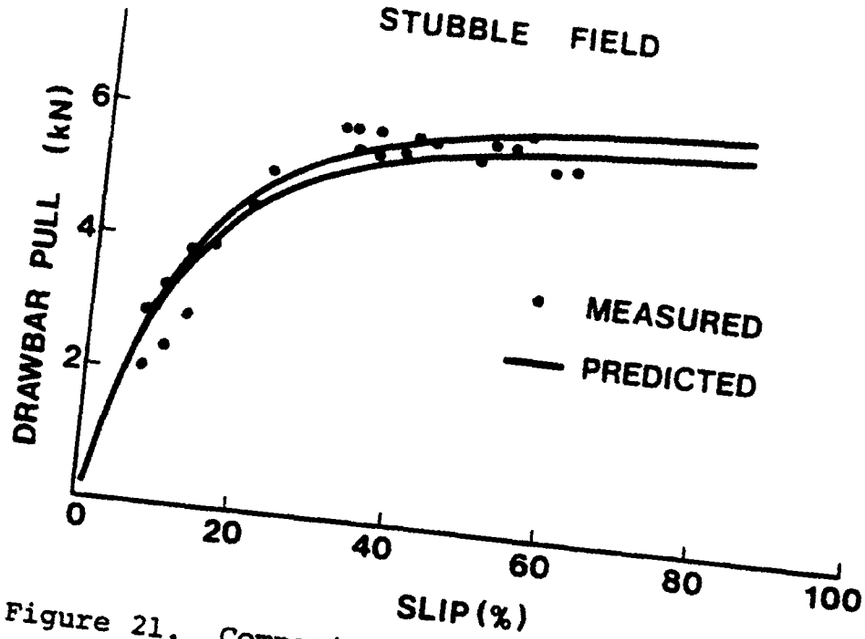

Figure 21. Comparison of the measured and predicted performance of a wheeled tractor on a stubble field

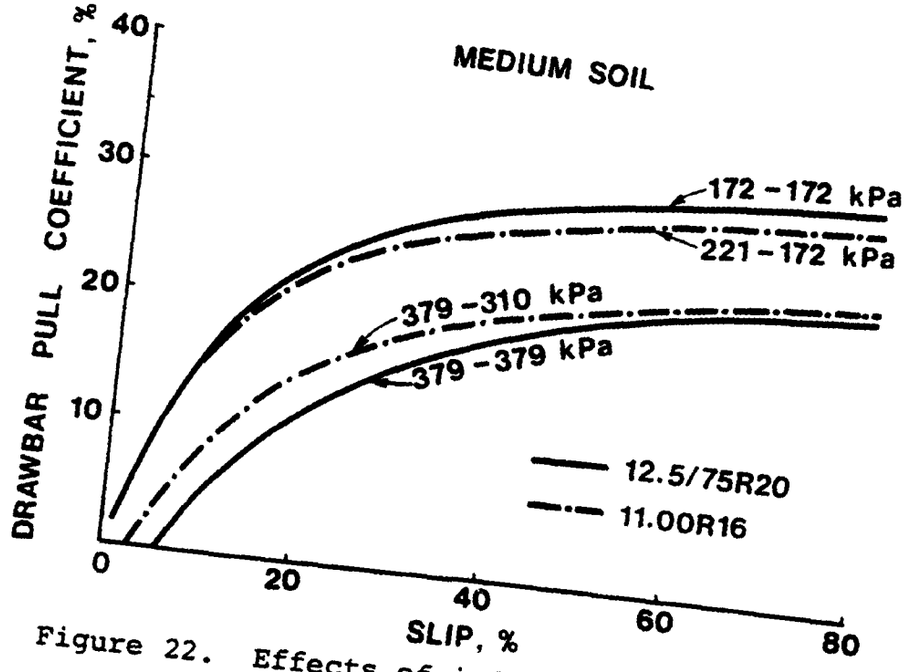

Figure 22. Effects of inflation pressure on the drawbar performance of a two-axle wheeled vehicle on a medium soil

Applications to Parametric Analysis and Design Optimization

The applications of NWVPM to parametric analysis of the performance and design of off-road wheeled vehicles and to the selection of tires for a given operating environment will be illustrated through examples.

Figure 22 shows the effects of tire design and inflation pressures of the front and rear tires on the tractive performance of a two-axle vehicle on a medium soil, predicted using NWVPM. The first and second numbers in the inflation pressure combinations shown in the figure represent the inflation pressure of the front tires and that of the rear tires, respectively. The effects of the static load distribution between the front and rear axles on the drawbar performance of the two-axle vehicle are shown in Fig. 23. It indicates that because of the "multipass" effect, a lighter static load on the front and a heavier static load on the rear will give improved tractive performance on the medium soil (Wong, 1989).

Concluding Remarks

Computer simulation models based on empirical relations have played a useful role in the past. However, with an improved understanding of the physical nature of vehicle-terrain interaction and of terrain response to vehicular loading, a new generation of computer simulation models has emerged over the past decade. They are based on detailed analyses of the mechanics of vehicle-terrain interaction and take into account all major vehicle design features and terrain characteristics. These comprehensive and realistic computer simulation models have played and will continue to play an increasingly important role in the future development of off-road vehicles. For instance, the computer simulation model NTVPM for vehicles with flexible tracks have been successfully used to assist vehicle manufacturers in the development of new products and governmental agencies in the evaluation of vehicle candidates in Europe, North America and Asia.

To further develop computer simulation models (computer-aided methods) for performance and design evaluation of off-road vehicles, the following guidelines are suggested.

a) It should be clear that the objective of a model is to provide a framework that will enable the engineering practitioner to realistically evaluate the performance or design of off-road vehicles under a variety of operating environments. The development of the model is an engineering endeavour and not an academic exercise.

b) The model should address the needs of the vehicle user, designer, or procurement manager and not that of the theoretician.

c) The model should be developed and implemented in such a manner that will be conducive to practical results and should appeal to a wide spectrum of engineering practitioners.

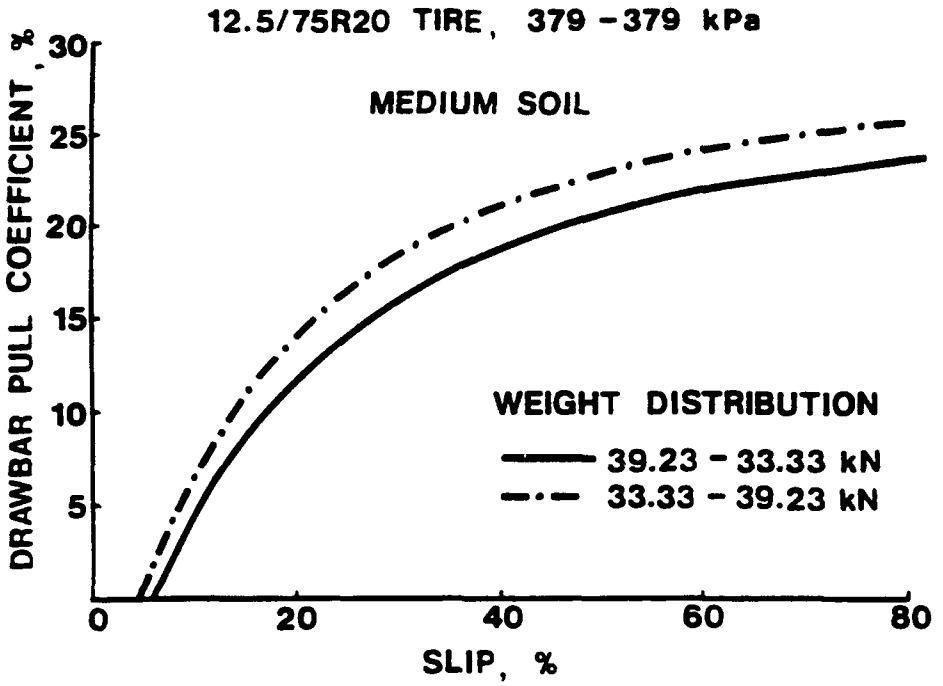

Figure 23. Effects of static weight distribution on the performance of a two-axle wheeled vehicle on a medium soil

d) In the development of the model, including the characterization of terrain behaviour, a pragmatic engineering approach should be followed. It should not be unduly dwelling on theoretical niceties.

e) An off-road vehicle is a complex mechanical system. In the development of the model, emphasis should be placed on an adequate representation of the vehicle, so that meaningful results can be obtained to guide its development, design and procurement.

f) While an understanding of the mechanical behaviour of the terrain (soil) is essential, the development of the model is not an exercise in soil mechanics.

g) The success or failure of a model is eventually judged by the market place or by the engineering practitioner, and not by the theoretician or the bureaucrat.

Acknowledgements

The provision of field test data by Caterpillar Inc., Peoria, U.S.A., for the validation of the computer simulation model RTVPM is appreciated. This does not imply, however, that the views expressed in this presentation necessarily represent those of Caterpillar Inc.

References

Jurkat, M.P., Nuttall, C.J. and Haley, P.W. (1975), "The U.S. Army Mobility Model (AMM-75)," Proceedings of the 5th International Conference of the International Society for Terrain-Vehicle Systems, Vol. IV, pp. 1-48.

Wong, J.Y. (1986), "Computer-Aided Analysis of the Effects of Design Parameters on Performance of Tracked Vehicles," Journal of Terramechanics, Vol. 23, No. 2, pp. 95-124.

Wong, J.Y. (1989), *Terramechanics and Off-Road Vehicles*, Elsevier Science Publishers, B.V., Amsterdam, the Netherlands.

Wong, J.Y. (1992a), "Optimization of the Tractive Performance of Articulated Vehicles Using an Advanced Computer Simulation Model," Proceedings of the Institution of Mechanical Engineers, Part D, Journal of Automobile Engineering, Vol. 206, No. D1, pp. 29-45.

Wong, J.Y. (1992b), "Computer-Aided Methods for Optimization of the Mobility of Single-Unit and Two-Unit Articulated Tracked Vehicles," Journal of Terramechanics, Vol. 29, No. 4/5, pp. 395-421.

Wong, J.Y. (1993), *Theory of Ground Vehicles*, John Wiley, New York.

Gao, Y. and Wong, J.Y. (1993), "A Computer-Aided Method for Design and Performance Evaluation of Vehicles with Rigid Link Tracks," Proceedings of the 11th International Conference of the International Society for Terrain-Vehicle Systems, Vol. I, pp. 76-85.

Gao, Y. and Wong, J.Y. (1994), "The Development and Validation of a Computer-Aided Method for Design Evaluation of Tracked Vehicles with Rigid Links," Proceedings of the Institution of Mechanical Engineers, Part D, Journal of Automobile Engineering, Vol. 208 (in press).

Wong, J.Y. and Preston-Thomas, J. (1986a), "Parametric Analysis of Tracked Vehicle Performance Using an Advanced Computer Simulation Model," Proceedings of the Institution of Mechanical Engineers, Part D, Transport Engineering, Vol. 200, No. D2, pp. 101-114.

Wong, J.Y. and Preston-Thomas, J. (1986b), "Development of Vehicle Performance Prediction Software," Unpublished Report prepared for the Division of Energy, National Research Council of Canada.

Wong, J.Y. and Preston-Thomas, J. (1988), "Investigation into the Effects of Suspension Characteristics and Design Parameters on the Performance of Tracked Vehicles Using an Advanced Computer Simulation Model," Proceedings of the Institution of Mechanical Engineers, Part D, Transport Engineering, Vol. 202, No. D3, pp. 143-161.

Wong, J.Y. and Gao, Y. (1994), "Applications of a Computer-Aided Method to Parametric Study of Tracked Vehicles with Rigid Links," Proceedings of the Institution of Mechanical Engineers, Part D, Journal of Automobile Engineering, Vol. 208 (in press).

Soil Property Determination Keynote Lecture

DETERMINATION OF ENGINEERING PROPERTIES OF SOIL IN-SITU

Shrini. K. Upadhyaya
Professor

Department of Biological and Agricultural Engineering
University of California, Davis CA 95616

SUMMARY:

Soil-tire/Soil-track interaction is of particular interest to researchers involved in off-road mobility and traction research. This includes scientists and engineers involved in research in the field of agriculture, construction, forestry, military, and mining. In agriculture and forestry soil compaction caused by traction devices is also a serious concern. A sound mathematical model is a pre-requisite to obtain a clear understanding of the soil-tire/soil-track interaction process. A key ingredient for any such model is a constitutive relationship which describes the stress-strain behavior of soil. Any suitable constitutive model requires soil physical properties which describe the elastic behavior of soil, onset of yield and subsequent plastic flow, material hardening or softening rules etc. Since in-situ soils seldom behave like remolded laboratory soils or disturbed field samples, it is important to "identify" or "calibrate" the engineering properties of field soil by means of in-situ tests. The technique of obtaining material parameters based on actual system response is known as "back analysis", "inverse solution", "identification", or "calibration procedure". For complex problems such as soil-traction device interaction where closed form analytical solutions do not exist a numerical technique such as a finite element technique is commomnly used to solve underlying system differential equation. For such cases the back analysis procedure can take one of the two forms: (1) inverse method, and (2) direct method. This paper addresses the advantages and disadvantages of such techniques, and discusses a new technique which overcomes some of their limitations. This new technique consists of developing a so called "response surface" in the parameter space and then using this pre-determined surface to "identify" engineering properties of the material based on in-situ tests. Two case studies - (1) a two parameter hypo-elastic model for soil, and (2) a complex five parameter model for soil which includes nonlinear material behavior in elastic range, yield based on Drucker-Prager yield criteria and associated plastic flow upon yield are presented to illustrate the methodology.

INTRODUCTION AND REVIEW OF LITERATURE:

One of the challenges in the design of an off-road vehicle is to equip it with a traction device(tire or track) which can develop high traction efficiently(i.e. optimum tractive efficiency) while deterring soil compaction. Even an increase of one percentage point in the tractive efficiency leads to an annual savings of over 100 million liters(about 25 million gallons) of fuel in U. S. alone[1]. On the other hand, soil compaction has been recognized as a worldwide problem with serious implications on agricultural sustainability[2]. Although, certain amount of soil compaction may even be desirable for some crops under certain environmental conditions (optimum soil compaction), excessive soil compaction can lead to diminished soil porosity, reduced water infiltration, increased resistance to root penetration, increased tillage energy requirements, decreased biological activity, and a reduction in crop yield[3 - 14]. A necessary pre-requisite for the successful design of a traction device is a sound mathematical model for the soil-traction interaction process. This interaction is an extremely complex, dynamic process. A key ingredient of such a model is a constitutive relationship which describes the stress-strain behavior for soil. Schafer et al.

[15] stated that an accurate description of soil constitutive relationship is necessary for the integrity and robustness of the model. Soil is perhaps one of the most complex material from engineering point of view[16].

Numerous constitutive models are currently available for soils. Among these are the elasticity models, higher order nonlinear elasticity models, hypo-elasticity models, plasticity models and visco-plasticity models. Desai [16], Desai and Siriwardane [17] and Chen and Baladi[18] have discussed these models and their applicability to a specific loading situation in detail. Piece-wise linear elastic models (hyperbola, parabola, splines and Ramberg-Osgood formulas) tend to be good for a specific loading case but are poor to simulate general loading conditions. Higher order nonlinear elasticity models tend to include too many parameters and have limited appeal. Hypo-elasticity models appear to show some promise. Plasticity models which utilize Von Mises, Mohr-Coulomb and Drucker-Prager failure criteria have been widely used. To include volume changes due to shear in geological materials and also to account for strain hardening or softening behavior critical state models have been developed. CAM and CAP models account for growth of the yield surface and have become increasingly popular in civil engineering. Applicability of critical state models to unsaturated agricultural soils has been a much debated issue. Hettiaratchi and O' Callaghan[19], Hettiaratchi[20] and Kirby[21] have found that critical state concept is applicable to unsaturated soils both qualitatively and quantitatively except that the critical state parameters depend on the soil moisture content. They found that it is reasonable to use total stress in the model(i.e. soil moisture tension can be ignored). Bailey et al.[22] and Bailey and Johnson[23] developed a constitutive model for agricultural soil that relates volumetric strain to octahedral normal and shear stress. This model predicts volumetric strain of soil samples accurately at limiting values of stresses(i.e. zero and very large applied stress). Raper and Erbach[24] and Raper et al.[25] have used this constitutive equation to compute tangent moduli in a finite element program to predict soil compaction.

All the aforementioned constitutive models require material parameters. These material properties describe the elastic behavior of soil, onset of yield and subsequent plastic flow, material hardening or softening rules etc. Typically these parameters are determined using laboratory tests. Sometimes remolded soils are employed in the laboratory tests which may not behave like field soil. Use of soil properties obtained from remolded samples can often lead to predictions which are unrealistic and of little value to engineers interested in improving tire design. Even if field samples are obtained, one of the main problem with the soil material is that these samples undergo disturbances during excavation and testing, and may not behave like in-situ soil under actual loading conditions in the field. Use of cone penetrometer, grouser plate, and sinkage plate often yield some composite soil parameters which depend on the geometry of the test device and loading conditions. These composite soil parameters are of little use in subsequent model studies based on constitutive relationship. It is preferable to determine the soil material parameters based on undisturbed in-situ tests. The technique of obtaining material parameters based on actual system response is called "back analysis", "inverse solution", "identification", or " calibration procedure". The process of "calibrating" actual field response to model behavior is expected to "identify" the material parameters which can accurately predict system response in subsequent analysis which utilize the same constitutive model.

The back analysis technique has been successfully used in Geomechanics in studying tunneling problems in rocks and in investigating settlement problems[26-43]. If a closed form solution exists for the underlying differential equation describing the physical problem, then back analysis to obtain the material parameters involves optimizing the difference between the analytical and experimental responses. However, most real life problems in geomechanics are geometrically and/or materially nonlinear, and an analytical solution may not exist. In such cases a numerical procedure such as a finite element

method[FEM] may be used to obtain solutions to the governing differential equation. When finite element analysis is used, back analysis may take one of the two forms - 1) inverse method, and 2) direct method.

In the inverse method nodal values of displacements and stresses obtained by a FEM technique are used as known boundary conditions and the unknown displacements and stresses are eliminated from the global matrix equation by reduction[41]. A brief discussion of the method is as follows:

Let the FEM result in the following matrix equation:

$$[K]\{u\} = \{F\} \tag{1}$$

where K is the global stiffness matrix, u is the nodal displacement vector and F is the global forcing vector. Let us partition the global stiffness matrix by collecting all nodes at which nodal values are measured in the field as follows:

$$\begin{bmatrix} K_{11} & K_{12} \\ K_{21} & K_{22} \end{bmatrix} \begin{Bmatrix} u_1^* \\ u_2 \end{Bmatrix} = \begin{Bmatrix} F_1 \\ F_2 \end{Bmatrix} \tag{2}$$

where u^*_1 is a vector containing measured nodal values and u_2 is a vector containing unknown nodal values. F_1 and F_2 are known nodal force vectors, and K_{ij} 's [i= 1,2; j= 1,2] are partitioned global stiffness matrix elements. Note K_{ij} 's are functions of unknown material parameter vector, p'. Eliminating u_2 out through reduction, we get

$$[K^*]\{u^*\} = \{F^*\} \tag{3}$$

where

$$[K^*] = [K_{11} + K_{12}K_{22}^{-1}K_{21}]$$

$$\{u^*\} = \{u_1^*\}$$

$$\{F^*\} = \{F_1 - K_{12}K_{22}^{-1}F_2\}$$

In equation (3) only unknowns are p_i s contained in the elements of matrix [K*]. An iterative scheme or a least square optimization scheme can be used to solve equation for unknown material parameters. This inverse technique is quite sensitive to experimental error and may not converge at all in some cases[35,40,42]. The direct approach results in more accurate parameter values. In the direct method, nodal values of the response are computed using a finite element method for a set of assumed parameter values. These responses are a function of assumed parameter vector ($\underline{p}$), say $u(\underline{p})$. The actual values of response at the same nodes can be obtained by field or in-situ tests. If u^* is corresponding observed response to $u(\underline{p})$ then $e_i=(u^*_i - u(p)_i)$ is a measure of error in the i^{th} value. A suitable objective function such as $\phi=\Sigma e_i^2$ can be optimized using a nonlinear optimization technique[35,40,42]. The direct search methods such as simplex method or its modification such as Rosenbrock's version or gradient based methods such as conjugate gradient method or quasi-Newton method can be successfully used depending on the

application[26,32,43]. Nodal displacement values are usually better than stress values in parameter identification[32,35,36]. Moreover, it is preferable to map all the parameters to same range through scaling[32]. Even in the case of simple linear elastic constitutive model, the objective function, ϕ will be a nonlinear function of material parameter vector, $\underline{p}$. Because of this situation, the objective function, ϕ may have several local minimas[43]. Therefore, the optimal solution may be sensitive to initial guess values. Sometimes different combination of two or more parameters may lead to same response[non-unique solution][43]. More than one type of test or tests using different geometry and/ or loads may be helpful in such cases. Bayesian approach and Kalman filtering have been found to be helpful in improving the accuracy of results in the presence of experimental errors[27,33,40]. The direct method can be computationally very expensive since at each iteration a new FEM analysis with updated parameter vector($\underline{p}$) needs to be carried out[42].

Rubinstein, Upadhyaya, and Sime[44] proposed a new methodology which utilized orthogonal regression technique to develop a response surface in the parameter space based on an analytical or numerical (such as a finite element analysis) solution to the system differential equation. This response surface was used in the optimization step. Their methodology consists of following steps:

1. A response surface is built using an orthogonal regression technique based on an analytical or numerical solution to the governing differential equation of the system. The response surface will be a function of unknown material parameters.

2. This response surface is updated using higher order corrections so that the response surface behavior is close to the real surface behavior everywhere in the parameter space. This response surface will be used to predict the response corresponding to the experimental values(i.e. at the same load and nodal point).

3. Experimental results are transformed such that the real surface and the response surface will have one-to-one correspondence everywhere in the region.

4. Experimental results are optimized against the response surface predictions to obtain material properties of the test material.

The proposed technique is particularly useful in dealing with complex problems which require numerical solution such as a FEM solution to the underlying system differential equation. The main advantage of this technique is that once the response surface is created using an FEM analysis, there is no need to go back to the FEM analysis. In the classical direct or indirect approach, hundreds or even thousands of time consuming and expensive FEM evaluations are necessary to determine material parameters through optimization technique. In this methodology during the optimization technique only the response surface is used to estimate $u(\underline{p})$. This approach is expected to make this technique computationally very efficient. These in-situ soil properties can be used in subsequent model studies based on constitutive relationships which utilize these soil parameters. In fact, the methodology is quite general and can be used in other fields to estimate constitutive equation parameters based on in-situ measurements.

MATHEMATICAL MODELING

Response Surface Development:

Let us consider a general material constitutive model for soil (or any other material) consisting of m parameters: $p_1, p_2, p_3, \ldots, p_m$. For example, if we select a nonlinear constitutive model with extended Drucker-Prager yield criteria and associated flow rule, then six parameters will be involved[45,46]. These parameters are p_1=logarithmic bulk mod κ; p_2= Poisson's ratio, υ; p_3=yield surface shape factor(i.e. related to the third invariant of stress), K; p_4=cohesion, c; p_5= internal angle of friction, ϕ; p_6=initial void ratio, e. The last parameter, e is really related to initial stress condition. The response of a system to applied load depends on its geometry, material properties and the load itself. If the applied load and the geometry are fixed(i.e. for a given geometry and loading), the system response is a function of material constants used in the constitutive equation. There is a function $\Phi=\Phi(p_1, p_2, p_3, \ldots, p_m)$ which represents the system response as the material properties used in the constitutive equation are changed. In most real situations the differential equation describing the response is nonlinear, this function is seldom known explicitly. One of the goals of this study is to find an approximate representation for this real response, Φ. This approximation to the real response is termed the response surface, F in this study. One convenient way of determining the response surface F is to determine the variation of F as one of the material parameter, p_i is changed while all other parameters are held constant. Let this response function for the single variable p_i be $f_i(p_i)$. If we repeat this process for each of the m material parameters(i.e. for i=1,2 ....., m), then one easy way of obtaining the response surface is simply to multiply these component equations, $f(p_i)$, i.e.

$$\Phi \equiv F = C f_1(p_1) f_2(p_2) f_3(p_3) \ldots\ldots f_m(p_m) \qquad (4)$$

where
F = response surface
f_i = a component equation which is a function of parameter p_i only.
C = constant.
Note that this type of solution is often sought in the solution of linear partial differential equations and is known as separation of variables. For example, in the case of a circular plate placed on a linear elastic medium and subjected to a uniformly distributed load, the real response, Φ is given on page 350 of Das[47] as

$$\Phi = 1.58\, qb \frac{1-\upsilon^2}{E} \qquad (5)$$

where

Φ = the plate sinkage.
E = Young's Modulus, $E=p_1$.
υ = Poisson's ratio, $\upsilon=p_2$.
q,b = constants (respectively, uniformly distributed load and plate radius).

Equation (5) is a multiplication of two functions of the parameters, p_1=E and $p_2=\upsilon$, i.e., $f_1=1/E$ and $f_2=(1-\upsilon^2)$. Therefore, in this case the response surface, F can be represented by a multiplication of the component equations as we assumed in equation (4). However,

in general such a representation is accurate only in a small region due to geometric and/or material nonlinearities in the system. The error is expected to be small if the range of p_i is small for each of the m parameters.

Thus the process of building the response surface requires holding all relevant factors except parameter p_i constant(i.e. geometry, loading, all other material properties p_j, j=1,2 .... m but j≠i) and determining the component equation $f(p_i)$. Once all the component equations are determined, equation (4) can be used to build the response surface. It should be recognized that for each given geometry and loading there will be one response surface. In the case of plate sinkage tests, for a given plate size and load level there will be a response surface. Since there are m unknown parameters, at least m field measurements are needed to solve for these m parameters. In practice, it is preferable to have more than m points(i.e. n>m) so that the m parameters can be determined with the help of an optimization algorithm. Since each unreplicated in-situ measurement corresponds to a given geometry and loading, each of these experimental values correspond to a point(or contour) on one response surface. Thus each of the n unreplicated measurements will correspond to a point(or contour) on one of the n distinct response surfaces. Note that more than one observations at a given geometry and loading refer to the same point (or contour)on a response surface that corresponds to that geometry and loading. Thus replicates do not provide additional equations to solve for the parameters, but help in controlling experimental error. Upadhyaya et al.[48] suggested that at least eight replicates to adequately deal with the spatial variability in the case of in-situ plate tests. Suppose we have n distinct combination of geometry and load level there will be n response surfaces, F_i, i=1,2 .....n. From equation (4) we get

$$\begin{aligned} F_1 &= C_1 f_{11} f_{12} \ldots f_{1m} \\ F_2 &= C_2 f_{21} f_{22} \ldots f_{2m} \\ &\cdot \\ &\cdot \\ &\cdot \\ F_n &= C_n f_{n1} f_{n2} \ldots f_{nm} \end{aligned} \qquad (6)$$

where f_{ij} is the component equation corresponding to response i and parameter p_j and C_i is the constant corresponding to the same response surface i.
Since each of the material parameter has its own range, some properties such as Poisson's ratio, υ vary in a very narrow range (0.0 to 0.5) whereas others such as Young's modulus, E may vary over a very large range(thousands of kPa). From the point of optimization as well as orthogonal regression, it is preferable to map each of the parameter to the same range through scaling[32,49]. Each of the unknown parameter was nondimensionalized and mapped to vary from -1 to +1 by the following transformation:

$$p_i' = \frac{2(p_i - \bar{p}_i)}{p_{i\,max} - p_{i\,min}} \qquad (7)$$

where:

p_i' = nondimensional value of parameter i.

$\bar{p}_i$ = mid point value of parameter i.

$p_{i\,max}$ = upper bound value of parameter i.

$p_{i\,min}$ = lower bound value of parameter i.

The value of the mid point is zero, upper bound is 1 and the lower bound is -1 for each of the nondimensionalized parameter.

Let f'_{ij} be the nondimensionalized component equation corresponding to the nondimensionalized parameter p'_j and test condition i. The relationship between f'_{ij} and f_{ij} is given by

$$f'_{ij} = \frac{f_{ij}}{\bar{F}_i} \tag{8}$$

where

$\bar{F}_i$ = computed value of the response surface F_i for test i when all the parameters are set equal to the mid point value of zero.

Moreover, it is convenient if we nondimensionalize the system response to avoid numerical problems in the analysis. The nondimensionalized response surface is given by:

$$F'_i = C'_i f'_{i1} f'_{i2} \ldots f'_{im} \qquad i=1,2,3,\ldots,n \tag{9}$$

Where

F'_i = nondimensionalized response surface values corresponding to the i^{th} test condition,
C'_i = correction constant, approximately equal to 1.

The data for the creation of response surfaces can be obtained from any analytical or numerical models. We propose to use an orthogonal regression technique to determine the component equation f'_{ij}. The use of an orthogonal regression technique not only provides an equation to accurately predict the overall system response, but also provides an accurate estimate of regression parameters[49,50,51]. An accurate estimation of regression parameters is essential in order to identify the unknown material parameters by optimization. The function f'_{ij} is an orthogonal polynomial of parameter p'_j and is given by:

$$f'_{ij} = \sum_{r=0}^{k} a_{ir} p'^{r}_{j} \tag{10}$$

The values of a_{ir} ,r=1,2 .....k are determined by using model response (analytical or numerical such as FEM) and orthogonal regression techniques. Only requirement for the use of orthogonal regression in curve fitting is that p'_j be equally spaced during model evaluation while all other material parameters be held at the mid point values. The theoretical value of the correction constant, C'_i in equation(9) is one. However, when curve fitting is employed to determine the regression coefficients,a_{ir}, the value of this correction constant may be slightly different than one. The actual value of C'_i can be found by a employing linear regression technique between F'_i and $(f'_{i1} f'_{i2} \ldots f'_{im})$. To accomplish this linear regression, model response at orthogonal points used in building the response surface and some additional random points may be used.

Higher Order Correction:

As stated previously, in general the orthogonal response surface is expected to be close to the true model response only near the mid point and the parameter axes(p'_i axis). As we

start moving away from the origin or the parameter axes, the two surfaces will depart from each other. At large distances from the origin and the parameter axes this error can be significant. The relation between the nondimensionalized true response, Φ'_i and the response surface, F'_i is given by:

$$\Phi'_i = F'_i + \varepsilon_i \tag{11}$$

where ε_i is the error in our approximation ,$\Phi'_i \cong F'_i$.

By assuming that the function Φ'_i is "well behaved"(i.e. analytic everywhere in the parameter space),this function can be represented in a Taylor series as follows:

$$\Phi'_i = 1 + b_1 p'_1 + b_2 p'_2 + \ldots + b_m p'_m + b_{11} p'^2_1 + b_{12} p'_1 p'_2 + \ldots + b_{1m} p'_1 p'_m + b_{111} p'^3_1 + b_{112} p'^2_1 p'_2 + \ldots + b'_{11m} p'^2_1 p'_m + b_{123} p'_1 p'_2 p'_3 + \ldots + b_{12m} p'_1 p'_2 p'_m + \ldots \tag{12}$$

where coefficients,b_i, b_{ij}, b_{ijk}, etc. for i=1,2, ...m; j=1,2 ....m; k=1,2,.....m are respectively related to the partial derivatives of the function, Φ'_i with respect to p'_i, $p'_i p'_j$, $p'_i p'_j p'_k$ etc. at the origin(mid point). Equation (12) reduces to f'_{ij} along p'_j axis. i.e.

$$f'_{ij} = 1 + b_j p'_j + b_{jj} p'^2_j + b_{jjj} p'^3_j + \ldots \tag{13}$$

Using equations (9), (11), (12) and (13) we get,

$$\varepsilon_i = d_{12} p'_1 p'_2 + \ldots + d_{1m} p'_1 p'_m + d_{23} p'_2 p'_3 + \ldots + d_{2m} p'_2 p'_m + \ldots + d_{112} p'^2_1 p'_2 + \ldots + d_{11m} p'^2_1 p'_m + d_{123} p'_1 p'_2 p'_3 + \ldots \tag{14}$$

where "d" s are constant coefficients related to the cross derivatives of Φ'_i at the origin. It should be noted that strictly from a theoretical point of view, an orthogonal response surface can be created based on equation (12) rather than equation (9) which relies on the product of component equations. In such a case, very little difference is expected between the real surface and orthogonal response surface. If nine equidistant values of each of the parameter p'_i, i=1,2, ...,m are used in evaluating real surface, 9^m model evaluations will be needed. If m=2 then 81 model evaluations are needed. On the other hand, if m=6, then an astronomical 531441 model evaluations are necessary. In most real problems, where FEM evaluation of a complex model is necessary, using equation (12) as a basis for the response surface is infeasible except for the case of a two parameter model. The response surface represented by equation (9) requires only [8*m+1] model evaluations(i.e. for m=2, 17 model evaluations are necessary whereas for m=6, 49 model evaluations are necessary).

Second Order Correction:

In practice, equation (14) will be truncated at some convenient point. The truncated function is an approximation to ε_i and is called the correction function,E_i . If we limit ourselves to only the product of the type $p'_i p'_j$ for i=1,2, ...,m and j=1,2, ...,m, but $i \neq j$, then E_i will be a second order function. This second order function, E_i contains $n_{c\,min}$ unknowns given by :

$$n_{c\,min} = \frac{m(m-1)}{2} \tag{15}$$

In order to determine the second order correction function, E_i model responses are obtained at n_c additional check points, where n_c is greater or equal to $n_{c\,min}$. The additional check points can be selected randomly or in a deterministic way. It can be shown that the form of the second order correction is:

$$E_i = \sum_{j=1}^{m-1} \sum_{k=j+1}^{m} e_{i,\frac{(j-1)(2m-j)}{2}+k-j} p'_j p'_k \tag{16}$$

The "e" coefficients can be derived from a set of n_c linear equations with $n_{c\,min}$ unknowns. A multiple linear regression technique based on equation(16) can be used to estimate the "e" coefficients. Modification to the response surfaces can be accomplished by adding equation (16) to equation (9). The resulting improved response surface is given by:

$$F_i = C_i f_{i1} f_{i2} \ldots f_{im} + E_i \qquad i=1,2,3,\ldots,n \tag{17}$$

It is important to emphasize that the second order correction neglects all higher orders of ε_i. There may be some situations where these higher order corrections are necessary. In such cases, it is possible that the second order correction may even give poorer results than not including any corrections. In situations like these, use of equation (9) may give more accurate results than equation (17). More discussion on this important issue will follow when we consider examples.

Third Order Correction:

In order to get more accurate results to the function E_i, we should consider the higher order corrections. In this study we will limit ourselves to a third order correction. The third order correction consists of all cross product terms of the parameters upto and including the third order terms. The third order function E_i is the summation of n_{cmin} combination of cross products, therefore we have $n_{c\,min}$ unknown coefficients. It can be shown that the number of combinations, $n_{c\,min}$ is given by:

$$n_{c\,min} = \frac{3m(m-1)}{2} + \frac{1}{2}\left[\frac{(m-1)(m-2)}{2} + \sum_{j=1}^{m-2} j^2\right] \tag{18}$$

The function E_i for the third order correction is:

$$E_i = \sum_{j=1}^{m-1} \sum_{k=j+1}^{m} e_{i,\alpha(m,j,k)} p'_j p'_k + \sum_{j=1}^{m-2} \sum_{k=j+1}^{m-1} \sum_{l=k+1}^{m} e_{i,\beta(m,j,k,l)} p'_j p'_k p'_l + \sum_{j=1}^{m} \sum_{k=1}^{m} e_{i,\gamma(m,j,k)} p'^{2}_j p'_k (1-\delta_{jk}) \tag{19}$$

Where:

$$\delta_{jk} = \begin{cases} 1 & j = k \\ 0 & j \neq k \end{cases} \tag{20}$$

$$\alpha(m,j,k) = \frac{(j-1)(2m-j)}{2} + k - j \tag{21}$$

$$\beta(m,j,k,l) = \frac{m(m-1)}{2} + \frac{1}{2}\left\{\frac{j-1}{2}[2m(m-j-1)+j] + \sum_{r=1}^{j-1} r^2\right\} + \frac{k-j+1}{2}(2m-k+j-2) + l - k \tag{22}$$

$$\gamma(m,j,k) = \frac{m(m-1)}{2} + \frac{1}{2}\left[\frac{(m-1)(m-2)}{2} + \sum_{r=1}^{m-2} r^2\right] + (m-1)(j-1) + \delta \tag{23}$$

$$\delta = \begin{cases} k & k < j \\ k-1 & k > j \end{cases} \tag{24}$$

Once again, "e" coefficients can be derived from a set of n_c ($n_c \geq n_{c\,min}$) linear equations with $n_{c\,min}$ unknowns. A multiple linear regression technique based on equation (19) can be used to estimate the "e" coefficients. The modified response surface is given by equation (17).

Estimation of Material Parameters:

Let U_i be one of the n independent experimental observations. In order to make U_i consistent with F'_i, we transform it into a nondimensional value, U'_i. The relation between U_i and U'_i is given by:

$$U'_i = \frac{U_i}{\bar{F}_i} \tag{25}$$

The subtraction of equation (25) from equation (17) yields a set of n nonlinear equations in m unknowns.

$$\begin{aligned} F'_1 - U'_1 &= 0 \\ F'_2 - U'_2 &= 0 \\ &\cdot \\ &\cdot \\ &\cdot \\ F'_n - U'_n &= 0 \end{aligned} \tag{26}$$

In general equation (26) is seldom an equality due to the presence of approximation as well as experimental errors. One method of determining engineering properties of the material involves optimizing sum of squares of residuals, SSR defined by:

$$SSR = \min\left\{\sum_{i=1}^{n}(F'_i - U'_i)^2\right\} \tag{27}$$

The expression for the SSR in equation(27) is used as an objective function and a nonlinear optimization technique is used to solve for material parameters. Since F'_i is an approximation to Φ'_i, and F'_i can be obtained from equation (9) which corresponds to the original orthogonal response surface or equation (17) which includes higher order correction, we can get different solutions in the vicinity of the real solution depending on which expression for F'_i is used. The SSR of these solutions is of the same order, thus the minimum value of the SSR does not necessarily indicate the best solution. Of course, the best solution can be obtained from the sum squares of the residuals which uses Φ'_i in equation (27), i.e.

$$SSR^* = \min\left\{\sum_{i=1}^{n}(\Phi'_i - U'_i)^2\right\} \tag{28}$$

Where SSR* is the minimum residuals of the real response surfaces and the test results. It is recommended to use equation (28) at these different optimum solutions suggested by different versions of F'_i to obtain the best results. We will return to this question when we consider example problems.

Transformation of Experimental Results:

As explained previously, the accuracy of function F'_i may be high in some region on the response surface and low in another region. This implies that the estimated parameters will be high in accuracy sometimes and poor in accuracy some other times. Generally speaking, the inaccuracy increases as we move away from the origin and parameter axes. At the origin, the nondimensionalized F'_i has a value of unity[cf. eq. (9)]. In some sense, as the values of F'_i change from unity the difference between the real and the response surface values(both corrected and uncorrected) tend to increase. Thus the values of F'_i can be used as a measure of this departure. This argument suggests that there exists a function $\Phi'_i = \Phi'_i(F'_i)$. Inverse of this transformation, $F'_i = F'_i(\Phi'_i)$ is of particular interest in our case. This relationship can be used as a transformation rule for experimental values by replacing the real response, Φ'_i by experimental value, U'_i. If we denote the transformed experimental value which corresponds to F'_i by U^*_i, then we have $U^*_i = U^*_i(U'_i)$. The transformation function can be obtained by conducting a polynomial regression between F'_i and Φ'_i in some acceptable range, $\Phi_{i\,min}$ and $\Phi_{i\,max}$, thus:

$$F'_i = \sum_j g_j \Phi_i^{'j} \tag{29}$$

where "g_j" s are regression coefficients. The corresponding transformation rule for the experimental values is given by:

$$U_i^* = \sum_{j=0}^{k} g_j U_i^{'j} \tag{30}$$

The value of U^*_i calculated from equation (30) can be used for replacing U_i in equation (26) and (27). This modification may significantly improve the accuracy of the parameters obtained through optimization. We will explore this aspect in more detail when we consider the example problems.

COMPUTER IMPLEMENTATION OF THE MODEL:

A FORTRAN program was developed to implement this inverse solution technique to estimate material parameter values. This task involves several steps as shown in figure 1. An interface program is used to transform the analytical or numerical results to a format accepatable to our inverse solution program. The inverse solution program uses model response (either analytical or numerical such as FEM analysis) for the creation of the orthogonal response surface. Higher order correction are implemented on to this orthogonal response surface in the next step. Following this expeimental data are input and a transformation is performed on these data to relate them to response surface points. In the last step, an optimization procedure is carried out to obtain the best estimates of the values of material parameters. This program allows for selection of any one of the following optimization subroutines called from IMSL library:

1. Nonlinear least squares techniques,
2. Complex algorithm,
3. Quasi-Newton method,
4. Modified Newton Method,
5. Conjugate Gradient Method.

CASE STUDIES:

Two Parameter Model:

A simple two parameter material model is selected to illustrate the main features of this technique. A cylindrical bar or soil column under uniaxial compression is considered. The bar is made of a hypoelastic material with an incremental constitutive law given by(p 139,Desai and Siriwardane [17]):

$$d\sigma = (E_0 + E_1\sigma)d\varepsilon \tag{31}$$

where E_0 and E_1 are the material parameters of interest in this model, σ is axial stress(positive in compression), and ε is axial strain. Integration of equation (31) yields:

$$u = \frac{L}{E_1} \ln\left(\frac{E_0 + E_1\sigma}{E_0}\right) \tag{32}$$

where:

u = deformation of the bar (the contraction).
L = length of the undeformed bar.
Equation (32) will be used as a basis to build the response surface, F'_i. The response surface will be developed in the following range of parameters E_0 and E_1:

$E_{0\ min}$= 689.5 kPa (100 psi) $E_{0\ max}$= 6894.8 kPa (1000 psi)
$E_{1\ min}$= 10.0 $E_{1\ max}$= 100.0
$E_{0\ mid\ point}$=3792.1 kPa (550 psi) $E_{1\ mid\ point}$= 55.0

The nondimensional parameters (equation 7) for this case are:

$$E_0' = \frac{2(E_0 - E_{0\ \text{mid point}})}{E_{0\ \max} - E_{0\ \min}} \quad \text{and} \quad E_1' = \frac{2(E_1 - E_{1\ \text{mid point}})}{E_{1\ \max} - E_{1\ \min}} \tag{33}$$

The response at the mid point of the parameters is(i.e. origin):

$$\bar{F}_i = \frac{L}{E_{1\ \text{mid point}}} \ln\left(\frac{E_{0\ \text{mid point}} + E_{1\ \text{mid point}}\sigma_i}{E_{0\ \text{mid point}}}\right) \tag{34}$$

The nondimensional representation of the real surface is obtained by dividing equation (32) by equation (34). The plot of the nondimensionalized real surface obtained by using an applied stress of σ= 689.5 kPa(100 psi), is given in Fig. 2. The approximation of the surface without any higher order correction is shown in Fig. 3, and the error of this approximation is shown in Fig. 4. The response surface describes the real function with reasonable accuracy except at the corners. The error is particularly high as both parameters (E_0 and E_1) approach their minimum values. The response surface for this case which includes second order correction is:

$$F_i' = f_1'(E_0')f_2'(E_1') + e_i E_0' E_1' \tag{35}$$

where f_1' and f_2' are orthogonal polynomial functions of E_0' and E_1' respectively and e_i is second order correction coefficient . The function f_1', f_2' and the coefficient e_i were found as described previously.

The second order correction for this case was obtained by using the edge points, the mid points of the lower and upper range for each parameter - a total of 16 combinations. The response surface with second order correction is shown in Fig. 5, and the difference between the real values and the response surface values is plotted in Fig. 6. The second order correction decreases the error in the zones of high error (e.g. in the region near the minimum values of E_0 and E_1). However, this correction to the response surface increased the error in some other regions where the error was negligible previously. The basic assumption of the second order correction is that all higher order(third order and higher) cross products are negligible. In this particular example, the plot of the error shown in Fig. 4 indicates a high curvature in a small region [in fact only about 3% region] where both parameters approach their minimum values. Thus, second order correction does not represent the error properly everywhere in the region.

Effect of including the third order correction (TOC) was also examined for this two parameter case. The form of the third order correction is:

$$E_i = e_{i1}E_0E_1 + e_{i2}E_0^2E_1 + e_{i3}E_0E_1^2 \tag{36}$$

Figure 7 shows the effect of including third order correction on the response surface. Inclusion of third order correction further reduces the error in the zone of high error (i.e. in the 3% region where E_0 and E_1 values are near or at their minimum). Figure 8 is a plot of

error when the third order correction is included. Comparison of this figure with figures 4 and 6 shows that although the response surface which includes third order correction reduces the error in the zone of high error , the error in other regions does not necessarily decrease. In fact, the error increases slightly in some areas.

In order to determine the material parameters(E_0 and E_1), seven different resoponse surfaces were created using seven different applied stresses. The stress values used were 344.7 kPa (50 psi), 517.1 kPa (75 psi), 689.5 kPa (100 psi), 861.8 kPa (125 psi), 1034.2 kPa (150 psi), 11206.6 kPa (175 psi) and 1379.0 kPa (200 psi). The adequacy of the method is illustrated by 12 examples. Table 1 lists the parameter values selected for the simulation purpose. The first set of parameter values are randomly selected. The other eleven examples are based on parameter values along the diagonal, $E'_0=E'_1$. The equation (32) was used to calculate the real response. These values were used instead of the experimental values in the optimization step. Since there is no experimental error in this case, we should, in principle, get exact values of the assumed parameters back. Inaccuracy in the results is solely due to the inadequacy of the response surface. Five different initial guess values of the parameters were considered in the nonlinear optimization process for each one of these examples. The first initial guess values were the mid point values of the parameters, three others were selected randomly and the fifth one was the exact solution.

The transformation equation was estimated using 50 random points of the real surface using equation (29) as a basis for regression.

Example 1: E_0 and E_1 were selected randomly:

The values of the simulated parameters were : E_0= 5666.1 kPa (821.8 psi) and E_1=61.8. The nondimensionalized real function value at an applied pressure of 689.5 kPa (100 psi) is 0.80. The results of optimization are listed in Table 2.

Note that both uncorrected response surface and respose surface with third order correction resulted very good solutions with negligible errors. However, the second order correction yielded relatively poorer results. When the transformation based on equation(30) was employed, all three correction methods yielded reasonably good results (Table 3). Transformation technique significantly improved the parameter estimation for the case in which no correction was employed. This transformation was beneficial in reducing error for the second order correction technique also, particularly at low parameter values. However, the transformation technique was not quite as beneficial in the case of the third order correction method. Even in this case the error in estimation of the parameters were reduced slightly. Thus, in general transformation technique leads to more accurate parameter estimation.

It should be noted that this particular soil model shows large increases in response when E_0 and E_1 values are very small compared to all other values of E_0 and E_1. This portion of the graph corresponds to only 3% of the parameter range (low values of the parameters). This makes it difficult to generate a response surface which is good everywhere in the region. Higher order corrections tend to predict the response better in this region. In so doing, they become less accurate in other regions - especially at large values of the parameters (see Figs. 3 through 8). This is an unusal situation which resulted in the uncorrected surface to generally estimate parameter values more accurately than when the third order correction was employed along with the transformation technique. In a well behaved system (i.e. no singularities or large increases in responses for small changes in parameter values) the method which employs third order correction is

expected to yield more accurate parameter valves. In fact, even very complicated models do not show such singularities or large changes in a small region as we will see with a five parameter Drucker-Prager model described below.

A Five Parameter Nonlinear Elastic Soil Model with Extended Druker Prager Yield Criteria:

The elasto-plastic constitutive material model with Druker-Prager yield criteria is widely used in geomechanics[45,46]. We assume that in-situ tests consist of plate penetration tests using circular plates. Here we will not consider the actual field data. Analysis of the field data to identify material parameters will be dealt later. We explore the feasibility of the proposed methodoiogy in this example for this fairly complex material model. A commercial finite element program, ABAQUS was used in this study to obtain model response. The orthogonal response surfaces were built using six parameters κ,υ,K,C,ϕ and e.

Two plates of diameters 50 mm(2 in.) and 100 mm (4 in.) were simulated, with applied load ranging from 137.9 kPa(20 psi) to 1034.2 kPa (150 psi) in increments of 68.9 kPa(10 psi), a total of 14 tests for each plate. A response surface was built for each of those tests in the following parameter range:

κ_{min}= 0.01	κ_{max}= 0.10	$\kappa_{mid\ point}$= 0.19	No. of points= 9
υ_{min}= 0.05	υ_{max}= 0.37	$\upsilon_{mid\ point}$= 0.21	No. of points= 9
K_{min}= 0.60	K_{max}= 1.0	$K_{mid\ point}$= 0.8	No. of points= 11
C_{min}= 9.0	C_{max}= 21.0	$C_{mid\ point}$= 15.0	No. of points= 9
ϕ_{min}= 22.5	ϕ_{max}= 47.5	$\phi_{mid\ point}$= 35.0	No. of points= 11
e_{min}= 0.6	e_{max}= 1.6	$e_{mid\ point}$= 1.1	No. of points= 11

A typical plot of the non-dimensional sinkage as a function of non-dimensional values of parameter κ for a 100 mm (4 in) plate subjected to 551.6 kPa pressure (80 psi) is shown in Fig. 9. Note that all other parameters are held constant at their corresponding midpoint values. Figures 10 through 14 are similar plots except that the dependent variable has been changed to υ, K, C, ϕ, and e respectively. These curves show an extremely good fit between the real response curve and the response curve obtained by the orthogonal regression (R^2 >0.997 for all cases).

The graph of the real surface versus the orthogonal response surface without any correction for a 100 mm (4 in.) plate subjected to an applied load of 103.4 kPa (15 psi) is shown in Fig. 15. This graph consists of 55 orthogonal points and an additional 60 random points. Figure 16 is similar to Fig. 15 except that the applied load is 551.6 kPa (80 psi) in this case. When the applied pressur low, soil deformation is small and the soil medium behaves similar to elastic materia in fact, in our case soil is modeled as nonlinear elastic but if displacements are small even nonlinear behavior can be approximated by linear behavior). In this case the real surface and orthogonal surface are almost identical (Fig. 15). As the load is increased, soil will yield and subsequent plastic

flow will take place as per the assumed model. Figure 16 reveals that under high load the orthogonal response surface begins to depart from the real surface when non-dimensionalized displacements are below 0.5 or exceed 1.5. Figures 17 and 18 are similar to figures 15 and 16 except that a second order correction has been added to the orthogonal response surface. These figures indicate that there has been only marginal improvements in these curves (especially Fig. 18). Perhaps a higher order correction is beneficial especially at high plate loads. Figures 19 and 20 are similar to figures 15 and 16 (also 17 and 18) respectively, except that a third order correction has also been added to the orthogonal response surface. Inclusion of third order correction has resulted in an orthogonal response surface which is almost identical to the real surface even at high loads. This indicates that an orthogonal response surface with third order correction can be used reliably to predict the real response without having to resort to FEM analysis.

Parameter Estimation:

Since we are dealing with a nonlinear problem the solution is not necessarily unique. Following recommendations may be used as a guide for selecting the best solution from several optimum solutions resulting from the presence of "local minimums":

1. Discard all solutions that have a significantly high SSR (cf. equation 27).

2. Use more than one geometry (i.e. 50 mm and 100 mm diameter plates) and look for optimum for each of the geometries and also the combination of all the geometries. Accept those solutions which are approximately same in all cases. From a practical point of view two plates will be sufficient.

3. Reject any solution in which more than one parameters hit the bounds of the search domain. The probability of more than one parameter hitting the bounds simultaneously is low. If in fact, if this really is the case for several initial guesses, and the above two criteria will be met.

4. In spite of these steps, if more than one optimal solutions are obtained, we recommend the use of equation (27) to compute SSR. If the response surface with higher order corrections has been properly verified as good (i.e. using figures such as 19 and 20 described earlier), then the solution which yields the minimum SSR should be accepted as the best solution. If possible one could use equation (28) to compute SSR* to provide additional verification. Although, such an approach is preferable, evaluation of equation (28) requires some limited FEM analysis (i.e. one for each plate for each competing solution).

To explore the suitability of this method to identify the material parameters of this complex constitutive equation for soil, we selected five different random sets of parameters and conducted simulation studies to obtain true response. Subsequently, these true responses were used as inputs into to the response surface methodology to re-predict those parameters. Since third order correction (TOC) to the orthogonal response surface appears to be necessary to obtain reasonable results, we will only explore the situation in which TOC is added to the orthogonal response surface. We chose five different random sets of parameter values to be re-predicted using the optimization technique. These random sets of points are as follows:

Point #1:	κ=0.127	υ=0.132	K=0.938	C=19.406	ϕ=26.984	e=0.630
Point #2:	κ=0.011	υ=0.343	K=0.611	C=16.813	ϕ=31.305	e=0.755
Point #3:	κ=0.056	υ=0.146	K=0.946	C=16.512	ϕ=28.985	e=1.095
Point #4:	κ=0.022	υ=0.093	K=0.776	C=13.893	ϕ=41.297	e=1.049
Point #5:	κ=0.083	υ=0.233	K=0.884	C=16.867	ϕ=34.856	e=1.123

The initial guess values selected were the "exact solution", "mid point values" and a set of five randomly selected parameter values listed below:

Point #6:	κ=0.356	υ=0.238	K=0.889	C=10.791	ϕ=34.579
Point #7:	κ=0.131	υ=0.297	K=0.996	C=45.693	ϕ=23.932
Point #8:	κ=0.039	υ=0.116	K=0.889	C=16.271	ϕ=30.728
Point #9:	κ=0.110	υ=0.088	K=0.610	C=20.472	ϕ=23.566
Point #10:	κ=0.014	υ=0.360	K=0.907	C=16.979	ϕ=23.778

The re-prediction process was carried out using 50 mm (2 in.) plate, 100 mm (4 in.) plate and a combination of 50 mm (2 in.) and 100 mm (4 in.) plates. For each case we used the exact solution and the mid point as initial guesses. The five randomly selected guess points were used only for point # 1 for both plates and also the combination of plates. However, for the 100 mm (4 in.) plate all seven initial guess values were use to seek the optimum solution for each of the five random set of parameter values.

The results of this analysis are listed in Table 4. An examination of the results indicates that the reasonable solution with minimum SSE usually leads to good solution except for point #4. Point #4 results in very large errors for both parameters κ and υ. However, an examination of SSE indicates that none of the solutions is reasonable. Our suspicion is that for this values of κ and υ, the soil is extremely hard and deforms very little. Under these circumstances, the nonlinear elastic model for soil with Drucker-Prager yield criteria is perhaps inappropriate.

DETERMINATION OF IN-SITU SOIL PROPERTIES:

Field tests were conducted during November, 1991 and September, 1992 using our instrumented soil-test device in a Yolo loam soil in the vicinity of the U.C. Davis campus. In November 1991 tests were conducted in an undisturbed soil using 50.8 mm (2 in.), 76.2 mm (3 in.), 101.6 mm (4 in.), 127 mm (5 in.), and 152.4 mm (6 in.) sinkage plates. When we conducted the field tests we were under the impression that more than one geometry (plate sizes) were necessary to obtain the engineering properties of soil by theinverse solution technique. However, later we found that this is not necessarily the

case. Even use of one plate size appears to be sufficient. In this study, field test results for 50.8 mm (2") and 101.6 mm (4") plates were only used to determine the engineering properties of soil by the inverse solution technique.

Eight replicates were obtained for each plate. Sinkage test data were analyzed using Recee's approach, i.e.

$$p = k\,(z/r)^n \qquad (37)$$

where

p = applied pressure
k = sinkage constant
z = soil sinkage
r = plate radius
n = empirical constant.

Table 9 lists the mean values of sinkage coefficients for each of the plate tested. The values of k and n for the 50.8 mm (2") and 101.6 mm(4") plate were used in estimating mean field response corresponding to a desired pressure for a given plate during the optimization process to "identify " soil parameters.

Soil shear tests were conducted using two different grouser plates [Plate #1: 203 mm long x 76 mm wide, and Plate #2: 178 mm long x 86 mm wide]. Each plate was tested at two different vertical loads and each test was replicated three times. Grouser plate test results were analyzed using the following equation:

$$\tau = [c + p * \tan(\phi)](1 - e^{-\frac{j}{K}}) \qquad (38)$$

where

τ = shear stress, kPa
c = cohesion, kPa
p = pressure on the plate, kPa
ϕ = soil internal friction angle
j = shear deformation, mm
K = shear modulus, mm

A nonlinear regression technique was employed to fit the data to equation (38) and obtain shear parameters. Maximum shear stress, τ_{max} for each test was calculated using the following equation:

$$\tau_{max} = c + p * \tan(\phi) \qquad (39)$$

The analysis of the experimental data resulted in a mean value of cohesion of 11.5 kPa and soil internal friction angle of 32.9 deg. for these tests.

Cone index, bulk density and moisture content data were also obtained in the test site. Eight replicates of cone index profiles were obtained in the top 152.4 mm (6") layer. The cone index values were averaged over the depth to get a representative cone index value for each location. Subsequently, all eight replicates were averaged to get a mean cone index value for this particular soil condition. Five bulk density and moisture content data were also obtained in the test site. Average cone index value was 816 kPa, dry bulk density was

1510 kg/m^3, and moisture content was 8.9% (dry basis). The void ratio was 0.755 based on a particle density of 2650 kg/m^3.

During September, 1992 only three sinkage plates were used for sinkage tests. Two distinct soil conditions (undisturbed and tilled/loose) were included in these tests. Once again eight replicates of sinkage tests were obtained for each plate and analyzed using equation (37). Sinkage parameters for the undisturbed and tilled soil conditions of the November 1992 tests are also listed in Table 5. Once again, the mean sinkage parameters corresponding to 50.8 mm (2") plate and 101.6 mm (3") plate were used in estimating field response for identifying Engineering parameters of soil.

Shear test procedure as well as data analysis techniques were similar to the procedure employed in analyzing the November, 1991 shear tests. The mean value of cohesion for the undisturbed soil condition was 32.3 kPa, and the internal angle of friction was 27.2 deg. The corresponding values for the tilled soil was 22.7 kPa and 22.8 deg.

Moreover, soil bulk density, cone index and moisture content data were also obtained as described for the November 1991 tests. The undisturbed (also referred as firm) soil had a mean dry bulk density of 1510 kg/m^3, moisture content of 5. 14 % (dry basis), and an void ratio of 0.755. The loose or tilled soil had a dry bulk density of 1433 kg/m^3, 4.55 % moisture content (dry basis), and a void ratio of 0.851. The cone index data were inconsistent and were ignored for these soil conditions.

Table 6 lists the Engineering parameters of soil estimated from the optimization process which utilized the orthogonal response surface including the third order correction. Both the best results based on SSE and SSR, and reasonable results based on our search criteria are listed in Table 6 for all the three soil conditions. The best estimates of the cohesion and soil internal friction angle values listed in Table 6 do not agree with the corresponding values listed in Table 5, which are grouser shear test results. This agrees with our hypothesis that the grouser shear test provides geometry dependent soil parameters, but not the basic soil constitutive property. Only the 101.6 mm (4 in.) plate was used for "identifying" soil parameters through optimization. Figures 21 and 22 show the experimental and simulated sinkage for a 101.6 mm (4 in.) plate obtained using back-calculated soil parameters for September 1992 tests in an undisturbed soil (firm soil). These results indicate that the estimated soil parameters are very good. However, when these same parameters were used to compare the response of a 50.8 mm (2 in.) plate in the same soil condition poor agreement was found between experimental and simulated sinkage (Figs. 23). This plot indicates that the parameters predicted from 101.6 mm (4 in.) plate tests are unable (under predict) to predict the behavior of 50.8 mm (2 in.) plate in the field. Similar results were obtained in the other soil conditions tested also. We feel that this is due to the edge effect which is not included in our model. Use of an interface element at the soil-plate interface appears to be necessary. Since 101.6 mm (4 in.) plate is less susceptible to edge effect compared to the 50.8 mm (2 in.) plate, we feel the parameters estimated from a 101.6 mm (4 in.) plate are more reliable. We recommend using a large diameter plates in future tests.

CONCLUSIONS

Based on this study we reached the following conclusions:

1) A response surface methodology based on an orthogonal regression in the parameter space has been developed to "identify" , or "calibrate" engineering properties of any material based on in-situ tests. The orthogonal response surface was created from an

analytical or numerical(such as FEM) solution to the underlying differential equation of the system which utilizes these engineering properties in a constitutive equation. A transformation technique was developed to map the model response or experimental data on to the response surface.

2) The proposed methodology worked very well (i.e. very little error) in the case of a two parameter hypo-elastic model for soil. When the second order correction was included with a transformation of data very small errors resulted in parameter estimation. Inclusion of third order correction to the orthogonal response surface reduced the chance of large error in parameter values.

3) When this technique was used in the presence of random noise, the predicted parameters were found to be insensitive to the noise.

4) When this methodlogy was applied to a complex five parameter model for soil (nonlinear elastic behavior with Drucker-Prager yield criteria and associated plastic flow upon yield), it appeared to work reasonably well. A third order correction to the orthogonal response surface appears to be necessary to obtain reasonably good solution. When both the logarithmic bulk modulus (κ) and Poisson's ratio (υ) are low, soil becomes very rigid and the methodlogy will not yield a good solution. Under such circumstances, perhaps the soil model chosen is inappropriate.

5) The response surface methodology was successfully employed to "identify" engineering properties of soil based on field tests for different soil conditions in a Yolo loam soil. We suspect that edge effect makes the parameter prediction using field data corresponding to small plates such as 50.8 mm (2 in.) diameter plate inaccurate. Use of larger plates such as 101.6 mm (4 in.) plate is recommended to reduce this edge effect. Use of Teflon coated plate with beveled edges and slip elements at the plate edge in the model may also increase the accuracy of parameter prediction.

The proposed methodology has not only applications in geomechanics, but also in other areas such as biological engineering(plants and animal tissues, food products etc.) where non-destructive in-situ tests are the only means of obtaining accurate estimate of engineering parameters.

ACKNOWLEDGEMENTS

The financial support received from the Goodyear Tire and Rubber Co. and the Bi-National (United States-Israel) Agricultural Research Development [BARD] agency to conduct this study is gratefully acknowledged.

REFERENCES

[1] W. R. Gill and G. E. VandenBerg, Soil dynamics in tillage and traction. agriculture Handbook No. 316, U. S. Govt. Printing Office, Washington, D. C. 511p. (1968).

[2] S. C. Gupta and R. R. Allmaras, Model to assess the susceptibility of soils to excessive compaction. In Adv. Soil Sci., Springer Verlag, NY, p 56-100 (1987).

[3] S. C. Gupta and W. E. Larson, Modeling soil mechanical behavior during tillage, In P. Unger et al.(eds.), Symposium on predicting tillage effects on soil physical properties and processes. Am. Soc. Agro., Pub. #44, Madison, WI, p 151-178 (1982).

[4] H. M. Taylor and G. F. Arkin, Root zone modification: Fundamentals and alternatives, In G. F. Arkin and H. M. Taylor(eds.), Modifying the Root Environment to Reduce Crop Stress, ASAE Monograph #34, St. Joseph, MI. p 3-19 (1982).

[5] R. Q. Cannel and M. B. Jackson Alleviating aeration stresses, In G. F. Arkin and H. M. Taylor(eds.), Modifying the Root Environment to Reduce Crop Stress, ASAE Monograph #34, St. Joseph, MI. p 141-193 (1982).

[6] W. J. Chancellor , Compaction of soil by agricultural equipment, Div. of Agr. Ser., Univ. Cal., Davis, Bulletin, 53pp (1977).

[7] LAWR - Cooperative Extension, Water penetration in California soils, Tech. Rep., Joint Infiltration Committee, Dept. of LAWR, Univ. Cal., Davis, Davis, CA (1984).

[8] A. Hadas, D. Wolf and E. Rawitz, Zoning soil compaction and cotton stand under controlled traffic operations, ASAE Paper 83- 1042, ASAE St. Joseph, MI 49085 (1983).

[9] A. Hadas, D. Wolf and E. Rawitz, Residual compaction effect on cotton stand and yields, Trans. ASAE 28, 691-696 (1985)

[10] A. Hadas, W. E. Larson and R. R. Allmaras, Advances in modeling machine-soil-plant interactions. Soil and Tillage Res. 11, 349-372. (1988).

[11] H. D. Bowen, Alleviating mechanical impedance, In G. F. Arkin and H. M. Taylor(eds.), Modifying the Root Environment to Reduce Crop Stress, ASAE Monograph #34, St. Joseph, MI. p 141-193 (1982).

[12] A. Hadas and D. Wolf, Soil aggregates and clod strength dependence on clod size cultivation and stress load rates, Soil Sci. Soc. Am. J. 43, 1157-1164 (1984).

[13] D. Wolf and A. Hadas,Conventional versus controlled traffic and precision system for cotton, ASAE paper 83-1040, ASAE St. Joseph, MI 49085, (1983).

[14] D. Wolf and A. Hadas, Soil compaction effects on cotton emergence, Trans. ASAE, 27,655-659 (1984).

[15] R. L. Schafer, A. C. Bailey, C. E. Johnson and R. L. Raper, A rationale for modeling soil compaction behavior: An engineering mechanics approach, Trans. ASAE, 34(4), 1609-1617 (1991).

[16] C. S. Desai, Some aspects of constitutive models for geologic media. Third Int. Conf. on Numerical Methods in Geomechanics,Achen, p2-6, (1979).

[17] C. S. Desai and H. J. Siriwardane, Constitutive laws for engineering materials with emphasis on geologic materials. Prentice Hall Inc., Englewood Cliffs, NJ, 468pp (1984).

[18] W. F. Chen and G. Y. Baladi, Soil plasticity - Theory and implementation, developments in Geotechnical engineering 38, ELSEVIER, NY, 231pp, (1985).

[19] D. R. P. Hettiaratchi and J. R. O' Callaghan, Mechanical behavior of agricultural soils. J. Agr. Eng. Res. 25, 239-259 (1980)

[20] D. R. P. Hettiaratchi, A critical state soil mechanics for agricultural soils. Soil use and Management, 3(3), 94-105 (1987).

[21] J. M. Kirby, Measurements of the yield surfaces and critical state of some unsaturated agricultural soils, J. Soil Sci. 40, 167-182 (1989).

[22] A. C. Bailey, C. E. Johnson and R. L. Schafer, Hydrostatic compaction of agricultural soils. Trans. ASAE, 27(4), 952-955 (1984)

[23] A. C. Bailey and C. E. Johnson, A soil compaction model for cylindrical stress state. Trans. ASAE. 32(3), 822-825 (1989).

[24] R. L. Raper and D. C. Erbach, Prediction of soil stresses using the finite element method. Trans. ASAE. 33(3):725-730 (1990).

[25] R. L. Raper, C. E. Johnson and A. C. Bailey, Coupling normal and shearing stresses to use in finite element analysis of soil compaction. ASAE Paper No. 90-1086, ASAE, St. Joseph, MI 49085, (1990).

[26] G. Gioda, A numerical procedure for defining the values of soil parameters affecting consolidation, In Design Parameters in Geotechnical Engineering, British Geotechnical Society London, Proceedings of the 7th European Conference on Soil Mechanics and Foundation Engineering, Vol. I, p169-172 (1979)

[27] A. Asaoka and M. Matsuo, Bayesian approach to inverse problem in consolidation and its application to settlement prediction, Third Int. Conference on Numerical Methods in Geomechanics, Aachen, p115-123 (1979)

[28] A. Asaoka and M. Matsuo, an inverse problem approach to settlement prediction, Soils and Foundations, Japanese Society of Soil Mechanics and Foundation Engineering, 20(4),53-66 1980

[29] G. Gioda and G. Maier, Direct search solution of an inverse problem in elastoplasticity: Identification of cohesion, friction angle, and in-situ stresses by tunnel tests, Int. J. for Numerical Methods in Eng., 15,1823-1848 (1980)

[30] S. Leroueil and F. Tavenas, Pitfalls in back analysis, 10th Conference of Int. Soc. for Soil Mechanics and Foundation Eng., p285-290, (1981).

[31] G. Maier, F. Giannessi and A. Nappi, Indirect identification of yield limits by mathematical programming, Engineering Structures, 4(2), 86-98 (1982)

[32] K. Arai, H. Ohta and T. Yasui, Simple optimization techniques for evaluating deformation moduli from field observations, Soils and Foundations, 23(1),107-113 (1983).

[33] A. Cividini, G. Maier and Nappi, Parameter estimation of a static Geotechnical model using Baye's approach, Int. J. Rock Mechanics, 20(5), 215-226 (1983)

[34] P. T. Brown and J. B. Burland, Soil parameter evaluation from large scale loading tests, Symposium Int., Paris, p25-28 (1983)

[35] S. Sakurai and K. Takeuchi, Back analysis of measured displacement of tunnels, Rock Mechanics and Rock Engineering, 16, p173-180 (1983)

[36] K. Arai, H. Ohta and K. Kojima, Estimation of soil parameters based on monitored movement of subsoil under consolidation, Soils and Foundations, 24(4), 95-108 (1984)

[37] A. Asaoka and M. Matsuo, An inverse problem approach to multi-dimensional consolidation behavior, Soils and Foundations, 2491), 49-62 (1984)

[38] V. U. Nguyen, Back calculations of slope failures by the secant method. Special Notes, 34(3), 423-427 (1984)

[39] A. Cividini, G. Gioda and G. Barla, Calibration of geological material model on the basis of field measurement, Fifth Int. Conference on Numerical methods in Geomechanics, Nagoya, p1621-1627 (1985)

[40] G. Gioda, Some remarks on back analysis and characterization problems in geomechanics, Fifth Int. Conference in Geomechanics, Nagya, p47-61 (1985)

[41] G. Gioda, A. Pandolfi, and A. Cividini, A comparative evaluation of some back algorithms and their application to in-situ load tests, Second Int. Symposium on Field Measurements in Geomechanics, Sakukai(ed.) p1131-1144 (1988)

[42] A. Anandarajah and D. Agarwal, Computer-aided calibration of a soil plasticity model, Int. j. for Numerical and Analytical Methods in Geomechanics, 15, 835-856 (1991).

[43] Y. Ichikawa and T. Ohkami, A parameter identification procedure as a dual boundary control problem for linear elastic materials, Soils and Foundations, 3292), 35-44 (1992).

[44] D. Rubinstein, S. K.Upadhyaya, and M. Sime. 1994. Determination of in-situ properties of soil using response surface methodology. Accepted for publication in J. Terramechanics.

[45] D. C. Drucker and W. Prager, Soil mechanics and plastic analysis or limit design, Quarterly Appl. Mech., 10, 157-165 (1952).

[46] ABAQUS, Thoery Manual, Version 4.8, Hibbitt, Karlsson and Sorensen, Inc. (1989)

[47] B. M. Das, Evaluation of soil settlement, In Advanced soil mechanics, Ch. 6, Hemisphere Publishing Corporation, NY, p339-401 (1983).

[48] S. K. Upadhyaya, D. Wulfsohn and J. Mehlschau, An instrumented device to obtain traction related parameters, Accepted for publication in J. Terramechanics, (1992).

[49] G. W. Snedecor and W. G. Cochran, Curvilinear regression, In Statistical Methods, Ch. 15, Sixth ed., p447-471 (1967).

[50] J. L. Glancey and S. K. Upadhyaya, A testing procedure for agricultural implements, ASAE Paper No. 90-1542, ASAE St. Joseph, MI 49085, (1990).

[51] J. L. Glancey, S. K. Upadhyaya, W. J. Chancellor and J. W. Rumsey, Prediction of implement draft using an instrumented analog tillage tool, ASAE Paper No. 91-1065, ASAE St. Joseph, MI 49085, (1991).

Table 1. Parameter values used in the simulation studies

Sequence number	True parameters values		Nondimensional parameters values	
	E_0 (kPa)	E_1	E'_0	E'_1
1	5666.1	61.8	0.604	0.151
2	999.7	14.5	-0.9	-0.9
3	1310.0	19.0	-0.8	-0.8
4	1930.5	28.0	-0.6	-0.6
5	2551.0	37.0	-0.4	-0.4
6	3171.6	46.0	-0.2	-0.2
7	3792.1	55.0	0.0	0.0
8	4412.6	64.0	0.2	0.2
9	5033.2	73.0	0.4	0.4
10	5653.7	82.0	0.6	0.6
11	6274.2	91.0	0.8	0.8
12	6894.8	100.0	1.0	1.0

Table 2. Parameter values obtained through optimization for the cases when no correction was included as well as the case for which second order and third order correction were included

No.	Without correction			Second order correction			Third order correction		
	% error of E_0	% error of E_1	SSE x 10^{-3}	% error of E_0	% error of E_1	SSE x 10^{-3}	% error of E_0	% error of E_1	SSE x 10^{-3}
1	1.34	0.07	0.1810	13.88	0.66	19.312	0.95	1.48	0.3104
2	31.03	17.89	124.01	31.03	0.65	96.300	1.88	4.32	2.2190
3	42.65	5.32	184.74	18.62	5.34	37.538	17.13	3.30	30.417
4	17.55	1.84	31.156	1.34	2.56	0.8340	17.02	2.21	29.463
5	5.81	0.53	3.3998	3.83	1.12	1.1594	8.92	1.12	8.0740
6	1.19	0.14	0.1448	1.56	0.36	0.2569	2.38	0.37	0.5784
7	0.03	0.00	0.0001	0.03	0.00	0.0001	0.03	0.00	0.0001
8	0.71	0.03	0.0503	4.55	0.56	2.1033	1.85	0.44	0.3632
9	2.52	0.27	0.6448	14.98	17.23	52.147	1.01	1.74	0.4030
10	4.63	0.43	2.1586	28.31	19.59	185.15	3.06	0.15	0.9370
11	14.06	9.50	28.790	44.41	7.77	203.25	15.69	8.03	31.064
12	8.34	0.00	6.9556	66.85	0.00	446.88	25.21	0.08	63.575

Table 3. Parameter values obtained through optimization when transformation technique was employed

No.	Without correction			Second order correction			Third order correction		
	% error of E_0	% error of E_1	SSE x 10^{-3}	% error of E_0	% error of E_1	SSE x 10^{-3}	% error of E_0	% error of E_1	SSE x 10^{-3}
1	0.86	0.24	0.0798	1.98	0.33	0.4030	1.78	0.55	0.3456
2	4.09	2.83	2.4780	2.81	1.88	1.1470	0.56	0.09	0.0395
3	1.49	3.92	1.7567	2.79	0.09	0.7796	2.06	5.47	3.4132
4	5.48	2.83	3.8048	0.06	1.75	0.3060	9.12	4.33	10.202
5	4.59	2.39	2.6734	2.47	2.62	1.3003	5.98	2.49	4.1949
6	4.14	1.49	1.9347	2.01	0.71	0.4562	3.95	0.78	1.6195
7	0.27	0.14	0.0091	0.89	0.47	0.1014	4.35	0.50	1.9139
8	2.69	1.04	0.8321	2.45	0.69	0.6496	9.73	0.65	9.5151
9	2.30	0.59	0.5612	4.38	10.15	12.225	9.22	0.37	8.5214
10	0.15	1.13	0.1288	14.03	21.95	67.882	1.93	2.44	0.9664
11	3.36	4.98	3.6090	22.54	9.89	60.572	9.50	9.54	18.118
12	0.00	2.47	0.6082	18.51	17.95	66.497	20.26	0.44	41.064

Table 4. Prediction of soil parameters using the orthogonal response surface developed when a third order correction was employed

Point #	Plate size	Reasonable solution #	% error of κ	% error of υ	% error of K	% error of C	% error of ϕ	SSE x 10^{-3}	SSR x 10^{-3}
1	2 in	1	0.82	3.77	10.07	6.82	1.00	16.390	0.010
		2	3.93	9.01	8.33	6.26	1.38	20.710	0.004
	4 in	1	4.93	14.83	3.28	14.39	3.07	47.140	0.010
		2	3.04	10.70	10.56	10.93	1.00	35.570	0.040
		3	0.72	0.84	8.39	4.79	0.21	9.470	0.040
	2 and 4 in	1	0.11	1.58	5.13	6.43	1.86	7.370	0.110
		2	0.09	1.51	5.20	5.11	1.54	5.780	0.110
2	2 in	1	6.60	6.79	3.42	22.34	6.21	63.900	0.110
	4 in	1	4.96	15.51	0.92	2.17	0.76	27.130	0.030
		2	3.34	15.88	14.55	30.12	16.90	166.810	0.750
	2 and 4 in	1	0.37	0.98	2.04	3.01	0.76	1.490	1.830
3	2 in	1	9.09	2.62	1.69	38.73	1.14	159.360	9.740
	4 in	1	9.09	5.14	3.63	6.56	2.65	17.220	2.390
		2	9.09	6.32	33.64	4.41	32.12	230.560	0.650
	2 and 4 in	1	9.09	2.05	3.80	15.13	28.45	113.960	5.700
4	2 in	1	30.51	79.76	1.61	0.55	11.84	743.630	0.120
	4 in	1	54.55	121.88	10.00	15.90	13.18	1836.000	0.950
	2 and 4 in	1	43.34	147.46	0.09	2.17	11.84	2376.830	0.120
5	2 in	1	4.90	6.10	2.60	3.42	0.24	7.970	0.010
	4 in	1	1.12	1.37	2.24	1.93	0.47	1.120	0.003
		2	15.12	19.22	8.39	4.64	2.43	69.570	0.004
		3	9.06	11.54	5.26	4.10	0.83	1.490	0.004
	2 and 4 in	1	5.40	6.78	2.14	3.50	0.06	9.190	0.020

Table 5. Sinkage parameters obtained from filed tests conducted in a Yolo loam soil.

Test Date	Soil* Condition	Plate Size, mm	Sinkage** Constant,k kPa	Sinkage Constant, n	Overall R^2
November, 1991	Undisturbed	50.8	695.6	0.609	0.774
	C=11.5 kPa	76.2	819.6	0.84	0.921
	ϕ=32.9 deg.	101.6	1091.2	0.828	0.911
	MC=8.9%	127.0	778.3	0.767	0.743
	ρ=1510, kg/m^3	152.4	1054.4	0.971	0.942
	e=0.755				
September, 1992	Undisturbed	50.8	959.5	0.646	0.776
	C=32.3 kPa	76.2	921	0.499	0.715
	ϕ= 27.2 deg.				
	MC = 5.14%	101.6	1839.4	0.992	0.934
	ρ=1510, kg/m^3				
	e=0.755				
	Tilled	50.8	607.6	0.918	0.776
	C=22.7 kPa	76.2	605.6	0.776	0.875
	ϕ=22.8 deg.				
	MC=4.55%	101.6	796.7	0.958	0.875
	ρ=1433, kg/m^3				
	e=0.85				

* C = cohesion; ϕ = soil internal angle of friction; MC = moisture content, dry basis; ρ= bulk density; e = void ratio.

** Logarithmic mean of all eight replicates.

Table 6. The parameter prediction from the soil tests

Test Description	Best Results	Reasonable Results No. 1	Reasonable Results No. 2
Test #1 Undisturbed Soil November, 1991	κ=0.0545 υ=0.1310 K=0.7124 C=12.348 kPa ϕ=22.5 deg. SSE=0.00380 SSR=0.00249	κ=0.0446 υ=0.2089 K=0.8928 C=11.371 kPa ϕ=22.5 deg. SSE=0.00490 SSR=0.00601	κ=0.0638 υ=0.0983 K=0.7955 C=15.344 kPa ϕ=22.5 deg. SSE=0.02146 * SSR=0.01295
Test #2 Undisturbed Soil September, 1992	κ=0.0513 υ=0.159 K=0.7365 C=14.321 kPa ϕ=28.333 deg. SSE=0.00665 SSR=0.00089	κ=0.0225 υ=0.370 K=0.8950 C=15.068 kPa ϕ=26.050 deg. SSE=0.01332 * SSR=0.00345	
Test #3 Tilled Soil September 1992	κ=0.1037 υ=0.1859 K=0.6247 C=8.997 kPa ϕ=31.820 deg. SSE=0.00378 SSR=0.00016	κ=0.0505 υ=0.370 K=0.8993 C=16.516 kPa ϕ=25.247 deg. SSE=0.00444 SSR=0.00337	

* Relatively high SSE indicating an unreasonable solution.

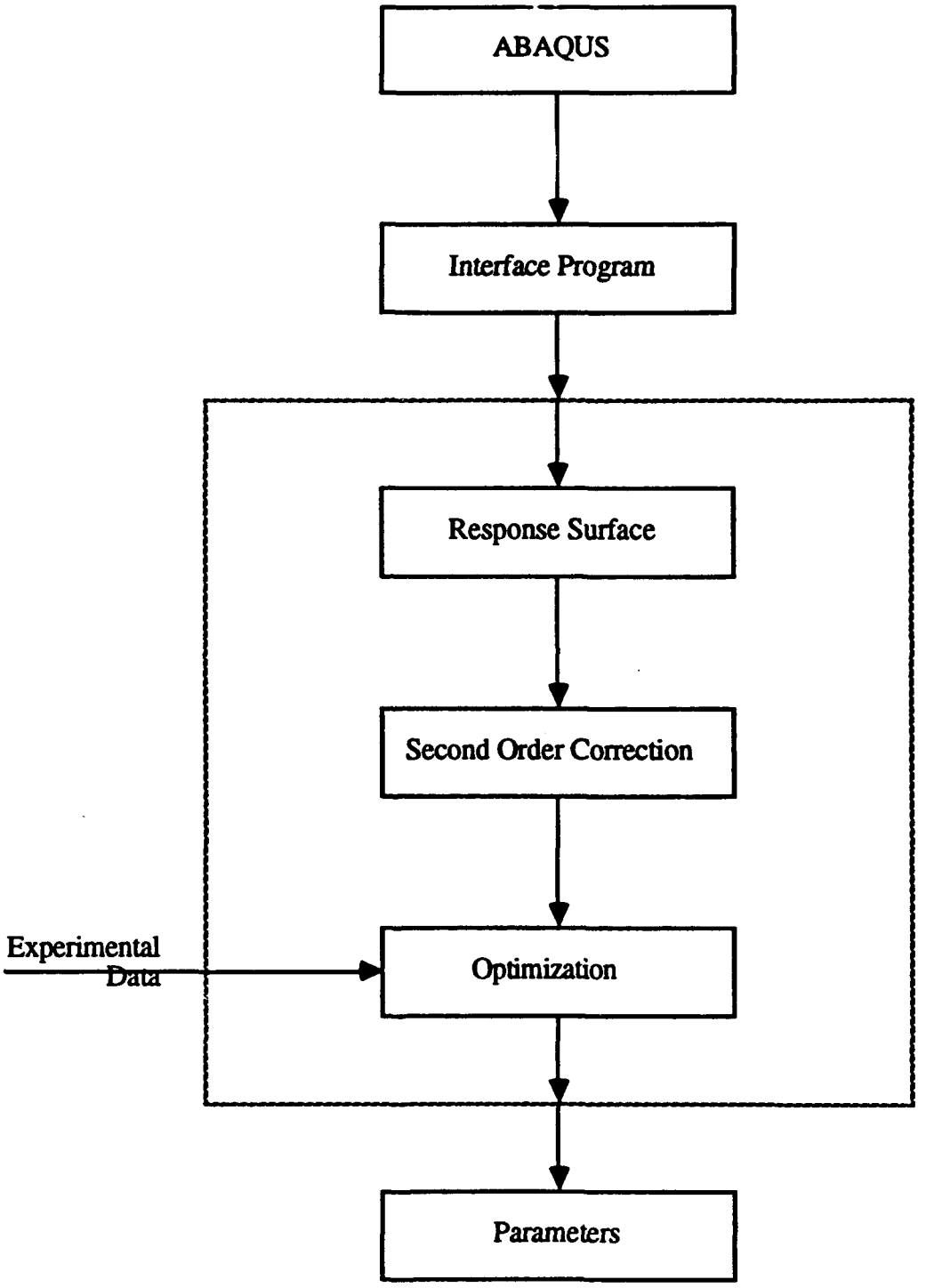
ABAQUS
Interface Program
Response Surface
Second Order Correction
Experimental Data
Optimization
Parameters

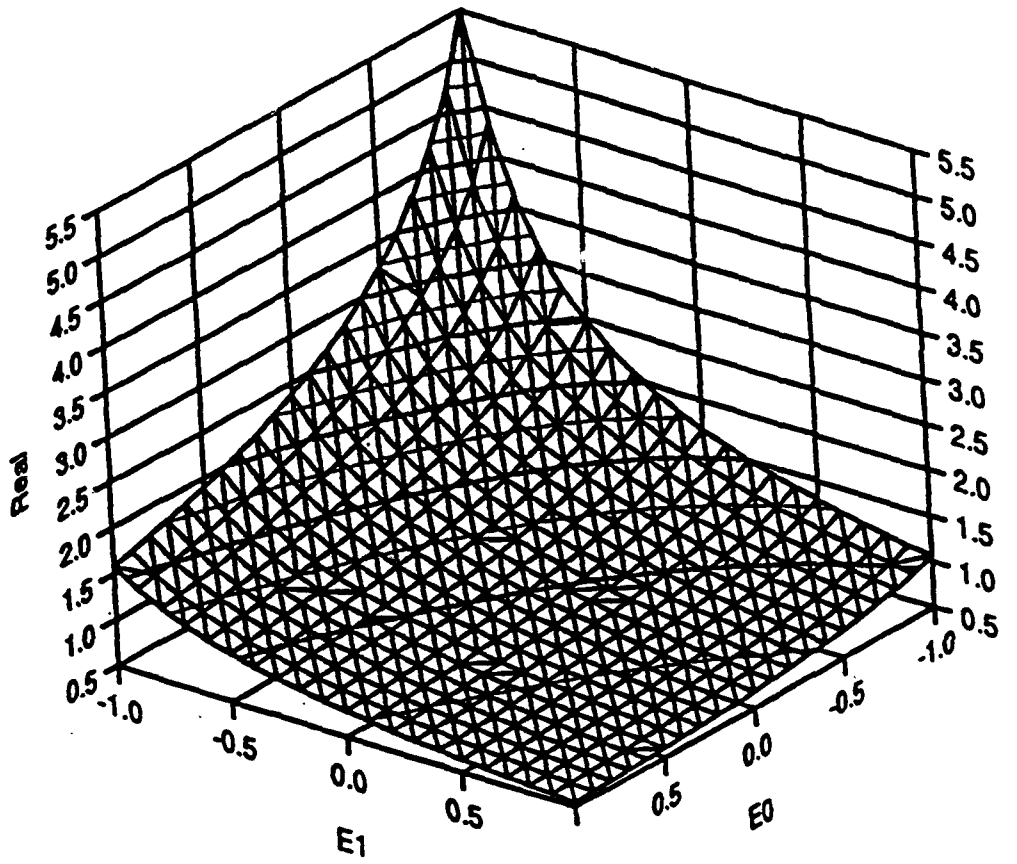

Figure 2. The plot of real function in E_0 - E_1 space

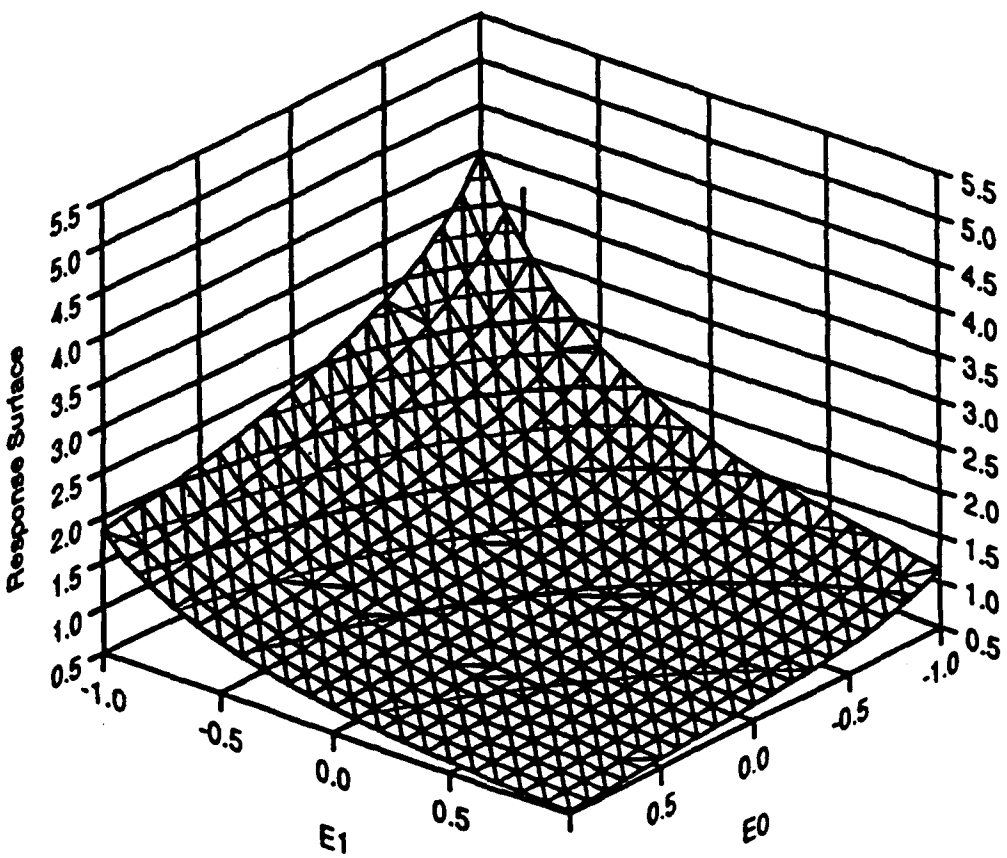

Figure 3. The plot of orthogonal response surface in E_0 - E_1 space

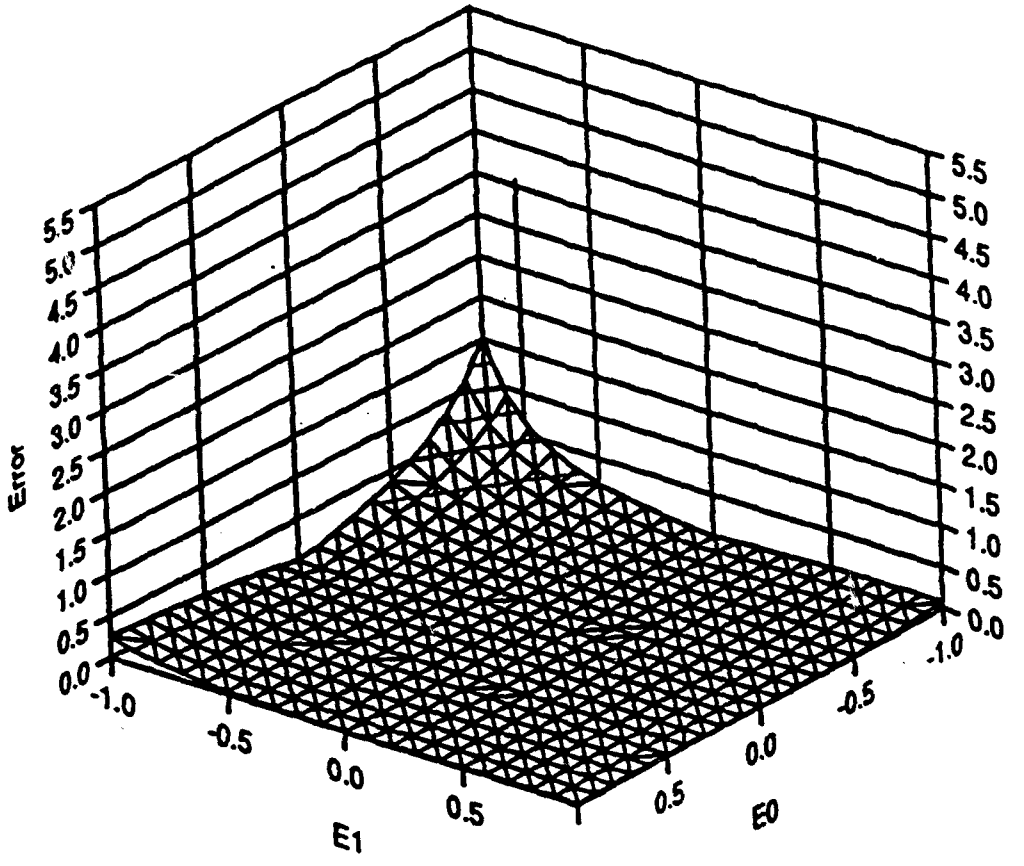

Figure 4. The plot of error without any correction in E_0 - E_1 space

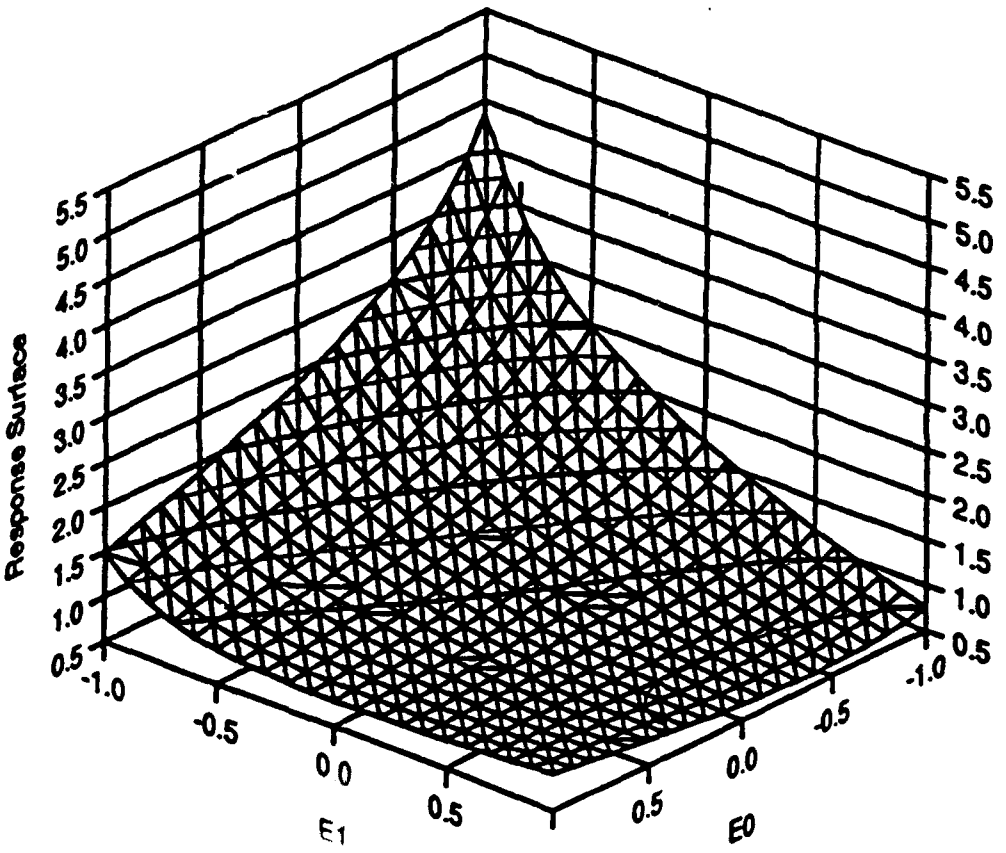

Figure 5. The plot of orthogonal response surface in E_0 - E_1 space when a second order correction was included

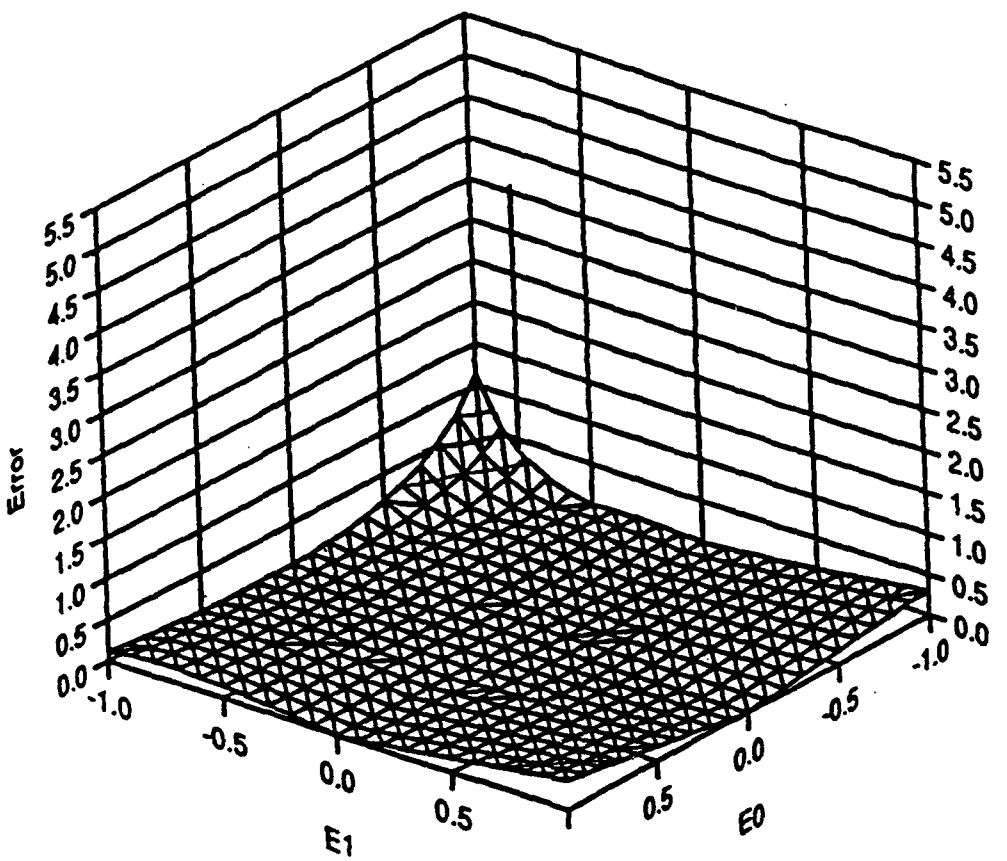

Figure 6. The plot of error in E_0 - E_1 space when second order correction is included

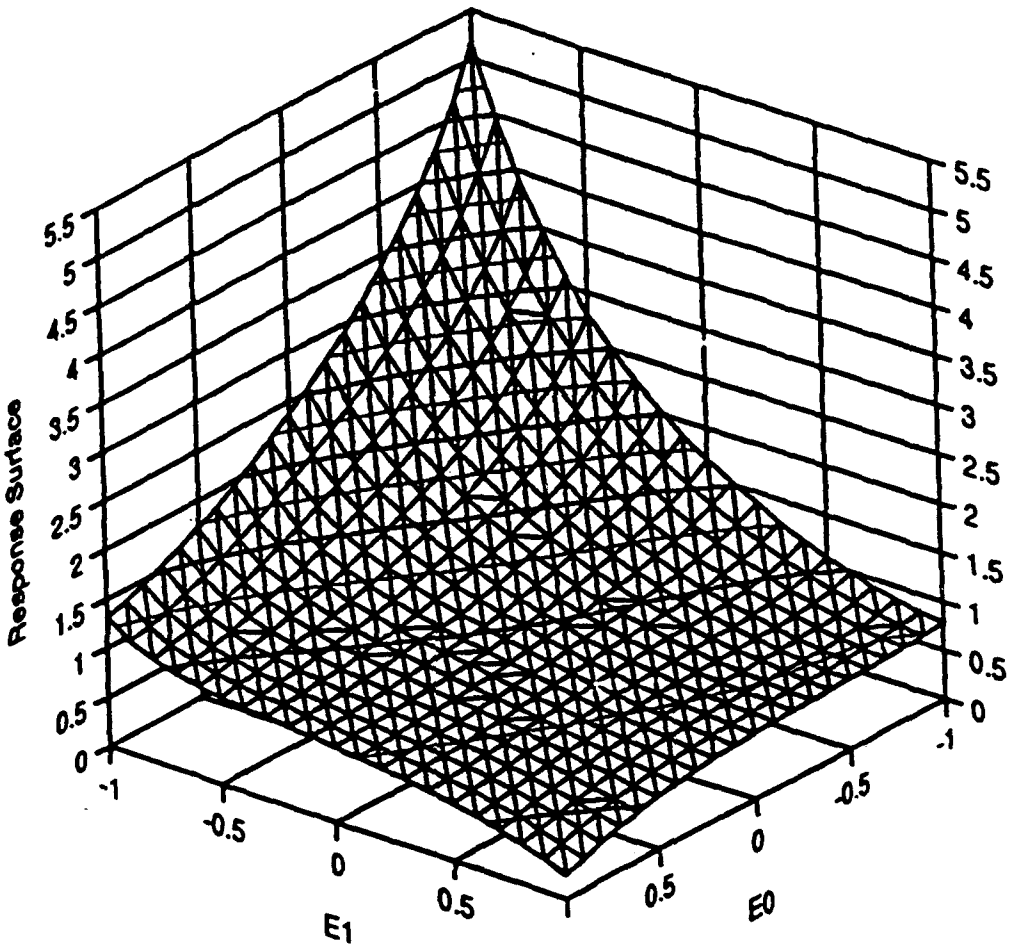

Figure 7. Plot of orthogonal response surface in E_0 - E_1 space when a third order correction was included

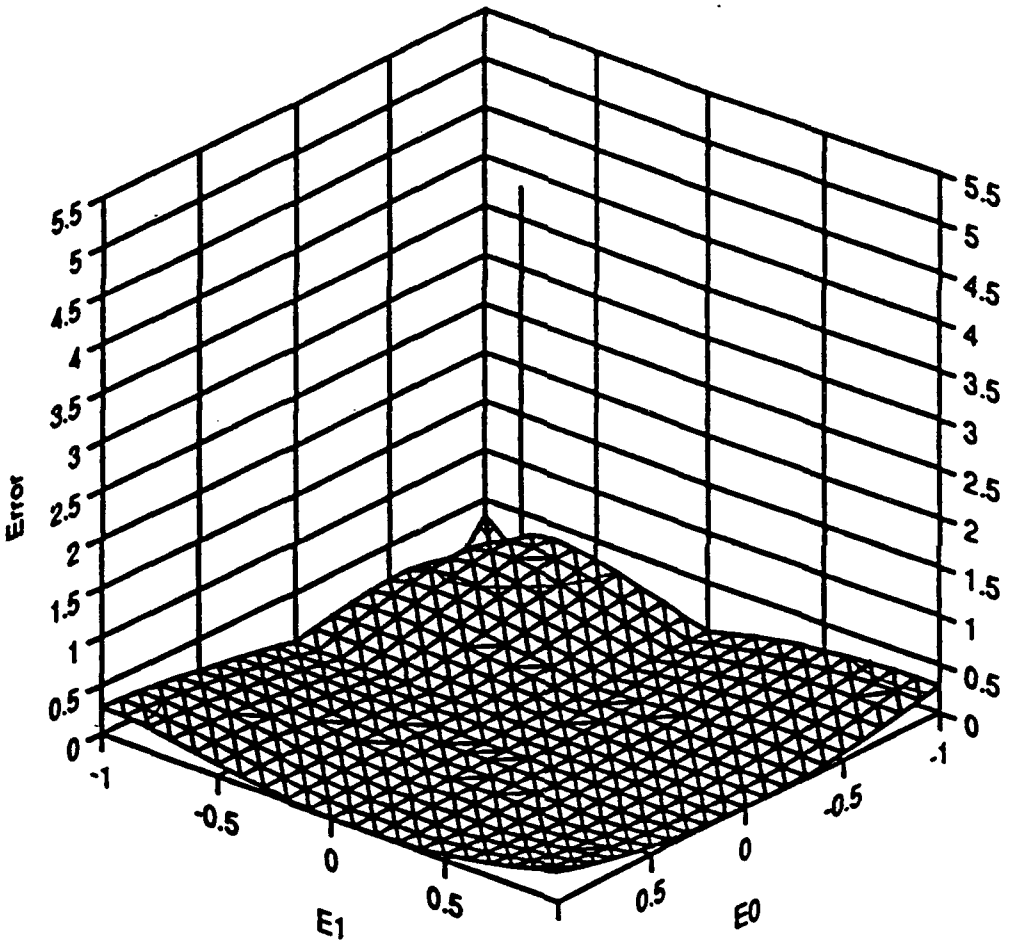

Figure 8. Plot of error in E_0 - E_1 space when a third order correction was included

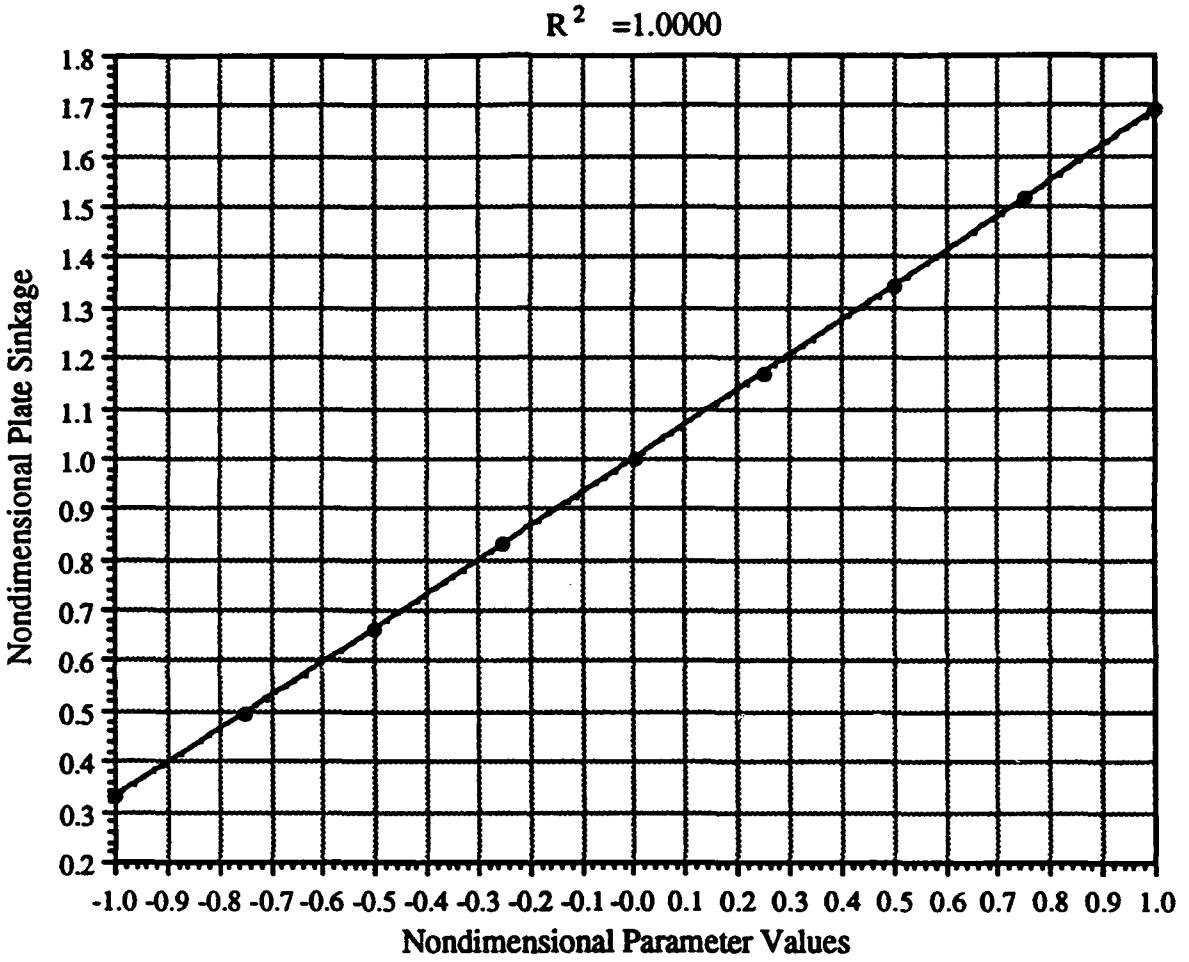

Figure 9. Plate sinkage vs. nondimensional values of parameter κ for a 4 in plate subjected to 80 PSI applied load

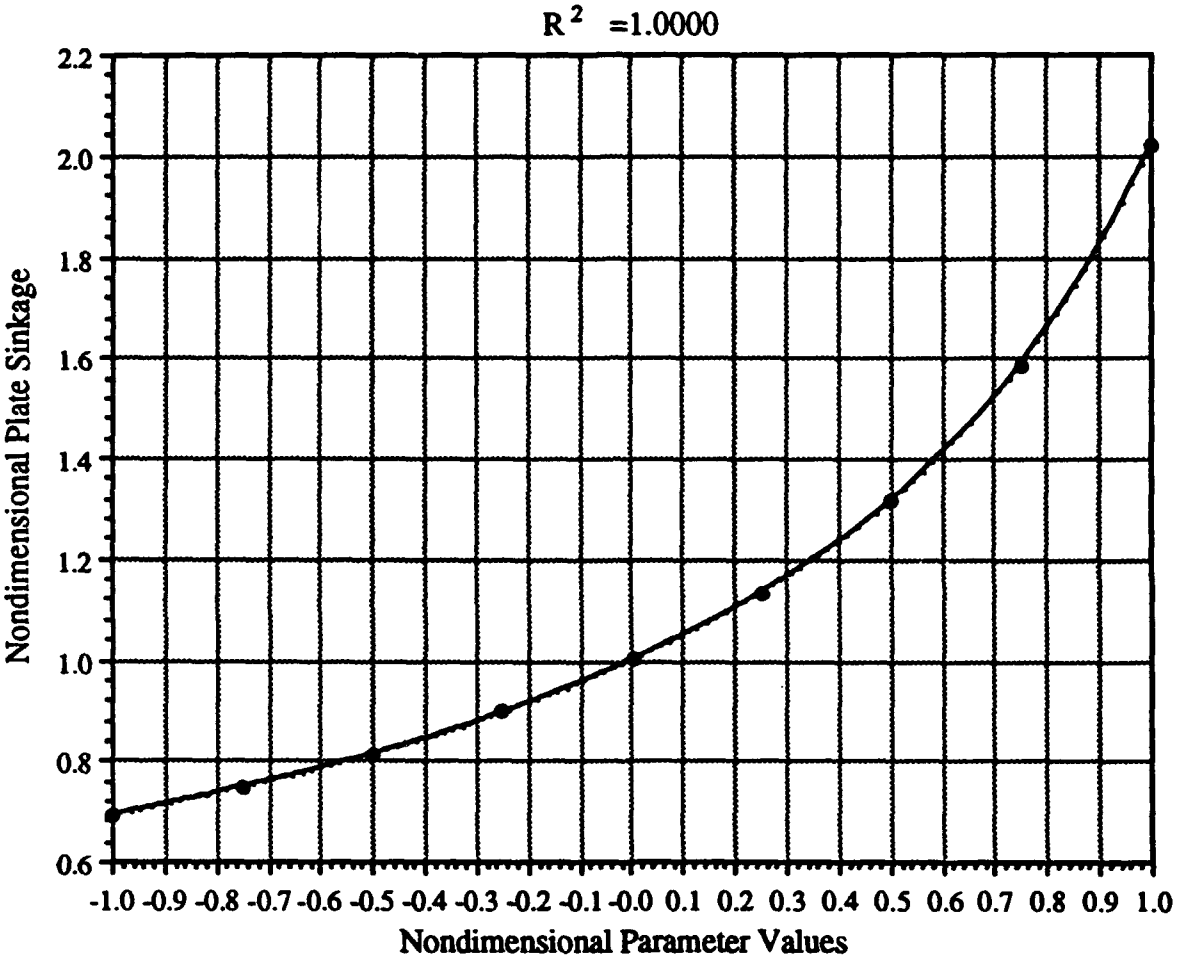

Figure 10. Plate sinkage vs. nondimensional values of parameter υ for a 4 in plate subjected to 80 PSI applied load

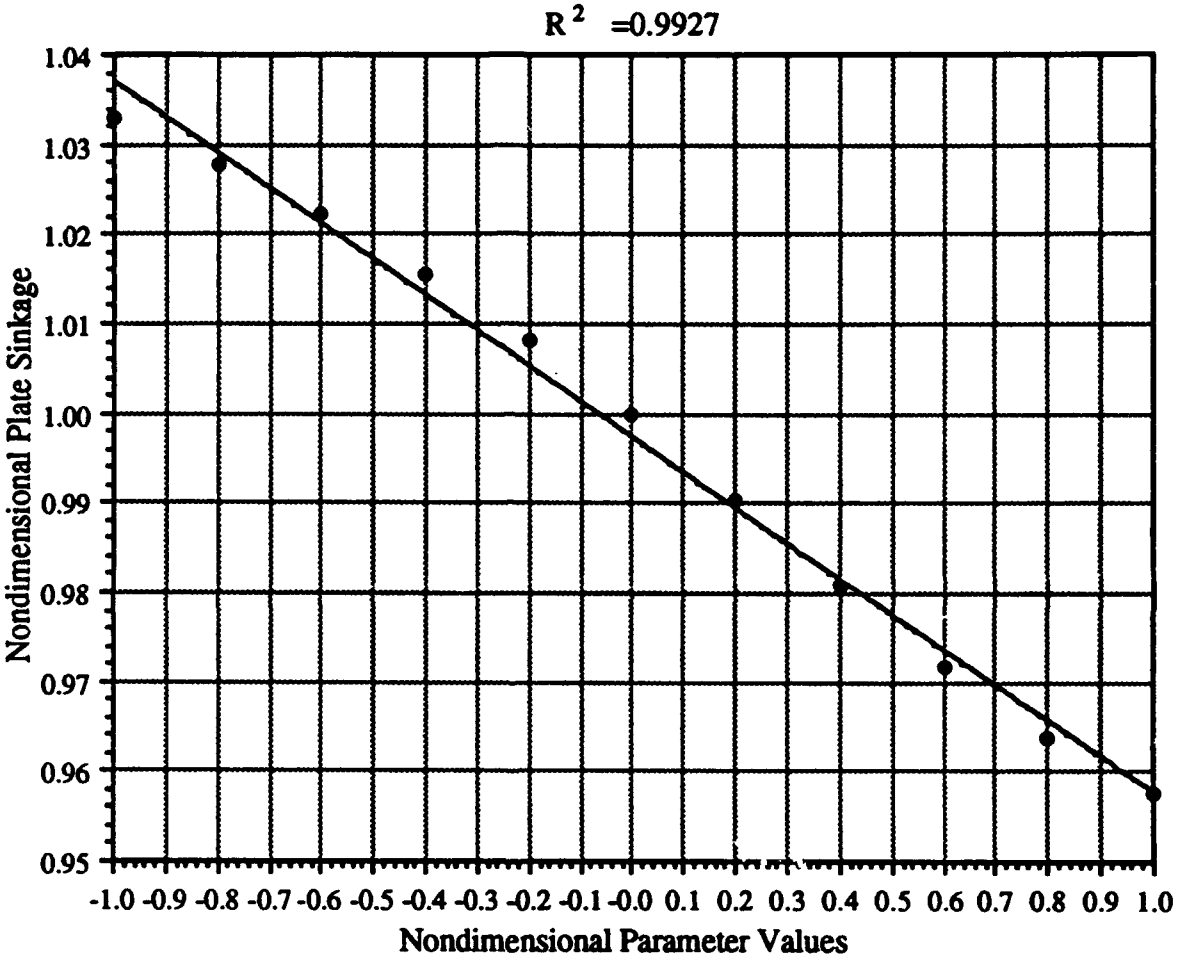

Figure 11. Plate sinkage vs. nondimensional values of parameter K for a 4 in plate subjected to 80 PSI applied load

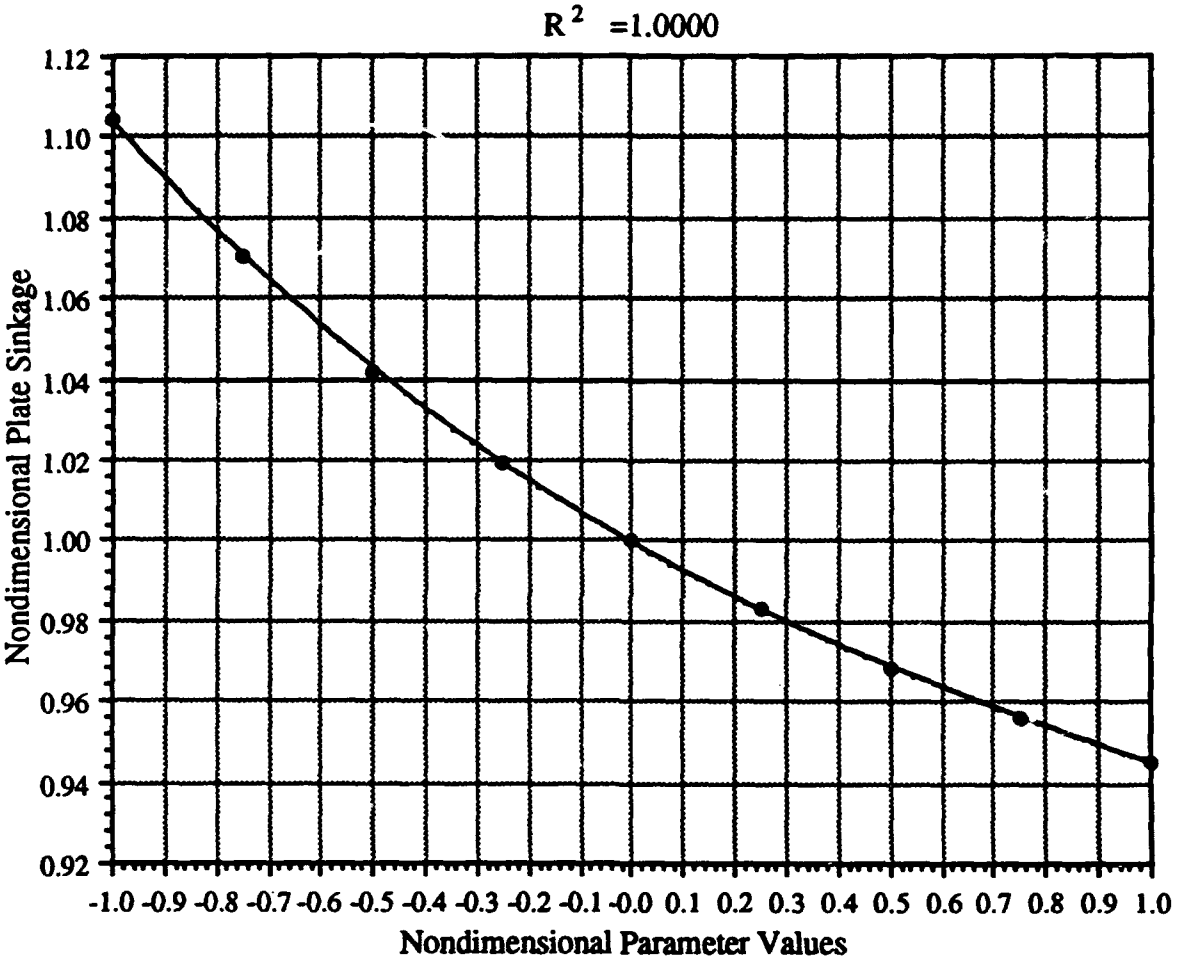

Figure 12. Plate sinkage vs. nondimensional values of parameter C for a 4 in plate subjected to 80 PSI applied load

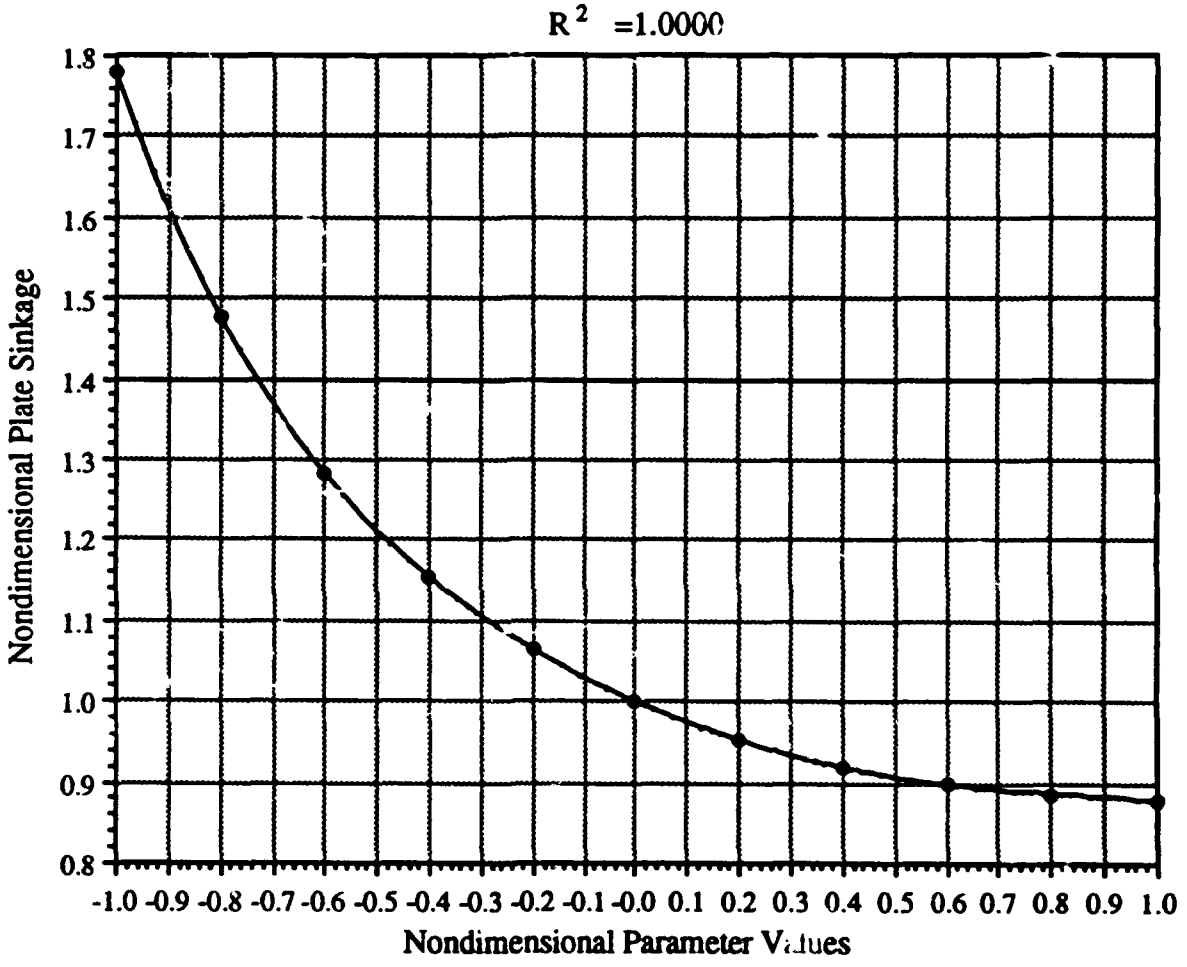

Figure 13. Plate sinkage vs. nondimensional values of parameter ϕ for a 4 in plate subjected to 80 PSI applied load

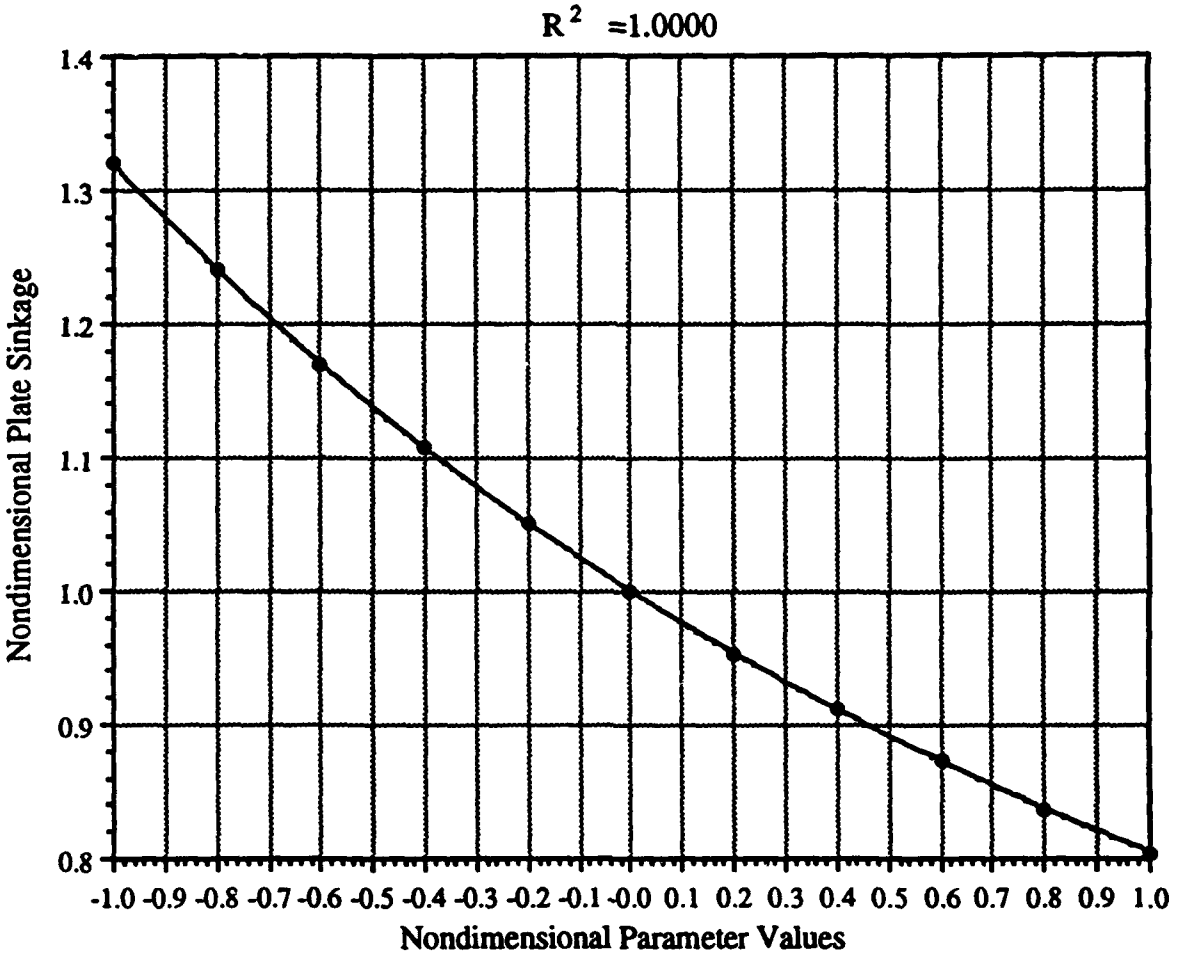

Figure 14. Plate sinkage vs. nondimensional values of parameter e for a 4 in plate subjected to 80 PSI applied load

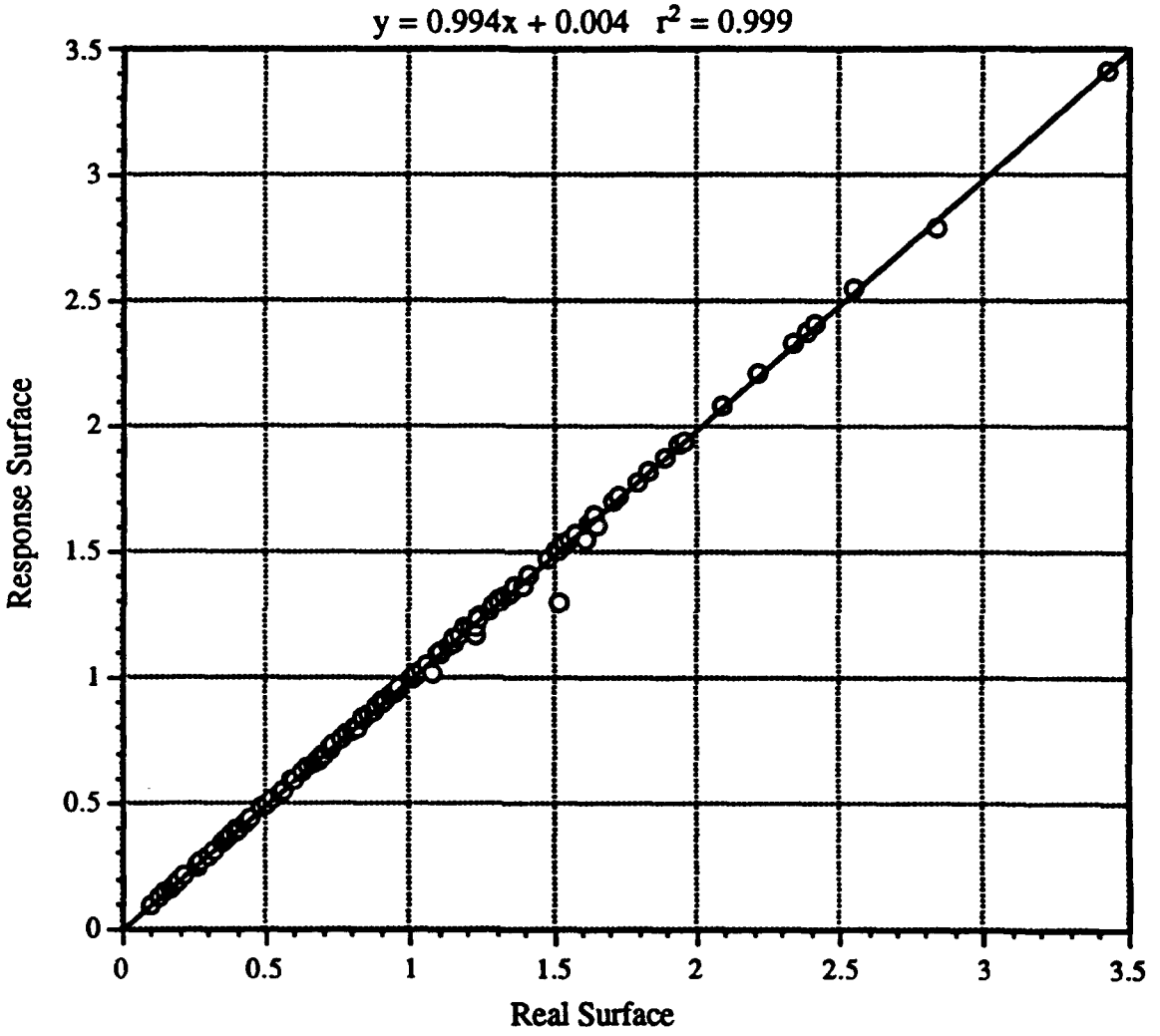

Figure 15. Response surface vs. real surface for a 4 in plate subjected to 15 PSI pressure - without correction

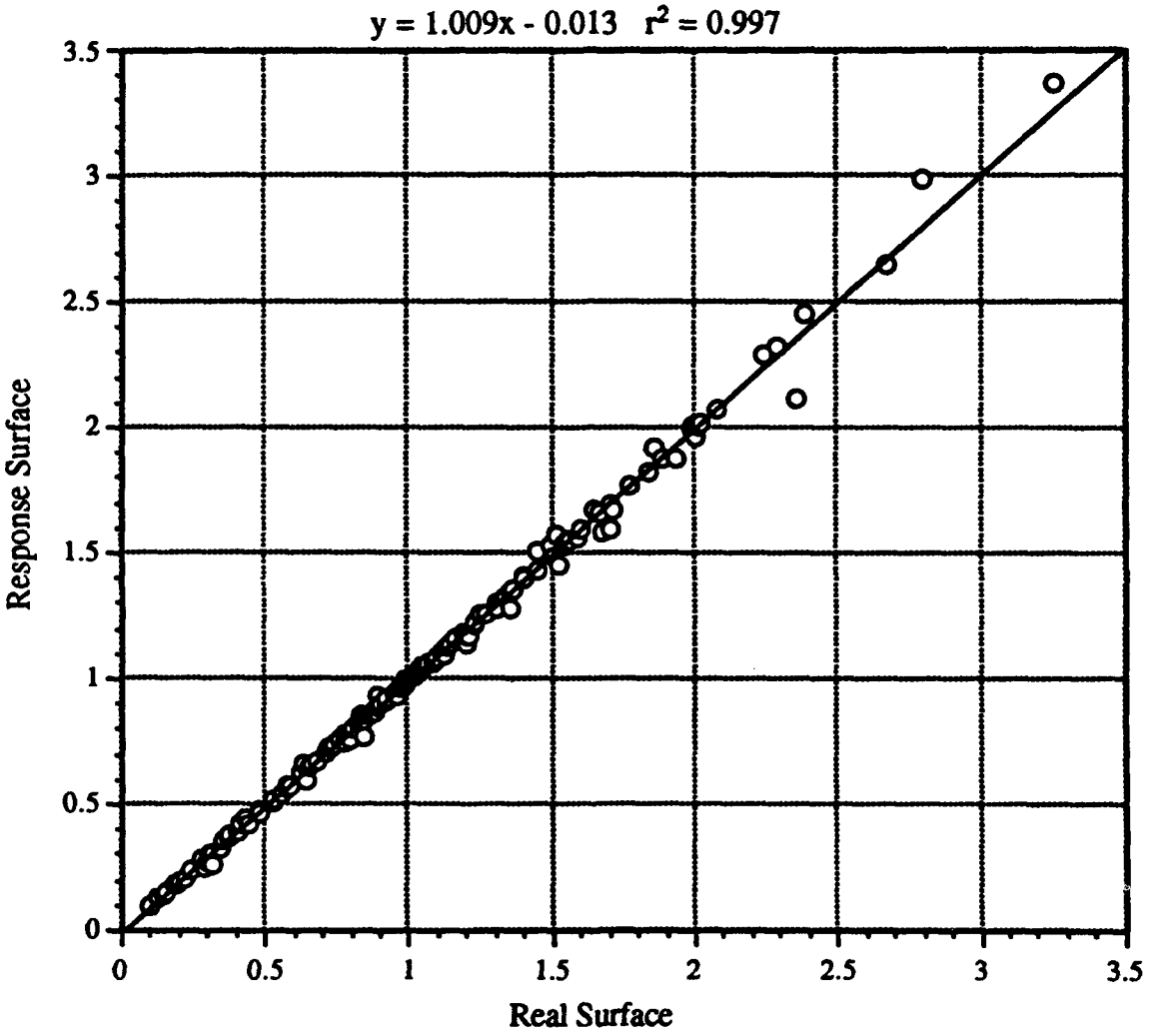

Figure 16. Response surface vs. real surface for a 4 in plate subjected to 80 PSI pressure - without correction

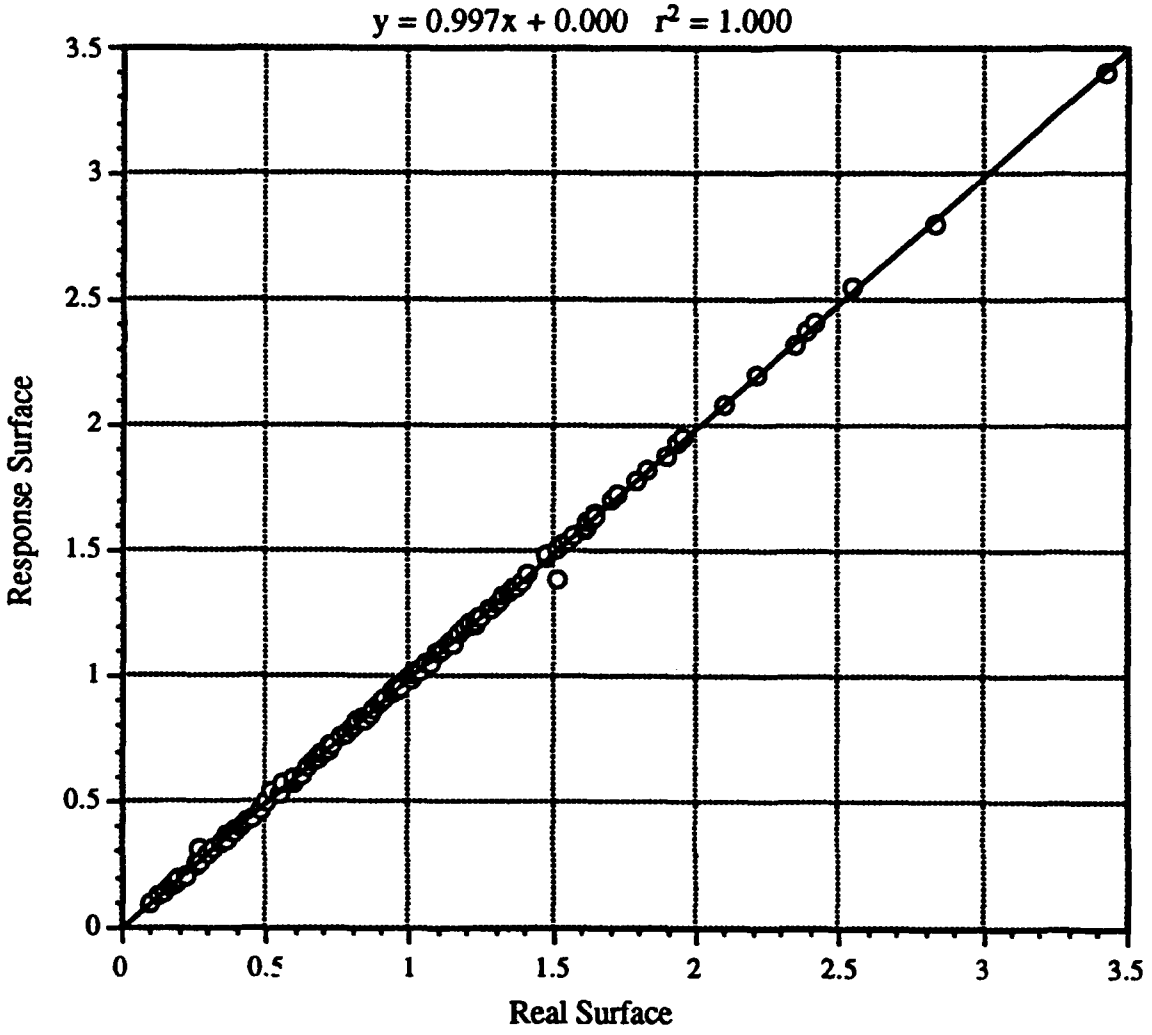

Figure 17. Response surface vs. real surface for a 4 in plate subjected to 15 PSI pressure - using second order correction

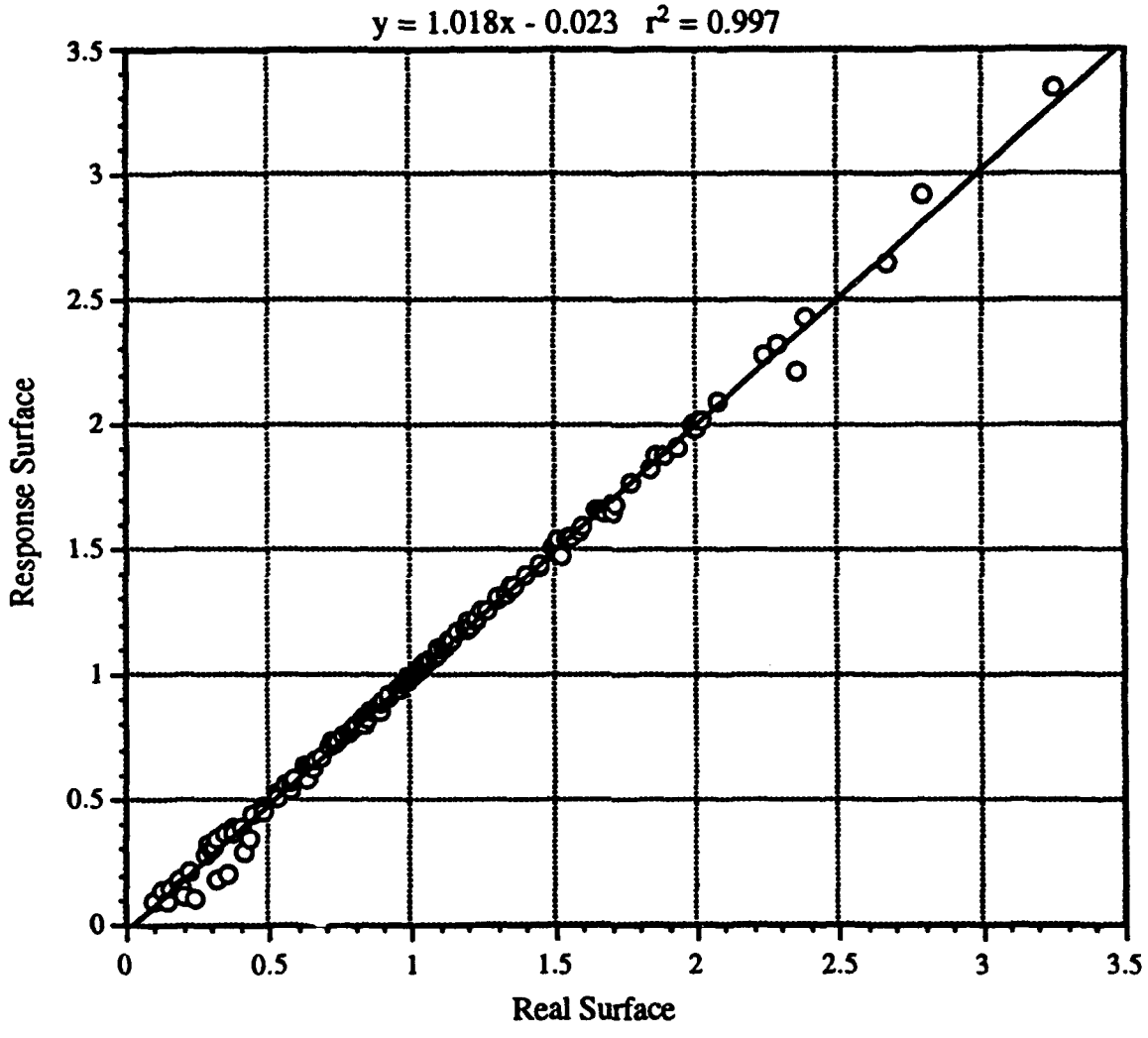

Figure 18. Response surface vs. real surface for a 4 in plate subjected to 80 PSI pressure - using second order correction

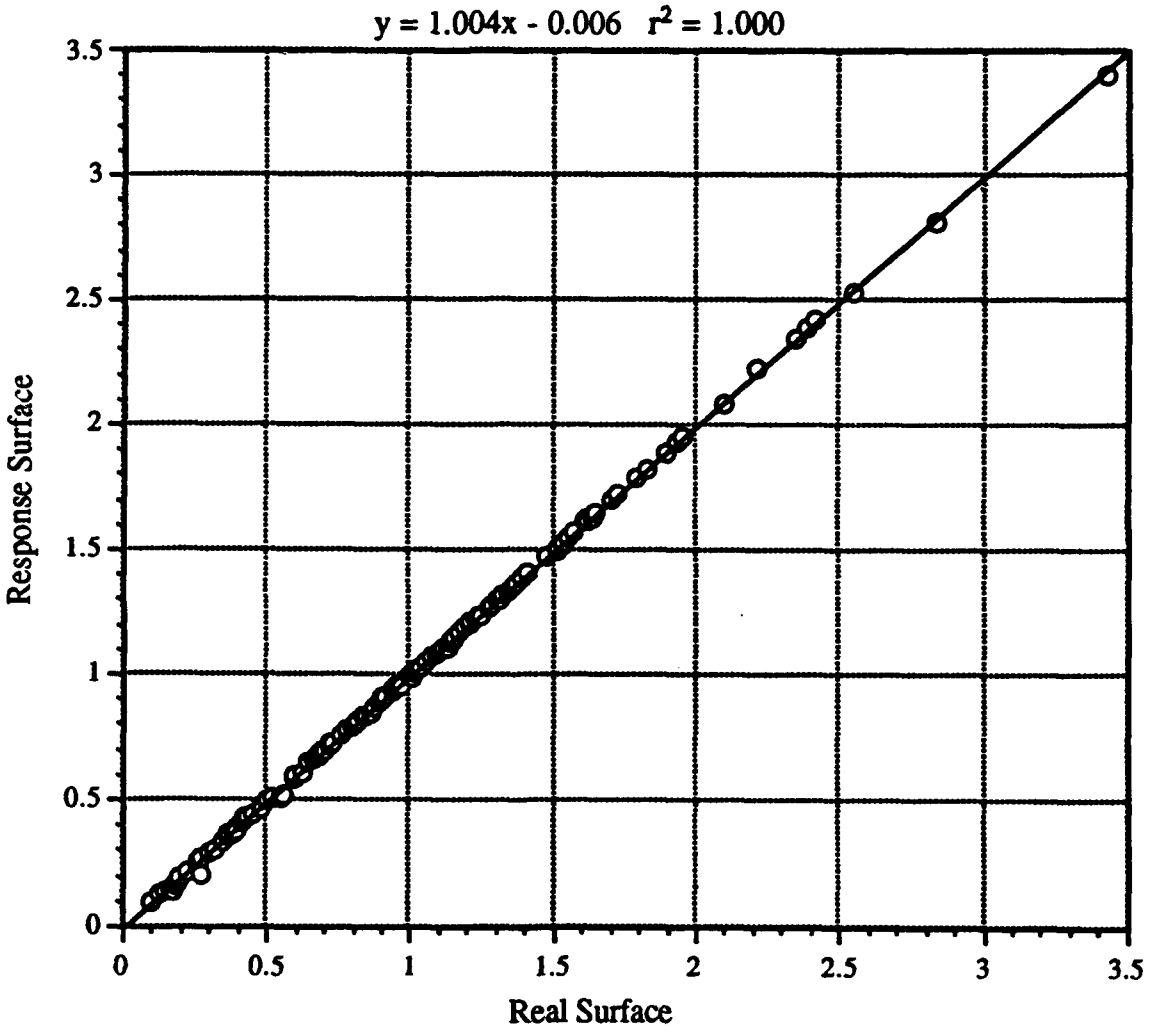

Figure 19. Response surface vs. real surface for a 4 in plate subjected to 15 PSI pressure - using third order correction

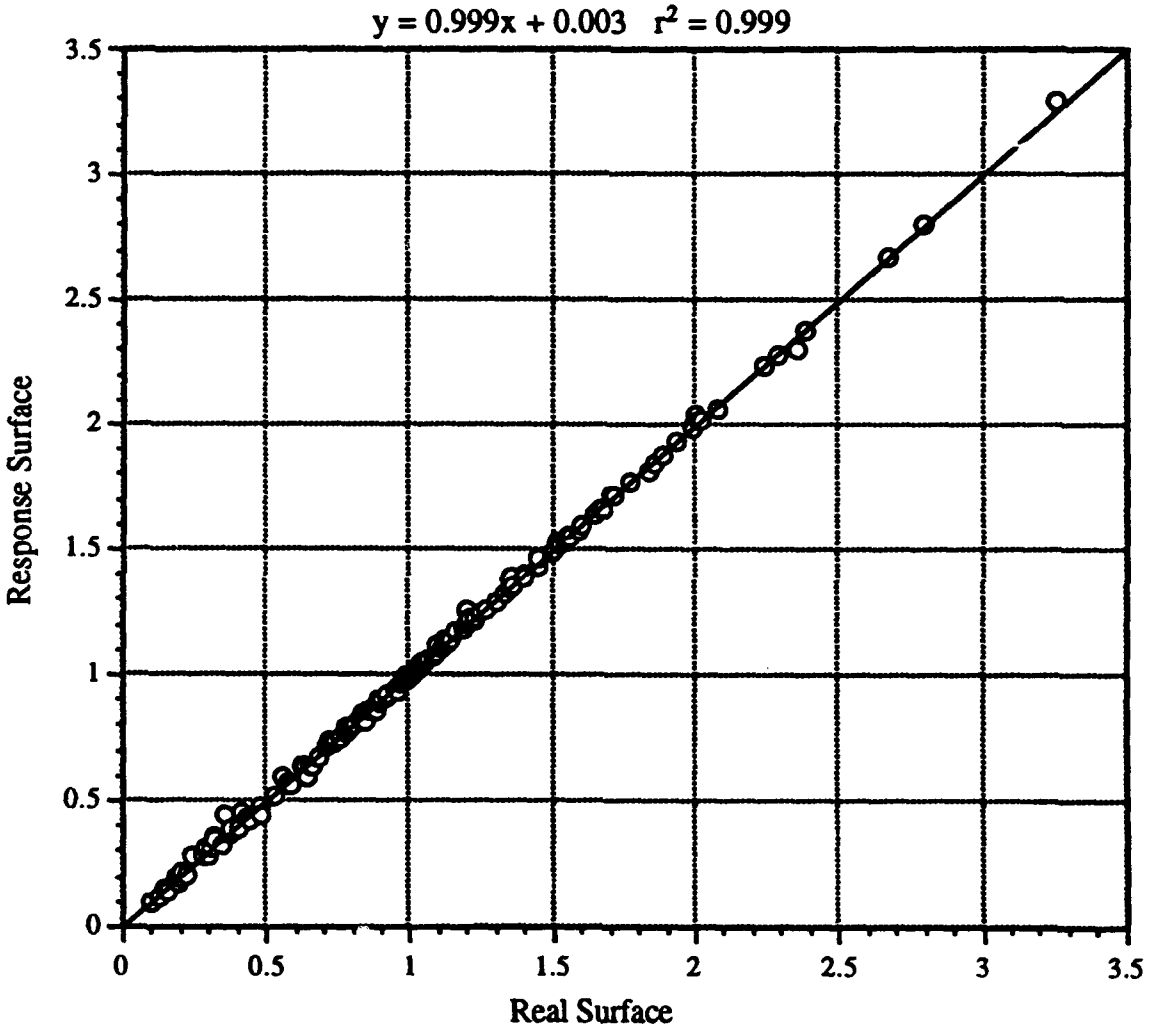

Figure 20. Response surface vs. real surface for a 4 in plate subjected to 80 PSI pressure - using third order correction

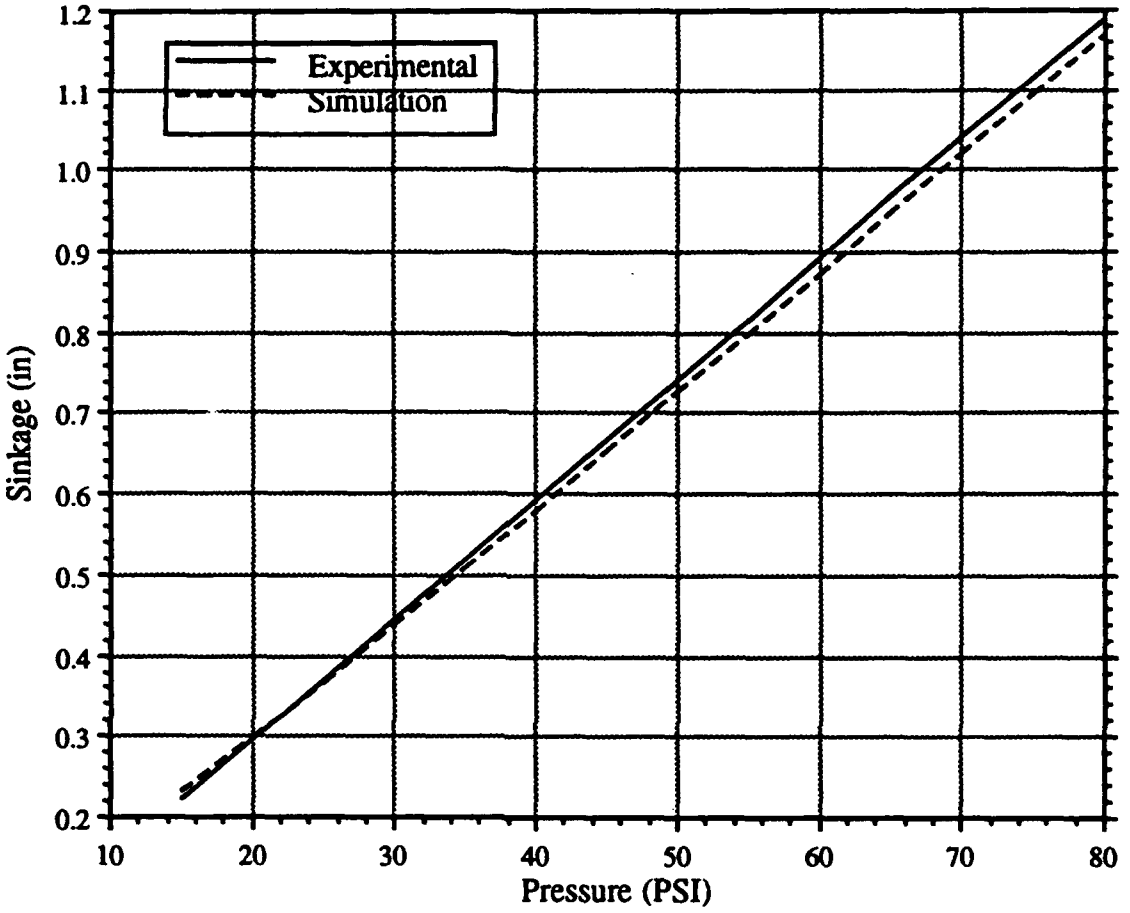

Figure 21. Experimental and simulated sinkage for a 4 in plate in an undisturbed soil. Experimental results correspond to September 1992 tests.

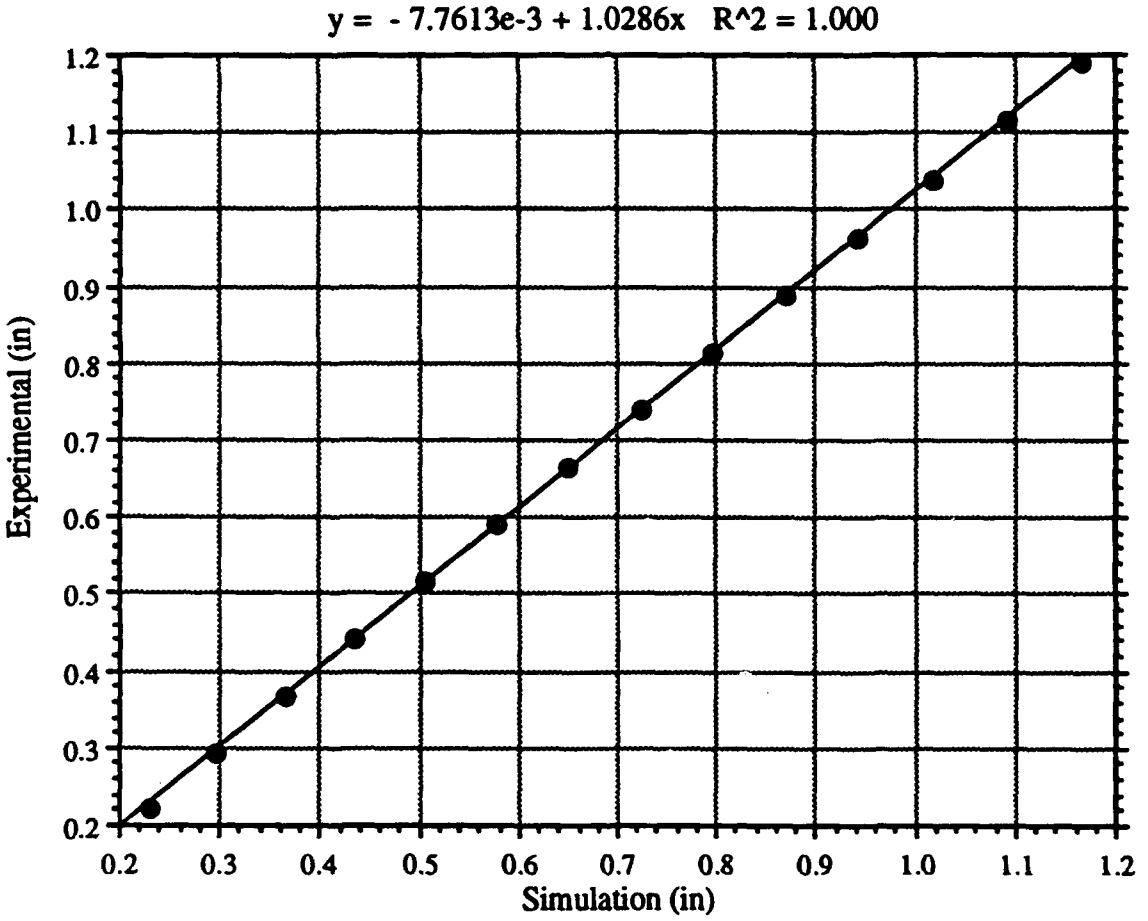

Figure 22. Experimental vs. simulated sinkage for a 4 in plate in an undisturbed soil. Experimental results correspond to September 1992 tests.

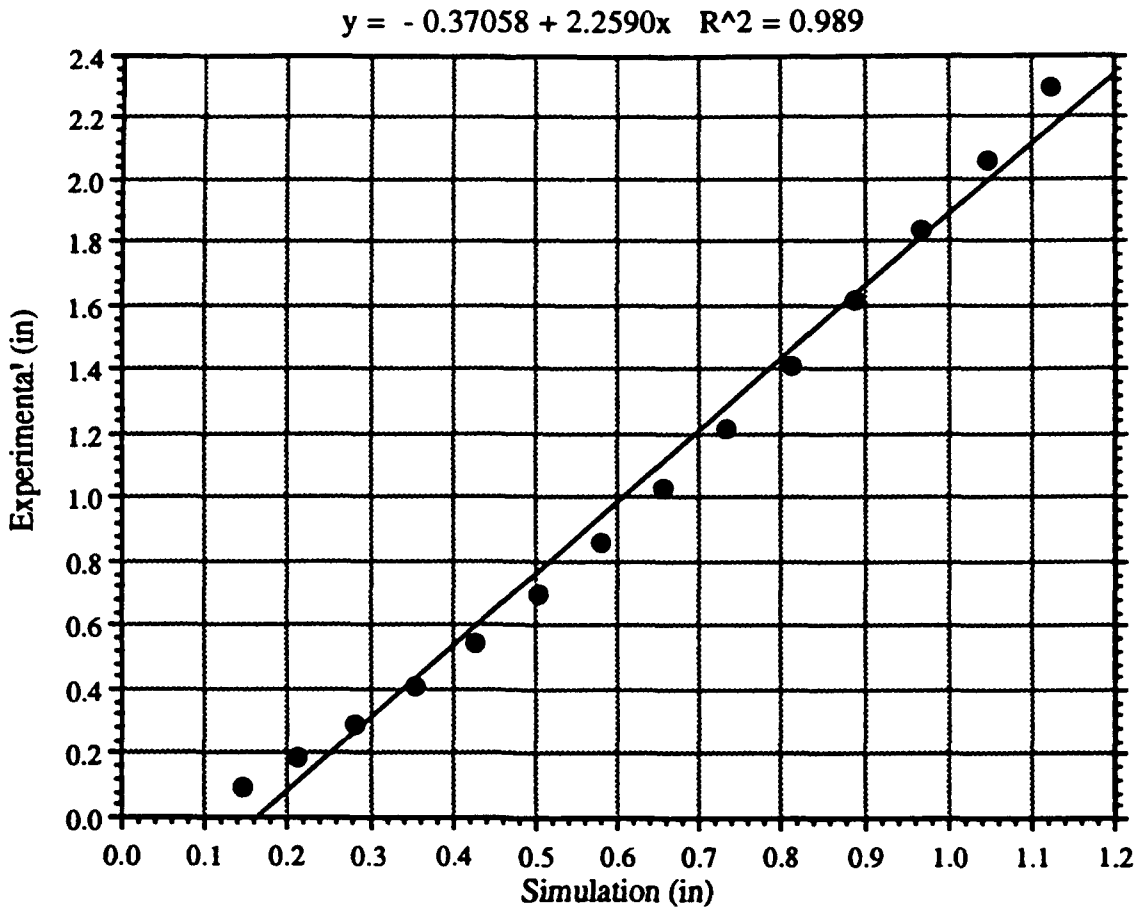

Figure 23. Experimental and simulated sinkage for a 2 in plate in an undisturbed soil when the soil parameters obtained using the inverse solution technique using a four inch plate test was used to simulate 2 in plate behavior. Experimental results correspond to September 1992 tests.

Appendix B
Technical Notes

SOIL STRESSES UNDER TRACTOR TIRES

A.C. Bailey, R.L. Raper, C.E. Johnson, T.R. Way, and E.C. Burt[1]

Introduction

Soil stress state transducers (SST's) have been used to determine the state of stress beneath tractor tires operating under a range of dynamic loads and inflation pressures. The stress state transducer has been described by Nichols *et al.*(1987). These SST's provide the data necessary to calculate the complete stress state at the transducer. The stress state is a 3 x 3 symmetric tensor with 6 independent stresses, and may be represented by the 6 independent stresses, the three principal stresses (σ_1, σ_2, σ_3) and their directions, or stresses on particular planes, such as the octahedral shearing (τ_{oct}) and normal (σ_{oct}) stresses and their directions (Bailey and Burt 1988).

Procedure

A recent experiment (Bailey *et al.* 1993) studied the effect on soil stresses of 4 combinations of tire loads and inflation pressures, Table 1. Treatments L and H are combinations of load and inflation pressures taken from the manufacturer's recommendations (Goodyear 1992). Treatment U (underload, load less than recommendation for the inflation pressure) used the load from the L level (13.1 kN) and the inflation pressure from the H treatment (124 kPa). Treatment O (overload) treatment used the load from the H level (25.3 kN) and the inflation pressure of the L treatment (41.4 kPa). The tire was operated at a constant forward velocity of 0.15 m/s and a constant slip of 10%.

Two soils, Norfolk sandy loam (NSL) and Decatur clay loam (DCL), and two profiles in each soil were used. One profile was relatively loose and uniform. A hardpan was present in the second profile. A SST was placed at the depth of the hardpan (hardpan depth) and a second SST placed midway between the surface and the hardpan (shallow depth). Both SST's were aligned directly under the centerline of the path of the tire. Soil bulk density samples were taken in each tireprint at the depth of each SST after completion of the tests.

Results and Discussion

Typical data from a SST are shown in figure 1. The data shown are from the H treatment at the hardpan depth in the NSL with a hardpan. The value of 0 on the distance axis represents the horizontal location of the tire axle, and data at positive distances represent

---

[1]The authors are: Alvin C. Bailey and Randy Raper, Agricultural Engineers, National Soil Dynamics Laboratory, USDA-ARS, Auburn, AL.; Clarence E. Johnson, Professor, Agricultural Engineering Dept., Alabama Agricultural Experiment Station, Auburn University, AL.; and Thomas R. Way, Agricultural Engineer, and Eddie C. Burt, Research leader, National Soil Dynamics Laboratory, USDA-ARS, Auburn, AL.

OTable 1. Mean octahedral stresses at peak σ_{oct} from all treatments

Treatment	Profile	Load, kN	Inflation pressure, kPa	NSL Deep depth σ_{oct} kPa	NSL Deep depth τ_{oct} kPa	NSL Shallow depth σ_{oct} kPa	NSL Shallow depth τ_{oct} kPa	DCL Deep depth σ_{oct} kPa	DCL Deep depth τ_{oct} kPa	DCL Shallow depth σ_{oct} kPa	DCL Shallow depth τ_{oct} kPa
L	uniform	13.1	41.4	32	32	44	52	34	39	56	79
U	uniform	13.1	124.0	43	55	49	55	53	85	71	108
O	uniform	25.3	41.4	51	55	53	56	84	151	71	104
H	uniform	25.3	124.0	57	54	82	89	91	140	59	70
L	hardpan	13.1	41.4	31	32	51	62	51	86	46	55
U	hardpan	13.1	124.0	39	42	63	51	86	85	65	98
O	hardpan	25.3	41.4	56	52	66	75	84	116	63	75
H	hardpan	25.3	124.0	79	83	106	142	105	177	120	146

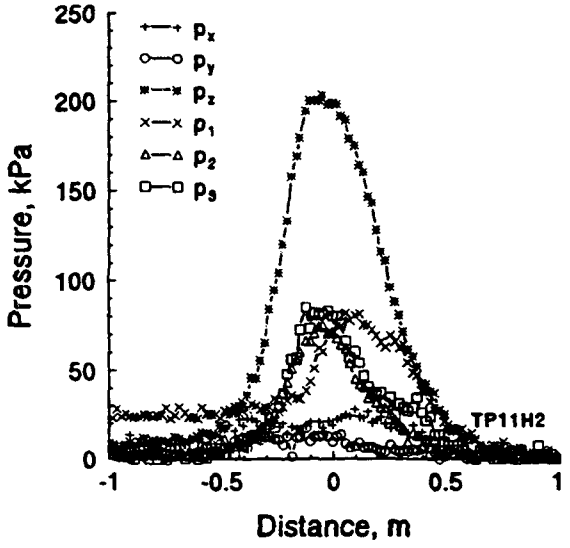

Figure 1. Typical measured pressures from the stress state transducer under the centerline of the tire.

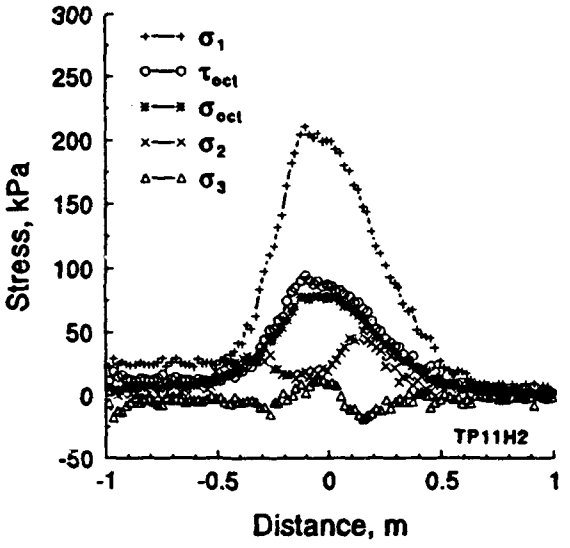

Figure 2. Calculated stresses from data shown in figure 1.

pressures in front of the tire. Figure 2 presents the calculated principal stresses (σ_1, σ_2, and σ_3) and the octahedral stresses (σ_{oct} and τ_{oct}) for the data from figure 1 using the same distance axis. The major principal stress, σ_1, is the greatest stress but displays the same trends as the octahedral shearing stress. For this discussion the octahedral stresses σ_{oct} and

τ_{oct} will be used to represent the stress state in the soil under the tractor tire. The peak values of σ_{oct} and the corresponding values of τ_{oct} were selected for further analyses. Table 1 presents of the means of the 4 replications of σ_{oct} and τ_{oct} from all treatments, soils, and profiles.

The peak values of σ_{oct} and the corresponding values of τ_{oct} were analyzed with SAS (1990) using a factorial design on each soil separately. Replications were nested within soil profile. The multivariate option MANOVA was also used to analyze both octahedral stresses together.

Higher levels of either dynamic load or inflation pressure generated higher octahedral stresses beneath the tractor tire in both soils when averaged across all depths and soil profiles (figures 3 and 4). Both dynamic load and inflation pressure were significant

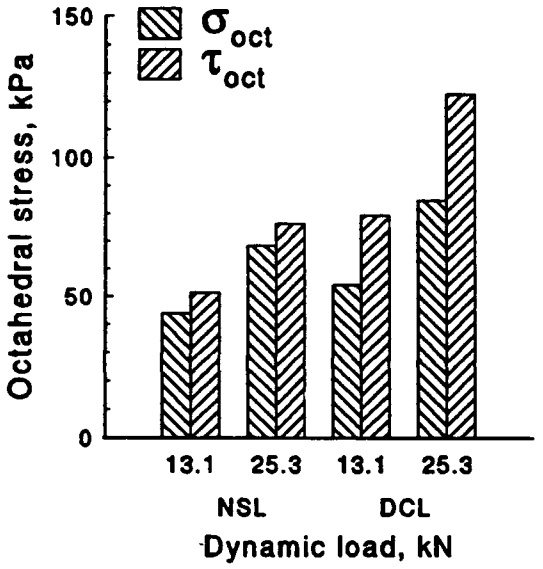

Figure 3. Effect of dynamic load on octahedral stresses for two soils averaged across profiles and depths.

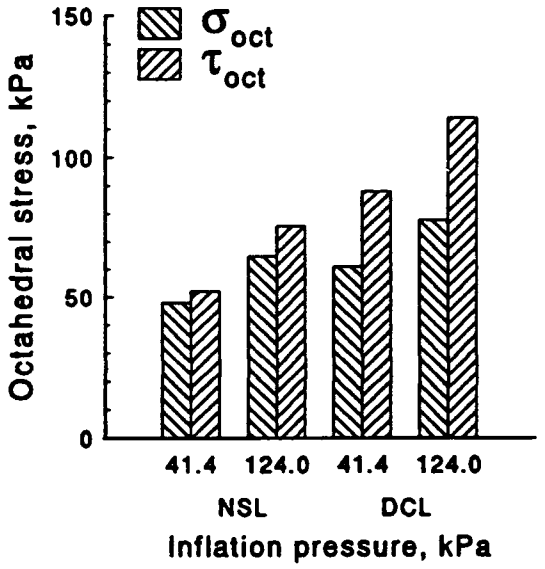

Figure 4. Effect of inflation pressure on octahedral stresses for two soils averaged across profiles and depths.

factors (5% level) affecting the two octahedral stresses, except for inflation pressure on τ_{oct} in the DCL. This exception is probably because the DCL had the greatest variability in τ_{oct} (a deviatoric stress contrasted to σ_{oct}, an average stress). Both dynamic load and inflation pressure were significant factors (5% level) affecting the bulk density and increase in bulk density at each depth level in each soil.

The mean net traction and tractive efficiency data for all treatments in each soil are presented in Table 2. An ANOVA of the net traction and tractive efficiency showed that inflation pressure and dynamic load both had significant effects on both performance variables, and that higher inflation pressures had lower net traction and tractive efficiencies at the same dynamic load. These results support the conclusions from the soil stresses and bulk density data. Higher inflation pressures at the same dynamic load have lower tractive efficiencies and generate higher soil stresses and soil compaction.

Table 2. Mean tractive performance data.

			NSL		DCL	
Treatment	Load, kN	Inflation pressure, kPa	Net traction kN	Tractive Efficiency	Net traction kN	Tractive Efficiency
L	13.1	41.4	5.4	0.674	13.2	0.698
U	13.1	124.0	3.9	0.584	13.2	0.636
O	25.3	41.4	11.6	0.687	12.7	0.734
H	25.3	124.0	8.3	0.620	8.9	0.665

References

Bailey, A. C. and E. C. Burt. (1988) "Soil stress states under various tire loadings", *TRANSACTIONS of the ASAE* 31(3):672-676,682.

Bailey, A. C., R. L. Raper, T. R. Way, E. C. Burt and C. E. Johnson (1993) "Soil stresses under tractor tires at various inflation pressures", *Proceedings of the 11th International Conference of ISTVS*. 276-285.

Goodyear. (1992) "Optimum tractor tire performance handbook", The Goodyear Tire & Rubber Company.

Nichols, T. A., A. C. Bailey, C. E. Johnson, and R. D. Grisso (1987) "A stress state transducer for soil", *TRANSACTIONS of the ASAE* 30(5):1337-1341.

SAS. (1990) 'SAS/STAT User's Guide" Version 5, 4th edition. SAS Institute, Inc, Cary, NC.

Soil Compaction Research Needs

P. T. Corcoran[1]

Introduction

There are two needs for compaction research that are potential topics for the workshop on "*Modeling the Mechanics of Off-Road Mobility*". Those topics are predictive analytical models for machine compaction, and the forecasting of machine compaction performance on specific job site conditions.

These two needs are similar in that both are needed to reduce the requirements for machine testing. Analytical models for machine compaction can reduce the need for expensive prototype testing, and improve the understanding of relationships between machine and soil in the production of compaction. Performance forecasting can eliminate the need for proof testing, and improve the quality of soil structures.

Analytical Compaction Models

There has long been a need for accurate and complete analytical compaction models. The ideal is to have such models based on proven theory, and not be dependent on relationships defined only by empirical testing. Although empirical testing is often the most attractive as a low risk practical means to define machine/soil relationships, empirical testing is always inherently limited in application to those parameters and ranges of parametric values included in whatever experiments provide the data base for empirical relationships.

Conversely, theoretically based analytical models are essentially unlimited in range of application. The more complete the theory and the more detailed the model, the broader the range of application. Historically analytical soil compaction models have been limited by a lack of computational capacity and detail to handle the non-linear and fine grained characteristics of machine soil compaction problems. These technological hurdles are coming down with the computational speeds of modern computer work stations, and the sophistication in newer modeling software.

Recent work with a finite element soil compaction model is confirming the technological hurdles to a comparatively complete and detailed model are gone or greatly reduced. The challenge now becomes one of using this technological opportunity. The author is interested in sharing experiences with others addressing the need for predictive models, both analytical and empirical.

---

[1]Senior Project Engineer, Product Research, Caterpillar Inc.

Compaction Performance Forecasting

Compaction is very often a critical need in the construction industry. Achieving compaction specifications can be the critical path guiding the progress of a construction site, and therefore achieving compaction specification may be the determinant factor in scheduling and costing a job. Contractors need accurate information on the ability to meet compaction specifications, and traditionally this has required proof testing. Proof testing can be far from an accurate means to insure compaction specifications will actually be met. The common variability in job site soils, virgin soil conditions, and the influence of weather can destroy the accuracy of proof testing.

An ideal would be the ability to forecast the performance of compaction machines based on specific job site conditions, and adapt machines and operating procedures to the job site as needed for both maximum efficiency and performance. However, most contractors lack information and interpretation to achieve such an ideal.

There appear to be two major needs to allow for the improvements of performance forecasting and the reduction of need for proof testing; the quantitative relationships between machine parameters, job site conditions, and compaction specifications; and the relationship between laboratory compaction measurement and actual field capability.

Quantification of relationships between machine, soil, and specifications is perhaps little more difficult then recording information already available from most job sites to establish a data base. There may be some incremental additional information required, however, it would be contrary to the purpose of performance forecasting to require significant additional information than that normally available. A requirement for significant additional information would only trade-off one inefficiency for another and thus not bring about a net gain in overall job efficiency. A reasonably inclusive database should then give the opportunity to establish correlations yielding a forecasting capability.

Improving the relationship between laboratory compaction measurement and actual field capability may be more difficult. The problem is compaction machines in the field do not have the same energy efficiency nor use the same mechanism to produce soil compaction as standard laboratory procedures. Therefore, densities achievable in the laboratory are not necessarily achievable in the field at the same energy level and maybe not at any energy level depending on compaction equipment available. Additionally, as shown by energy/density relationships from laboratory testing, optimum moisture levels vary with compaction energy and may vary with method of compaction. The need is to provide information to guide field use of compaction machines both for the selection of the optimum machine, and the optimum use of the machine. Obtaining such information could require a significant amount of controlled testing and therefore be a relatively costly endeavor.

One possible alternative to establishing correlation between laboratory and field through empirical testing would be the development and verification of fundamental theory of soil compaction. Such a theory may already be in existence based on the compaction energy/density relationships defined by current laboratory testing. Therefore, expansion of a theory of this type to correlation between laboratory energy and actual field energy could become the foundation for performance forecasting and not require large amounts of machine tests.

There may be a significant amount of compaction forecasting information already available but not widely disseminated, or there may be a significant amount of information available from a wide distribution of sources but not consolidated, or there may simply be a lack of information pertinent to the need. The author is interested in sharing thoughts and ideas on the need, value, and feasibility for accurate performance forecasting of soil compaction and the availability of pertinent information.

Localized Energy Dissipation in Strained Granular Materials

Peter K. Haff[1]

A granular material is a mechanical system composed of distinct macroscopic interacting components. A soil, a sand dune, a heap of mine tailings, and a fractured rock mass, are all granular materials, with "grain sizes" ranging from microns to meters in diameter. There are two approaches that can be used to model granular systems quantitatively. A continuum method based upon a partial differential equation or a discrete method that retains specific reference to the particulate nature of the medium.

Continuum models require the existence of an "averaging volume", large compared to grain sizes, within which the characteristics of individual particles can be replaced by variables like velocity, density, components of stress, etc. Discrete models on the other hand retain reference to individual particle identities. In discrete models one can investigate "microscopic" behavior that is lost or obscured in the averaging transition to a continuum model. One such type of behavior in granular systems is the nature of frictional losses incurred when the medium is subjected to inelastic strain.

A drawback in using a discrete modeling technique is that the number of discrete particles that can be handled is limited (thousands to tens of thousands of particles), and hence we can study only a small volume of material at one time, while with a continuum model we can usually model large volumes. Consequently, discrete techniques are often best used to generate insight into microscopic mechanisms that can help us in interpretation of larger scale modeling, or to help construct constitutive relations for use in continuum models.

In a granular medium subjected to a given load (a generic prototype of a soil or similar granular material subjected to vehicle loading), the stress is distributed throughout the medium via grain contacts and fluid pressure forces. For simplicity, we consider here only dry, noncohesive materials. As strain develops in the material, compression of individual grains occurs at the grain-grain contacts. If the contacts do not slip, and the strain rate is small, then the strain is generally reversible upon unloading and energy loss is zero. At larger strains, grain contacts can slip. Since the contacting surfaces of earth materials are frictional, Coulomb-type losses are incurred, and contact positions do not return to their original configurations upon unloading.

Particle dynamics studies of energy dissipation in strained granular material point to the importance of fluctuations in the stress distribution at grain contacts. These fluctuations can influence the macroscopic lossiness of the material. When a compressive load is applied to a granular assembly, the allocation of stress among contacts is determined in large measure by the geometric placement of grains. Consider for simplicity a system of circular or spherical particles. Each particle has a set of neighboring particles with whom it is in contact. By drawing an imaginary line between the centers of every pair of contacting grains, we define a stress network. A normal force associated with grain stiffness is associated with each element in this network, as well as a tangential force due to friction between the contacting grains. The normal force exerted across each element of the network is a function of the deformation at that contact. If the elastic interaction is modeled by a stiff spring, then the force is a function of the instantaneous compression of the spring. In general the stresses will be different at each contact, i.e., spring compressions will differ, so that there is a distribution of local stress determined by the details of grain packing.

[1]Department of Geology
Duke University
Durham, North Carolina 27708-0230

Small amounts of strain can often be accommodated by reversible compression of the elastic springs at the contacts, but large strain must be accompanied by slippage and rotation of grains. Wherever slippage takes place, frictional forces will lead to energy loss. Because there is a distribution of normal contact forces, some contacts will slip more easily than others. If a contact is tightly compressed, so that the normal force is large, then a correspondingly large local tangential stress is needed at that contact to cause it to fail. Conversely, at a contact where the normal spring is not much compressed, slippage is relatively easy. The frictional energy lost in a slip event is the product of the tangential force acting during the slip and the amount of displacement incurred at the contact. Assuming for the sake of argument equal displacements, the greatest amount of energy lost per slipping contact is at the strong contacts. Conversely, the smallest amount of energy lost per slip event is at the weakly compressed contacts.

Particle-dynamics-model simulations of sheared granular materials suggest that for the system as a whole, most energy is lost at contacts of intermediate strength. The strong contacts do not slip sufficiently often to dominate the overall energy loss, while the weak contacts slip often but do not generate enough loss per contact to be the dominant loss mechanism. A consequence of this observation is that the macroscopic rate of energy loss in deformation is not a simple function of the grain-on-grain frictional properties of individual grains. The energy loss will usually be less than that expected from a simple averaging approach, the magnitude of the effect depending upon the detailed distribution of forces over the stress network. A corollary is that since strong contacts cannot slip easily, clusters of grains with strong contacts between them tend to rotate as a whole, with slip and energy loss occurring on the periphery of the cluster. As the material strains, the stress network continually adjusts to maintain force balance. Rotating friction-locked clusters eventually unlock as their internal stress-network becomes less well aligned with the overall stress field in the medium. At this point the local stresses readjust, slippage begins to occur within the previously rigid cluster, and new clusters spontaneously appear nearby.

The frictional losses and hence the energy absorption of the macroscopic granular medium depend upon the details of such microscopic mechanisms. By elucidating these mechanisms, discrete computational models can help to further our understanding of the dynamic response of granular systems such as soils to external loads.

A Case for Improved Soil Models in Tracked Machine Simulations

F.B. Huck[1]

Abstract

A planar, multibody dynamics model of a track-type-tractor was developed to provide an analytical tool to evaluate alternative new tractor designs and to resolve problems on current products. The model has been applied to studies of track chain vibrations, track/sprocket jumping, sprocket/bushing wear, and the influence of track and undercarriage kinematics on fundamental tractor rigid body vibration mode excitation. Applications of the model in studies of higher frequency vehicle vibrations associated with ride quality demonstrated the important influence that track/soil interface models have on machine vibration excitation and the need to improve our capabilities in this area.

Introduction

Earthmoving equipment manufacturers must identify ways to reduce product design and development time and cost to remain competitive in world markets. Manufacturers increasingly turn to engineering computer analysis as a time and cost savings methodology to supplement and ultimately reduce dependence on their more traditional and costly build and test approach to product design and development.

As computers continue to increase in speed and expand in memory capacity, engineering software functionality grows to quickly fill any vacant memory cell or unused CPU cycle. Performance analysts, as a result, are able to develop increasingly realistic and detailed interdisciplinary models to simulate the overall dynamic response of the complete earthmoving machine.

The response of the machine ultimately depends upon the external forces which act upon it. In the case of an earthmoving machine, these include gravitational forces, combustion of engine fuel, operator interactions, and soil reactions. None of these external influences, with the exception of gravity, is as well understood from an analytical standpoint as it needs to be to match the degree of sophistication now attainable in dynamics models of the machine itself. Of the three least understood forces, the soil force reaction, though possibly not as analytically intractable as the human operator, is the most critically lacking component in most earthmoving machine performance models.

---

[1] Senior Project Engineer - Research Department - Caterpillar, Inc.

Discussion

The Model

One example of a model that pushed the limits of computing resources and analysis software to their limits at the time of its development was a 2- dimensional, pitch plane, multibody dynamics model of a high-drive track-type-tractor. Initiated in the mid 1980's, the model was developed within the framework of the commercial, rigid multibody dynamics code, DRAM (Chase and Angell 1977). The model (Figures 1 & 2) (Huck, 1987) was unique from previous tracked machine models in that it treated each link in the track chain as a distinct rigid body. This level of model fidelity was required to address the range of questions being asked at the time.

Typical Model Applications

The model was applied primarily to questions related to track chain and undercarriage dynamics or to the influence of track and undercarriage dynamics on fundamental machine vibration modes excitation. In the area of track chain dynamics, the model was used to understand the relationship among track pitch, catenary length, track tension, and track speed on the excitation of transverse vibration modes in the track catenaries.

A second application demonstrated how premature wear develops when out-of-tolerance sprocket teeth segments lead to adverse track bushing and sprocket tooth engagement. A third application simulated the track/sprocket tooth jumping that can occur during rapid forward/reverse directional shifts.

The primary application for the model is to optimize undercarriage component placement in order to minimize the influence of track and undercarriage kinematics on the excitiation of the chassis' fundamental rigid body pitch vibration mode in the 4 to 6 Hz range. If overly excited, this mode can affect dozer controllability during finish grading applications.

Importance of Soil Models

The DRAM tracked machine model incorporates simple representations of soil behavior to simulate the ground reaction forces that support and propel the machine.

Early versions of these models applied Bekker pressure-sinkage like relationships to simulate the normal support force acting on each individual track shoe. (Bekker, 1969) Likewise, a model similar to that proposed by Kacigen & Guskov was applied to each track shoe grouser to simulate the soil shearing forces associated with traction.(Kacigen & Guskov, 1968) These models are simply nonlinear elastic representations of the soil. There is no coupling between the normal support and traction force models other than the dependence of the tractive force generated by a given track shoe on the normal pressure imposed on the soil by the adjacent shoe.

While such models may be adequate for steady state predictions of tracked machine pull-slip characteristics, they are quite inadequate for detailed dynamic models of the kind discussed here. Certainly a major deficiency is the inability for a nonlinear elastic, single

modulus, spring-only model to provide the energy dissipation in the soil that accompanies the passage of a tracked machine.

As mentioned above, the tracked machine model is commonly used to predict machine vibrations. Numerous studies over the years show, not unexpectedly, that its predictive accuracy is strongly dependent upon how the soil is characterized.

The plots in Figure 3 show the horizontal component of machine velocity predicted for the CG of a D8L tractor operating at a sprocket speed of 1.89 MPH (0.845 m/s) under high drawbar load. The two simulations are identical except for the presence or absence of an ad hoc damping term that was added to the traction force model. The top plot, from the simulation with no traction damping, shows the superimposition of a 1 Hz and a 4 Hz vibration in forward tractor motion. The 1 Hz component is the result of a 1 Hz variation in track tension. It is consistent with the natural frequency of the machine mass "bouncing" horizontally against the nonlinear traction "springs". The 4 Hz component (actually 3.88 Hz) represents the track first order chordal excitation. The introduction of a 50% critical damper into the traction model resulted in the response shown on Figure 3b. The vibration content of the machine is now almost purely due to chordal excitation as would be expected.

Similar results are obtained in predictions of vertical machine motion. As a result of these early model development observations, ad hoc viscous damping terms were added to both the normal and tractive force components of the track/soil interface model to account for energy absorption by the soil.

Soil Model Influence on Machine Vibration Predictions

During the course of normal use, track link rails will wear and develop a scalloped profile. The ride quality of the machine can be adversely effected if the amplitude of the scallop pattern becomes excessive. The pattern is usually adequately described as a Fourier series sine wave expansion to third order of track pitch. This pattern is well known to undercarriage designers; and, they normally account for it by properly positioning the track rollers.

In rare instances on certain soils, scallop patterns with fourth order content appear. A recent case provided the opportunity not only to apply the DRAM tracked machine model to an analysis of the situation but also to calibrate/validate the model.

Full scale machine vibration tests on the subject tractor were run to accumulate data on the fourth order vibration phenomenon. Triaxial accelerometers were positioned at the front and rear of the roller frames (RF), and at the front and rear of the main frame (MF) or chassis. Fast Fourier Transform (FFT) plots of the measured vertical acceleration data clearly show the fourth order content in the signal, particularly on the roller frame signals. (See Figure 4)

A DRAM tracked machine model was assembled for the subject tractor and simulations run to predict accelerations at points where they were measured on the machine. Frequency response plots of the predicted accelerations are shown in Figure 5. Note that the only model parameters changed for the six simulation results shown were the effective spring and damping coefficients in the normal soil support force model. Clearly, soil parameter changes have a strong influence, not only on the relative magnitude of a particular order but also on the order that predominates.

The simulation results with a Bekker coefficient of 2.0E6 and a damping coefficient of 6.0E4 most closely resemble the measured data. These parameters were chosen to "calibrate" the soil model for subsequent work on this project. Fourth order scalloped wear patterns are now routinely considered during undercarriage design studies that employ this model to determine track roller placement.

Improved Transient Soil Models

The work discussed above is just one example of the need to improve analytical descriptions of the soil's transient response characteristics. One would like more realistic models that can be simply and independently calibrated. It is far too costly and time consuming to conduct full scale tests, like the one above, to calibrate the model. Furthermore, it defeats a main purpose of analysis, which is to provide a reliable, predictive capability without the need to build and test a prototype.

To this end, Caterpillar has worked to develop improved track soil interface models. A new, semi-empirical visco-elasto-plastic model that more accurately characterizes the plastic deformation that occurs during dynamic, repetitive soil loading has been developed by Hornbrook (Figure 6) (Hornbrook 1992). This "dual stiffness" spring and viscous damper model is simple to implement, relatively easy to calibr .te, and does a very good job of matching measured force/sinkage characteristics of repetitively loaded flat plates in plastic soil with frictional and cohesive characteristics. (Figure 7)

The new, visco-elasto-plastic model has been implemented in the DRAM tracked machine model; but, it's impact on the total model's predictive accuracy in machine vibration simulation studies is yet to be verified.

Similar work is needed to improve the tractive force portion of the track/soil interaction model. To date, little effort has been devoted to that task.

Summary

Earthmoving machine manufacturers increasingly depend upon sophisticated engineering analysis techniques to help reduce the time and costs involved in new product introduction. Advances in computer technology now permit the development of detailed machine performance models with the capability to address a broad range of design and development questions. Model accuracy must approach test measurement accuracy if costly and time consuming full scale testing is to be minimized. However, earthmoving machine performance model accuracy is strongly dependent on methods employed to characterize machine/soil interactions. While some progress has been made, there remains an urgent need for computationally efficient, easy to calibrate models which accurately describe the *transient* response characteristics of soil.

References

Bekker, M.G. (1969) *Introduction to Terrain -Vehicle Systems*, Univ. of Michigan.

Chase, M.A. and Angell, J.C. (1977) "Interactive Simulation of Machinery with Friction and Impact Using DRAM*", *SAE*, No. 770050

Hornbrook, S.L. (1992) *Internal Research Report*, Caterpillar, Inc.

Huck, F.B. (1987) *Internal Research Report*, Caterpillar, Inc.

Kacigen, V.V. and Guskov, V.V. (1968) "The Basis of Tractor Performance Theory", *Journal of Terramechanics*, Vol. 5, No. 3, pp. 43-66.

*DRAM - Dynamic Response of Articulated Machinery, Mechanical Dynamics, Inc., Ann Arbor, Michigan

Rigid Body Dynamics Model

of

Earthmoving Tracked Machine

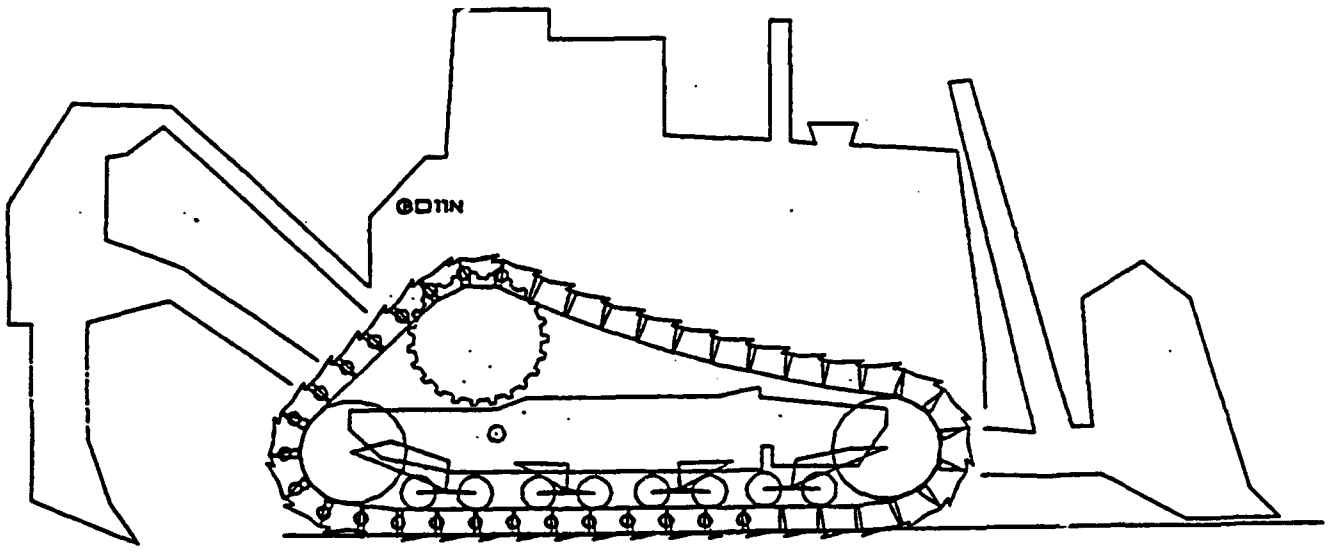

Figure 1

TRACKED VEHICLE DYNAMICS MODEL

EXPLODED VIEW SHOWING COMPONENTS
MODELED AS INDIVIDUAL RIGID BODIES

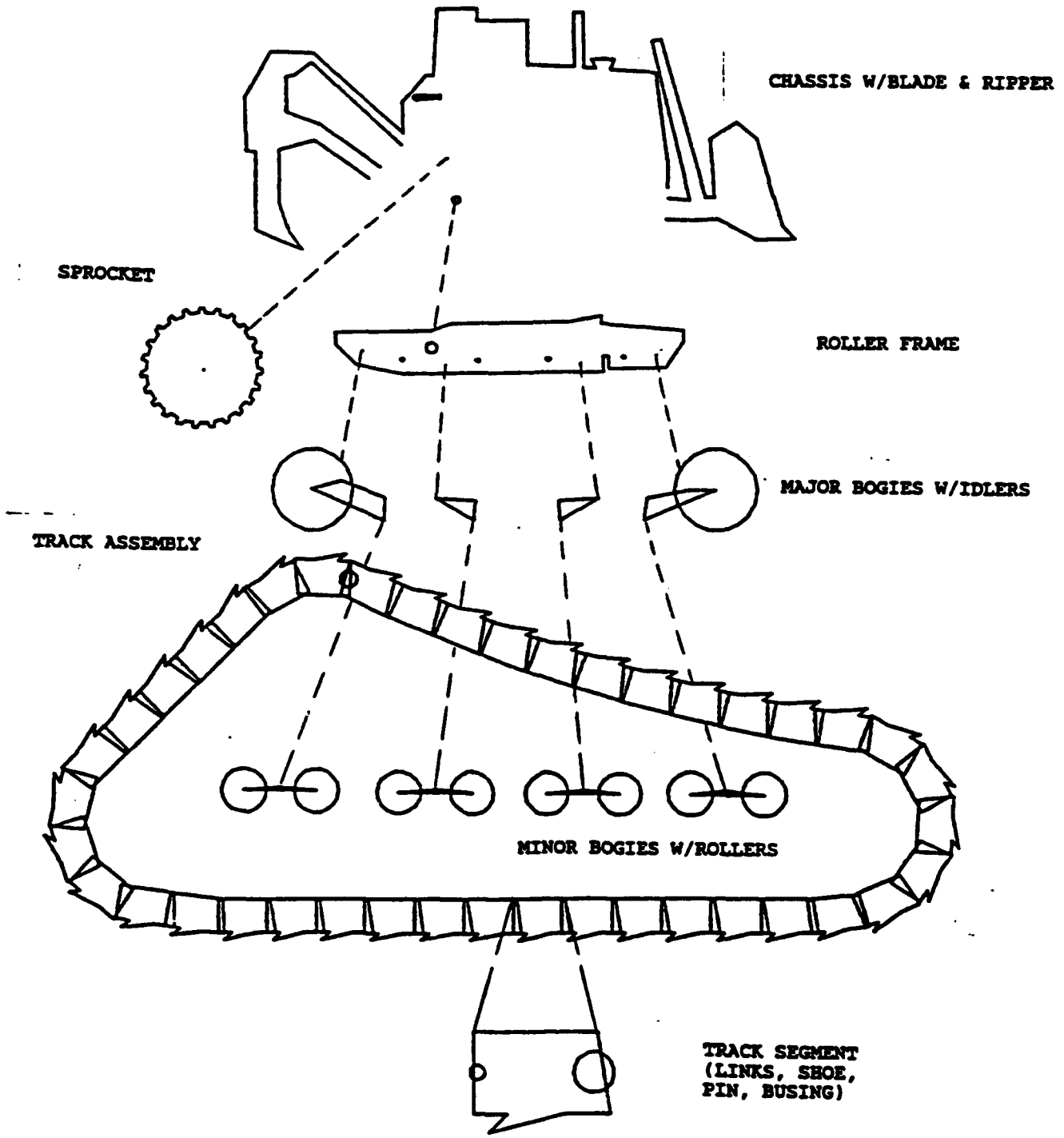

Figure 2

Sensitivity of Predicted Machine Response to Traction Model

Translational Velocity of Main Frame C.G.

D8L – 0.845 m/s Track Speed – 1 E5 Nt. DBP

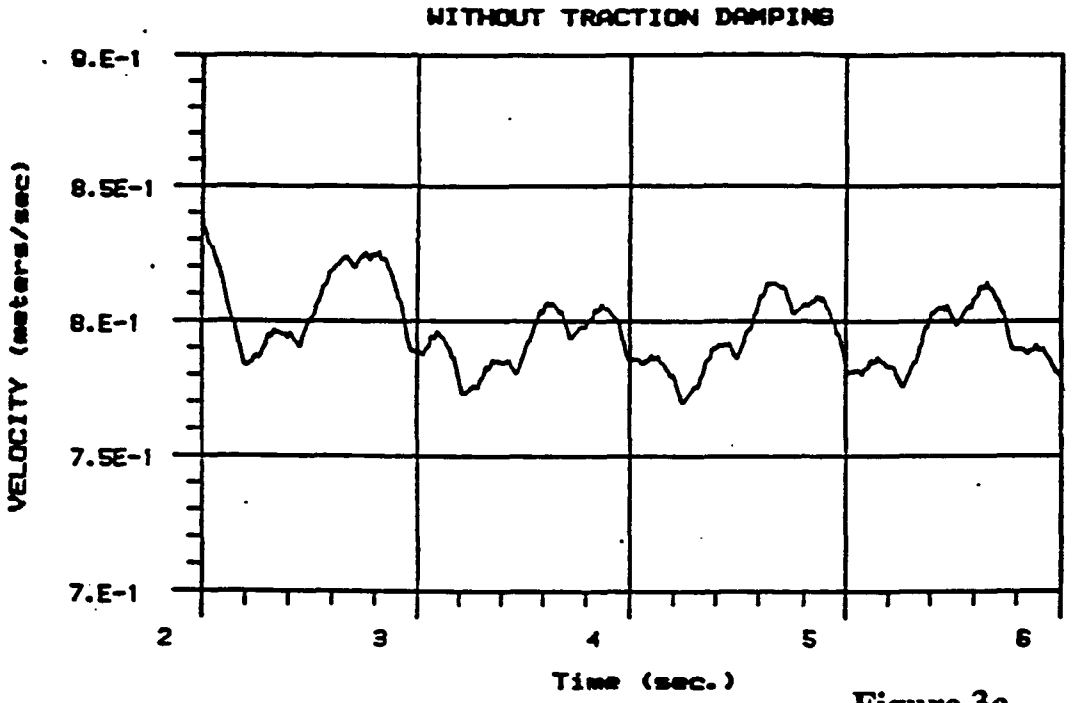

Figure 3a

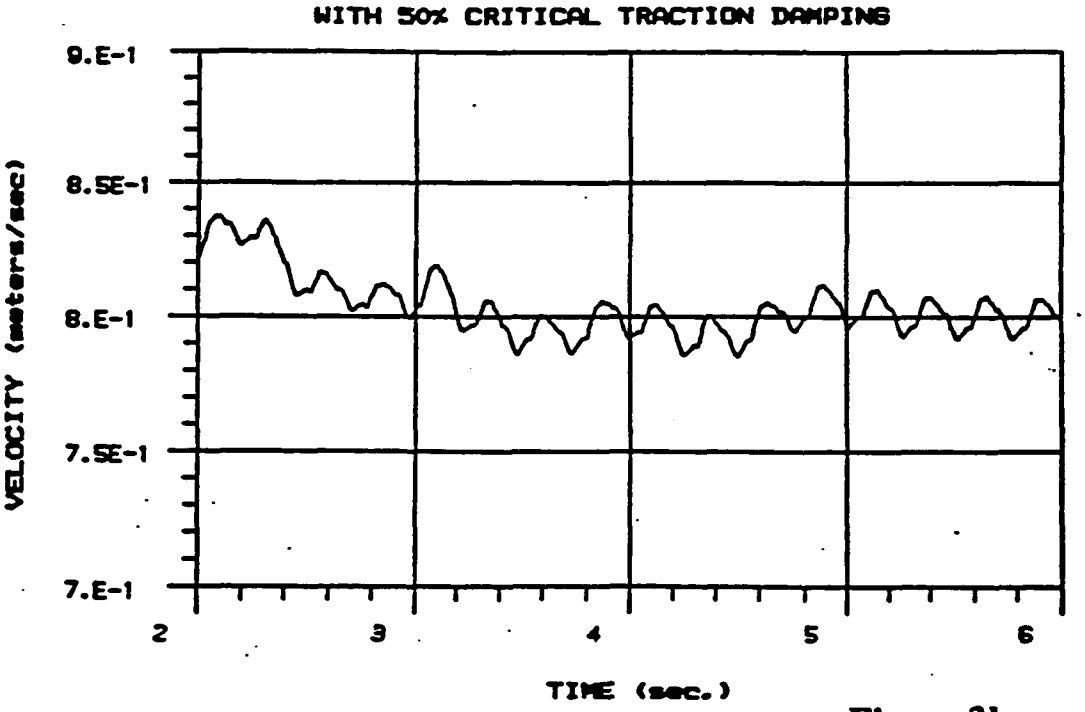

Figure 3b

Measured Scalloped Track Induced Frame Accelerations

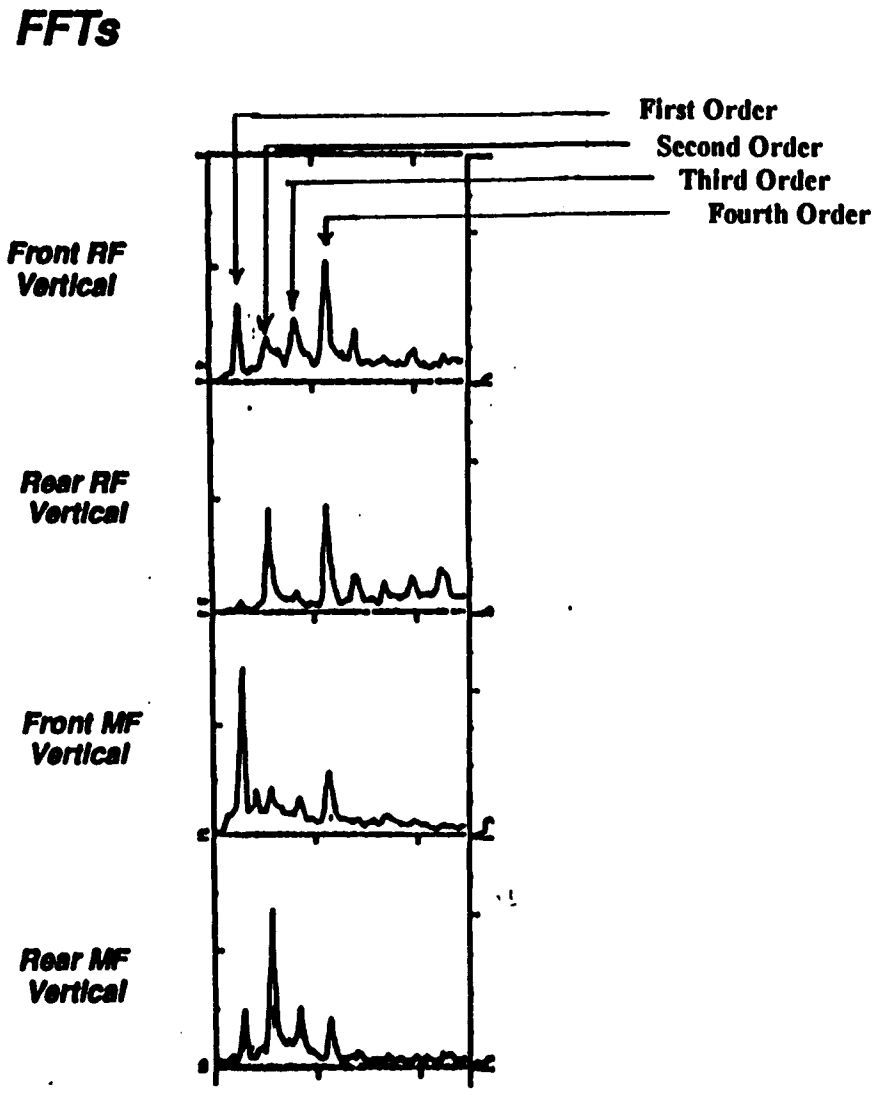

Figure 4

Model Predictions of Scalloped Track Induced Frame Accelerations

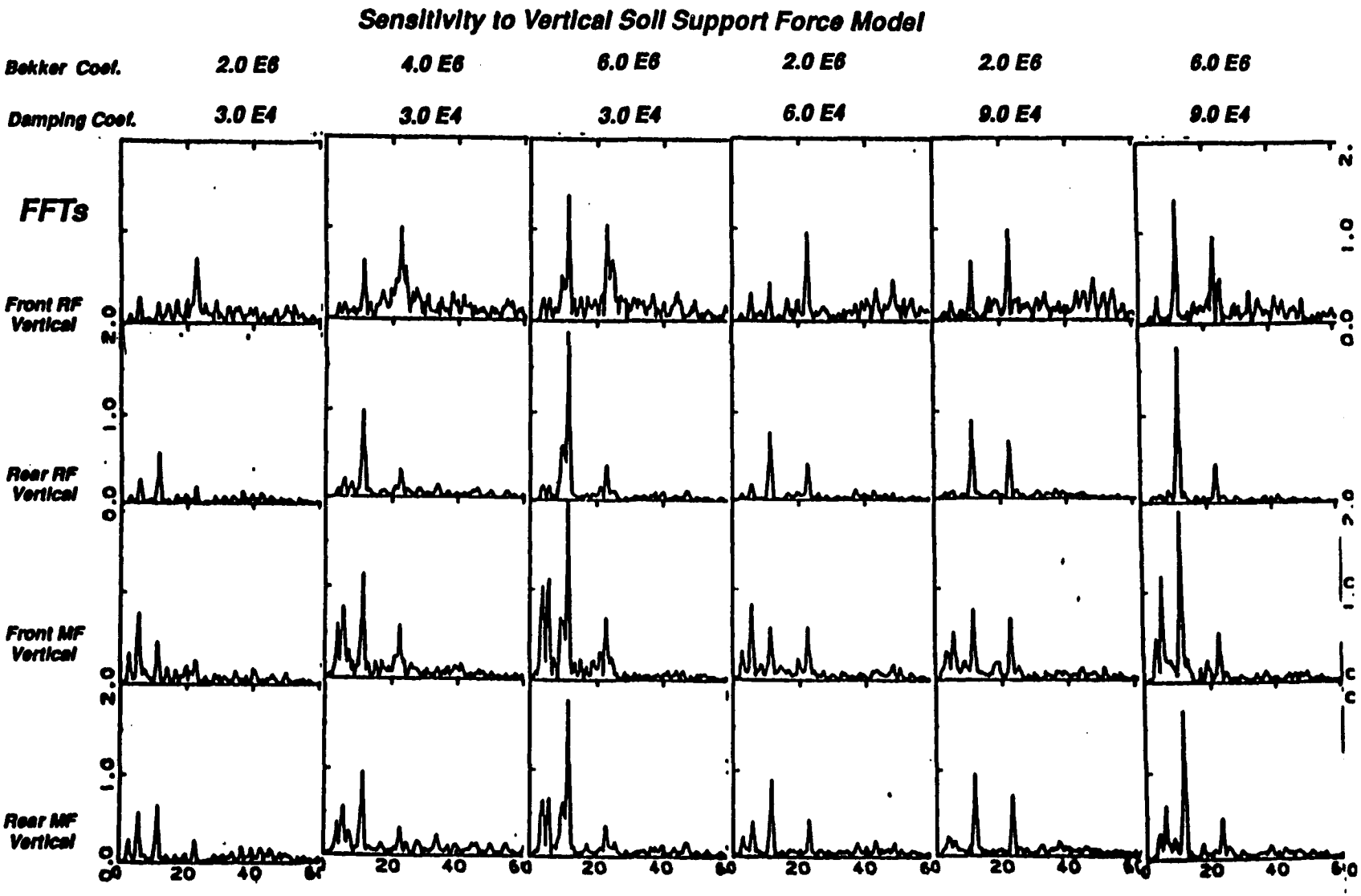

Figure 5

VISCO-PLASTIC-ELASTIC MODEL PREDICTION
PLASTIC SOIL
MEAN LOAD: 54 LB
AMPLITUDE: +/-27 LB AT 0.5 HZ

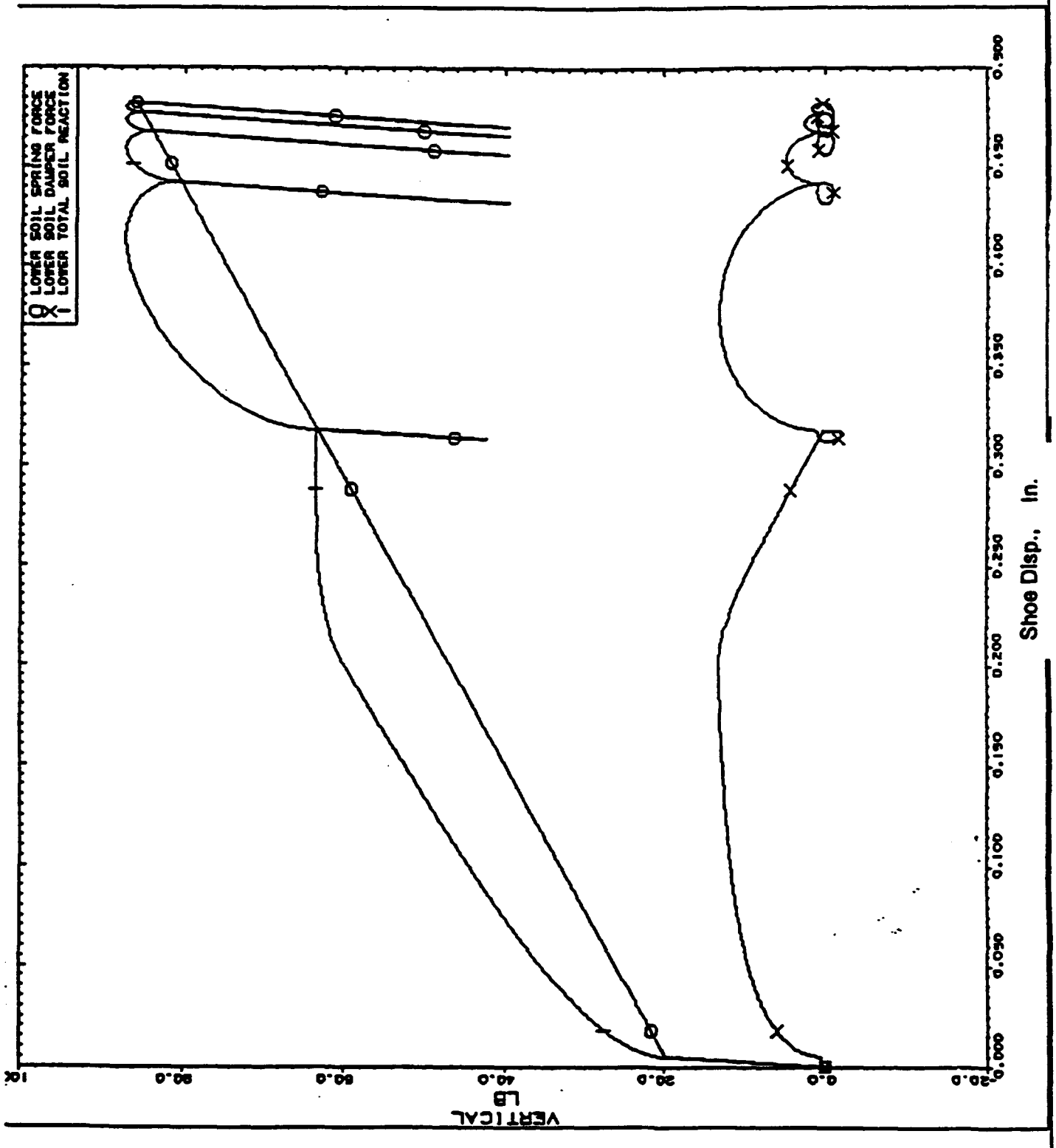

Figure 6

DYNAMIC SOIL RESPONSE TEST RESULTS
PLASTIC SOIL
MEAN LOAD: 54 LB
AMPLITUDE: +/-27 LB AT 0.5 HZ
10.00
8.00
6.00
4.00
2.00
0.00
S.S. VERT LBS. E 1
0.000000 -1.000000 -2.000000 -3.000000 -4.000000 -5.000000 -6.000000
SHOE DISP IN E -1

Figure 7

Prediction of Soil Compaction Behavior

Clarence E. Johnson, Alvin C. Bailey, and Randy L. Raper[1]

Introduction

Our research interests include the development of mathematical models of soil compaction behavior (constitutive relations) of agricultural topsoil necessary for prediction of stress propagation in the soil and resulting state of compactness. The source of the force systems which influence compaction may come from field machinery moving over the soil surface or through the soil beneath the surface. The initial state of the soil may be very loose (following a tillage operation) and it is often unsaturated either before or after application of the force system. The state of soil compactness influences vegetative response, soil erosiveness and degradation, and other utility of our natural resources.

Prevost (1987) recognized that modern tools, such as computer technology coupled with finite element techniques, provide the potential for solving problems associated with soil behavior of greater complexity than did past historical technology. But, he emphasized that,

> "Further progress in expanding analytical capabilities in geomechanics now depends upon consistent mathematical formulations of generally valid and realistic material constitutive relations."

The goal of our research is to develop a useful model of soil stress-strain-strength behavior to predict satisfactorily soil (and machine) "performance" in circumstances important to production agriculture, forestry and off-road mobility.

Current Status

Schafer *et al.* (1989) summarized the status of our soil compaction modeling effort. Our current deviatoric stress model, described by Bailey and Johnson (1989) is a modification of a previous model (Bailey *et al.*, 1986). For a monotonically increasing stress state, the current model is:

$$\epsilon_v = \ln(\rho_i/\rho) = (A + B\sigma_{oct})(1-\exp(-C\sigma_{oct})) + D(\tau_{oct}/\sigma_{oct}) \qquad [1]$$

where ϵ_v = natural volumetric strain, $\ln(v/v_i)$
ρ, v = bulk density and specific volume at stress state τ_{oct} and σ_{oct}
ρ_i, v_i = initial uncompacted virgin bulk density and specific volume
σ_{oct}, τ_{oct} = applied octahedral normal and shear stresses
A, B, C = compactibility coefficients
D = coefficient for the component of natural volumetric strain due to applied octahedral shearing stress.

The two idealized boundary conditions of (1) zero strain at a zero stress state and (2) linearly asymptotic

---

[1]The authors are: Clarence E. Johnson, Professor, Agricultural Engineering Dept., Alabama Agricultural Experiment Station, Auburn University, AL., Alvin C. Bailey and Randy L. Raper, Agricultural Engineers, National Soil Dynamics Laboratory, USDA-ARS, Auburn, AL.

at high hydrostatic stress states, proposed by Bailey *et al.* (1984, 1986), are maintained in this model. This model (equation 1) has an upper bound of octahedral shear stress at which plastic flow (strain at constant volume) is initiated described by:

$$\tau_{oct_y} = K\sigma_{oct} \qquad [2]$$

where τ_{oct_y} and σ_{oct} are stress values at maximum density and K is a coefficient representing

when yield is initiated by plastic flow. This follows the Drucker-Prager failure criteria with an intercept of zero (Desai and Siriwardane 1984).

Fig. 1 presents bulk density data from two Norfolk sandy loam samples displayed as a function of the octahedral stress ratio, τ_{oct}/σ_{oct}. The two straight lines representing the two different octahedral normal stress levels have the same slope. The evaluation of straight line slopes at all levels of octahedral normal stress indicated that the slope was independent of level of octahedral normal stress.

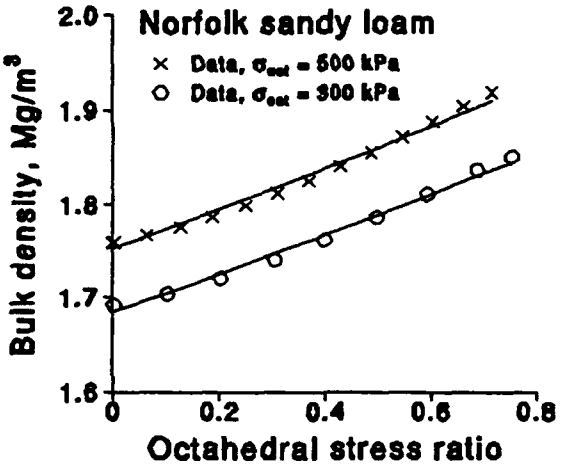

Fig. 1. Deviatoric loading portion of two Norfolk sandy loam tests as a function of the octahedral stress ratio.

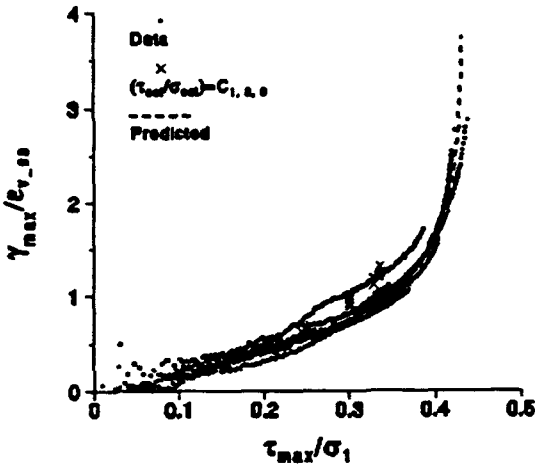

Fig. 2. Typical natural shearing strain ratio data for Hiwassee clay.

A shearing strain model for soil that includes soil behavior under compressive normal and shear stresses great enough to attain maximum compaction was developed (Johnson and Bailey, 1990). Representative data for the ratio of maximum natural shear strain to the volumetric strain occurring after application of shear stress versus the ratio of maximum shear stress to major principal stress are shown in Fig. 2. The maximum natural shearing strain, γ_{max}, was defined as the difference between the major and minor principal natural strains according to Ludwik in 1909 as reported by Hoffman and Sachs (1953). The data in Fig. 2 are for six stress loading paths and include data for three stress loading paths ($\tau_{oct}/\sigma_{oct} = C_1, C_2, C_3$) from Grisso *et al.* (1987). The volumetric strain occurring after application of shear stress in the ordinate term appears to account for much of the stress loading path or stress history effect. These data (Fig. 2) suggest that one form of the relationship is:

$$\tau_{max}/\sigma_1 = K' (1 - \beta \exp(-h\, \gamma_{max}/\epsilon_{v\_oct})) \qquad [3]$$

This relationship form with alternative "variables" of τ_{oct}/σ_{oct} and $\gamma_{oct}/\epsilon_{v\_oct}$, which appears to be more

compatible with variables in equations 1 and 2, is being investigated. Four soils, Decatur clay loam (Rodic Paleudults), Hiwassee sandy loam (Typic Rhodulults), Hiwassee clay (Typic Rhodulults, formerly classified as Lloyd clay), and Norfolk sandy loam (Typic Paleudults) from the NSDL soil bins were used to develop these models.

At first glance these model results may appear quite different than "critical state" concepts and resulting cam clay and cap models as reported in the literature (Roscoe *et al.* (1958) and Desai and Sirwardane (1984)) that were developed for saturated soils using the concept of effective stress. However, equations 1 and 2 geometrically represent a three-dimensional surface, illustrated in Fig. 3, which is similar to the "critical state" surface described by Roscoe *et al.* (1958). Fig. 4 illustrates a form of a cap model which is bounded by equation 2 and equation 1 with the natural volumetric strain being held constant (plastic flow condition) at a value caused by a hydrostatic stress of 500 kPa and $\tau_{oct}/\sigma_{oct} \leq K$ (equation 2).

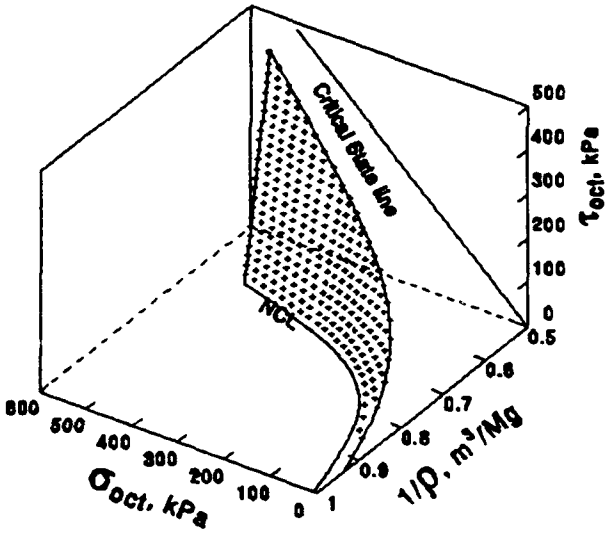

Fig. 3. Surface represented by models (Equations 1 and 2) for Hiwassee clay.

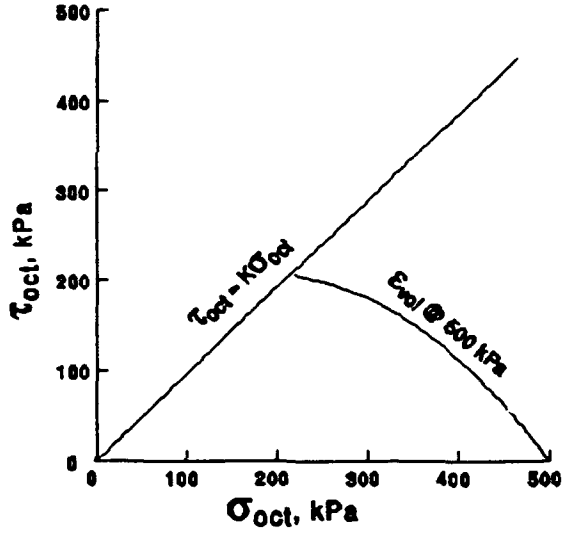

Fig.4 Projection of model boundaries on the octahedral stress plane at a constant volumetric strain for Decatur clay loam.

Future Plans

Elastic rebound properties will be determined from data currently being collected and analyzed for repeated loading and unloading in a conventional triaxial cell using two different stress paths (constant σ_{oct} and constant cell pressure) (Johnson *et al.*, 1992). These additional elastic rebound properties and tensile stress-strain-strength characteristics are needed to fully implement an elasto-plastic or "critical state"-cap type finite element model of the soil behavior.

The role of the intermediate principal stress will be investigated using apparatus designed and developed by Gibas *et al.* (1993). This will test the validity of the models developed from use of conventional triaxial cell (an axisymmetric stress state) for true three-dimensional stress states.

References

Bailey, A.C., C.E. Johnson, and R.L. Schafer (1986) "A model for agricultural soil compaction", *J. agric. Engng Res.* 33:257-262.

Bailey, A.C. and C.E. Johnson (1989) "A soil compaction model for cylindrical stress states", *TRANSACTIONS of the ASAE* 32(3):822-825.

Desai, C.S. and H.J. Sirwardane (1984) *Constitutive Laws for Engineering Materials with Emphasis on Geologic Materials*, Prentice-Hall, Inc., Englewood, NJ.

Gibas, D.M., R.L. Raper, A.C. Bailey, and C.E. Johnson (1993) "Cubical pneumatic cushion triaxial soil test unit", *TRANSACTIONS of the ASAE* 36(6):1547-1553.

Grisso, R.D., C.E. Johnson, and A.C. Bailey (1987) "The influence of stress path on distortion during soil compaction", *TRANSACTIONS of the ASAE* 30(5):1302-1307.

Hoffman, Oscar, and George Sachs (1953) *Introduction to the Theory of Plasticity for Engineers*, McGraw-Hill Book Co., Inc. New York.

Johnson, C.E. and A.C. Bailey (1990) "A shearing strain model for cylindrical stress states", *Amer. Soc. of Ag. Engineers, Paper No.* 90-1085.

Johnson, C.E., A.C. Bailey, and E. Cakir (1992) "Understanding soil response to multiple loading", *Amer. Soc. of Ag. Engineers, Paper No.* 92-1051.

Prevost, J.H. (1987) "Modeling the behavior of geomaterials", In *Geotechnical Modeling and Applications*, ed. S.M. Sayed, Gulf Publishing Co., Houston, TX.

Roscoe, K.H., A.N. Schofield, and C.P. Worth (1958) "On the yielding of soils", *Geotechnique* 9(8):71-83.

FINITE ELEMENT MODELING OF WHEEL PERFORMANCE AND SOIL REACTION AND DEFORMATION

Clarence E. Johnson, Winfred A. Foster, Jr., Sally Shoop and Randy L. Raper[1]

Introduction

Operation of wheeled vehicles over the land, off of developed roadways, is vital to the national security and economy of the United States. For example, part of our national defense relies on transport of supplies and manpower provided by wheeled vehicles in regions where there are minimal or no roadways. Also, our mechanized agricultural and forest industries depend on cost effective and efficient wheeled vehicle and equipment operation on soil without roadways to produce food and fiber for our national economy.

Thus, it is important to develop technology to predict tractive performance of wheeled vehicles and the reaction of soil to wheeled vehicle traffic under a variety of wheel configurations and soil conditions. This technology will aid the design, development and utilization of future wheeled vehicles with improved efficiency, effectiveness and/or economy without adverse environmental impact. This research project was initiated within the past year and has the following progressive objectives as follows:

1. Develop a plane strain finite element model for the analysis of a rigid wheel rolling on the edge of a semi-infinite linearly elastic plane.

2. Develop a plane strain finite element model for the analysis of a rigid wheel rolling on the edge of a semi-infinite elasto-plastic plane.

3. Develop a plane strain finite element model for the analysis of a rigid wheel rolling on the edge of a semi-infinite plane of soil.

4. Expand the objectives 1, 2 and 3 to a full three-dimensional analysis.

5. Expand the objectives 1, 2, 3 and 4 to include a non-rigid wheel where part or all of the wheel could be considered "elastic".

---

[1]The authors are: Clarence E. Johnson, Professor, Agricultural Engineering Dept., Alabama Agricultural Experiment Station, Winfred A. Foster, Jr., Aerospace Engineering Dept., Auburn University, AL., Sally Shoop, Research Civil Engineer, U.S. Army Corp of Engineers, Cold Regions Research and Engineering Laboratory, Hanover, NH and Randy L. Raper, Agricultural Engineer, National Soil Dynamics Laboratory, USDA-ARS, Auburn, AL.

Procedure

All models defined in the objectives will be analyzed using ABAQUS and some will also be analyzed using NASTRAN (finite element software) for comparison purposes. Data collected by Block (1991) at the National Soil Dynamics Laboratory (NSDL), Auburn, AL in two soils with an instrumented powered rigid wheel will be utilized to validate and calibrate the models. These data include data from five pressure cells spaced across the width of the wheel, data from force transducers measuring normal force and tangential force on the face of the wheel in contact with the soil, and stress state data within the soil at two depths beneath the path of the wheel. Data from various kinds of triaxial tests for development of the NSDL-AU constitutive model parameters (Bailey, Johnson and Schafer (1986) and Bailey and Johnson (1989)) are also available for these two soils.

Constitutive models of soil behavior for objectives 3 and 4 similar to the modified Cam Clay, Critical State and the NSDL-AU constitutive models may be utilized.

Current Status

As a starting point, we decided to simulate some circular plate (approx. 18-in dia) and spherical body sinkage data that Raper (1987) had collected in the NSDL soil bins. Data of force vs sinkage and soil stress state at four locations are available. A linear elastic axisymmetric model in both NASTRAN and ABAQUS for the circular plate situation using approximately the same grid size, etc. that Raper had used was developed. This would allow us to easily make comparisons with results from his program also. Deformation loading with a circular plate, without gravitational loading, gave "same" results from all three finite element programs.

Gravitational loading (a stress boundary condition) combined with deformation loading (a "geometry" boundary condition) presented problems in both NASTRAN and ABAQUS. So next, we modeled the soil being loaded with a "massless" steel circular plate on the soil surface with vertical stresses acting near the center of the plate. This approach alleviated the "combined" boundary problem yet allows the soil to experience a deformation like loading since the plate is very rigid compared to the soil.

We found that the combination of non-linear elasticity and axisymmetry requires full 3D model elements. So a 3D grid for an axisymmetric section was developed that could be used in both ABAQUS and NASTRAN. Currently, we're using a non-linear bulk modulus (tangent) data array we developed from hydrostatic soil compaction data in a triaxial cell for the soil used in the "plate sinkage tests" and a constant Poisson's ratio of 0.35. Results from the linear elastic, nonlinear elastic, and elasto-plastic behavior models have similar mean normal stress distributions in the soil which compare favorably with Raper's data in a Norfolk sandy loam soil. Displacements within the soil are under predicted by all three behavior models.

Future Plans

Our next step is to develop interface or contract elements to work with a curved surface. These are the elements between a spherical surface and the soil surface in an axisymmetric model or between a cylindrical surface (rigid "wheel") and the soil surface in plane strain and plane stress models. This should help us when using either deformation or "stress" loading with a "rigid" curved surface at the soil surface.

References

Bailey, A.C., C.E. Johnson, and R.L. Schafer (1986) "A model for agricultural soil compaction", *J. agric. Engng Res.* 33:257-262.

Bailey, A.C. and C.E. Johnson (1989) "A soil compaction model for cylindrical stress states", *TRANSACTIONS of the ASAE* 32(3):822-825.

Block, W.A. (1991) *Analysis of soil Stress under rigid wheel loading Geologic Materials*, Unpublished Ph.D. Dissertation. Auburn University, Auburn, AL.

Raper, R.L. (1987) *Prediction of soil compaction using the finite element method*, Unpublished Ph.D. Dissertation. Iowa State University, Ames, IA.

GENERALIZED JANOSI'S SHEAR STRESS-SLIPPAGE RELATION

Hidenori Murakami[1] and Tatsunori Katahira[1]

ABSTRACT

The authors propose a shear stress-slippage relation for plane slippage in arbitrary directions to furnish a soil-track interaction relation for off-road mobility analyses of tracked vehicles. The relationship is obtained based upon a suite of plate shear tests conducted in a soil bin of loose, dry sand, and generalizes Janosi's shear stress-slippage relation proposed for slippage in longitudinal as well as lateral directions.

DESCRIPTION OF EXPERIMENTS

In order to develop a model for shear stress-slippage relation for tracks, plate shear tests were conducted in a soil bin filled with dry, loose sand (Fig. 1a). Two types of plates -- with and without grousers -- of width 8 cm and length 42 cm were tested. The grouser pitch is 2 cm and the height is 0.7 cm (Fig. 1b). A special load cell was employed to measure two shear force components under prescribed slippage, slip velocity, and normal force. The slip angle, θ, is measured from the longitudinal (x_1-) axis of the track in the clockwise direction in the plan view. For a prescribed set of slip direction, slip velocity, and normal force, the shear force components in the direction of slippage, Q_s, and in the transverse direction, Q_t, were measured along with the sinkage.

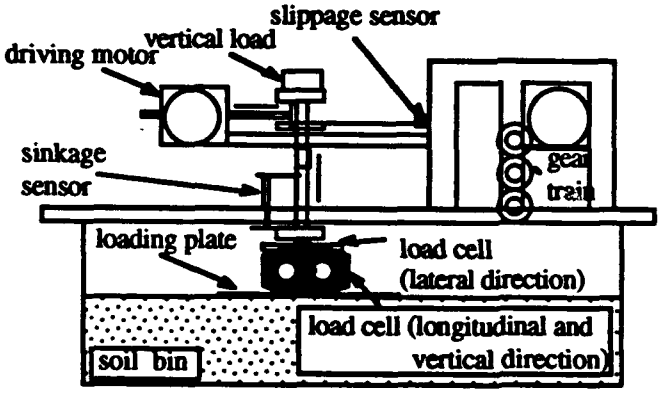

Fig. 1a The shear test apparatus

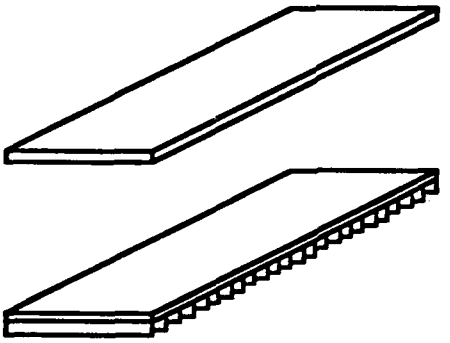

Fig. 1b Loading plates

EXPERIMENTAL DATA AND ANALYSES

Experimental Results

The shear force components and sinkage were measured for monotonic slippage in the slip directions, $\theta = 0°$ (longitudinal slippage) to 90° (lateral slippage) for every 15°at constant slip velocity, 0.3 cm/s. For a plate with grousers, the shear force components, Q_s versus slippage

[1]Department of Applied Mechanics and Engineering Sciences, University of California at San Diego, La Jolla, CA 92093-0411

and Q_t versus slippage, for the same slip directions are illustrated, respectively, in Figs. 2a and 2b. Similar results were obtained for a plate without grousers.

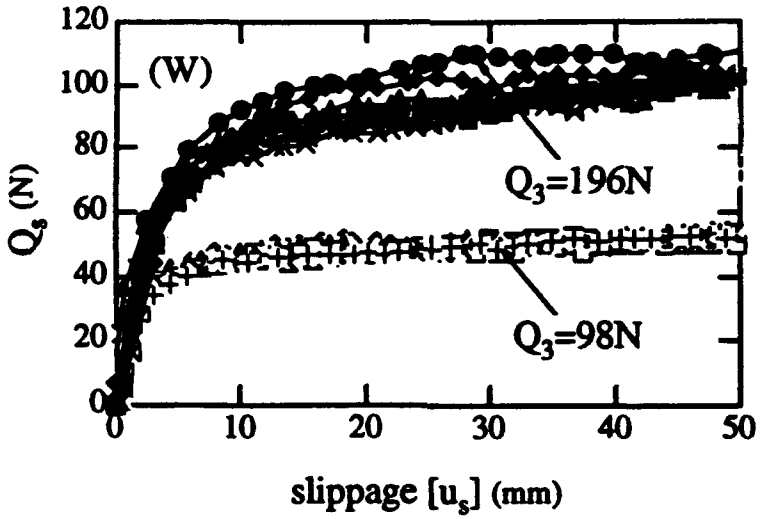

Fig. 2a Shear force component Q_s versus slippage for a flat plate with grousers

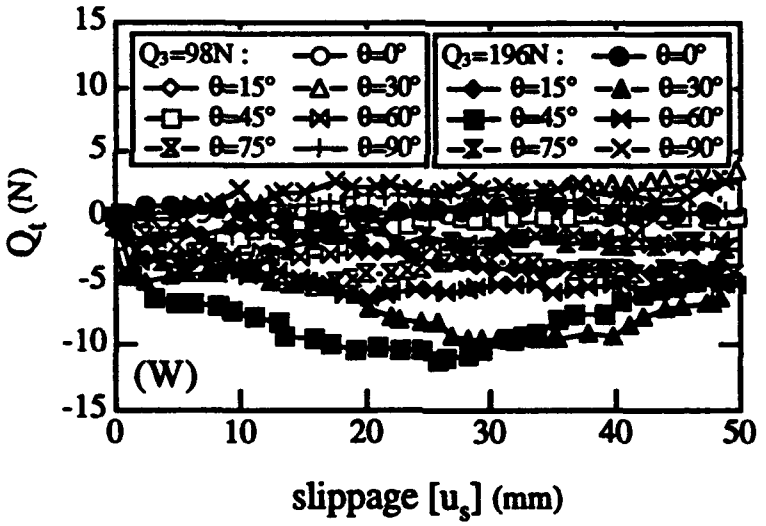

Fig. 2b Shear force component Q_t versus slippage for a flat plate with grousers

For longitudinal and lateral directions (θ=0° and θ=90° respectively) the shear force component, Q_t, vanishes as shown in Fig. 2b. The monotonic loading curves in the longitudinal and lateral directions were described by Janosi and Hanamoto (1961) as

$$Q_{eff} = Q_y(Q_3)\{1-\exp\{-\beta[u_{eff}]\}\} \quad (1)$$

where Q_{eff} is the shear force in the slip direction, Q_y is the critical shear force, $[u_{eff}]$ is the slippage, and β is a constant. The critical shear force Q_y increases with increasing normal force Q_3.

For other slip directions Q_t changes with slip directions. The comparisons of Figs. 2 with the results without grousers have revealed that, indeed, the plate with grousers exhibits orthotropic

dependency of shear force-slippage relations. The objective of this paper is to establish appropriate definitions of Q_{eff} and $[u_{eff}]$ so that all curves in Figs. 2 can be deduced from a single master curve.

Slip Surface in the Interaction Shear Force Plane

In order to find the shape of the critical slip surface in the interaction shear force plane, the shear forces Q_s and Q_t are transformed into the track axial and lateral components, Q_1 and Q_2, according to the coordinate transformation between the x_1, x_2 coordinate system attached to the track and the s, t coordinate system which described the slippage and transverse directions. The slippage [u] is also decomposed into the x_1 and x_2 components, $[u_1]$ and $[u_2]$.

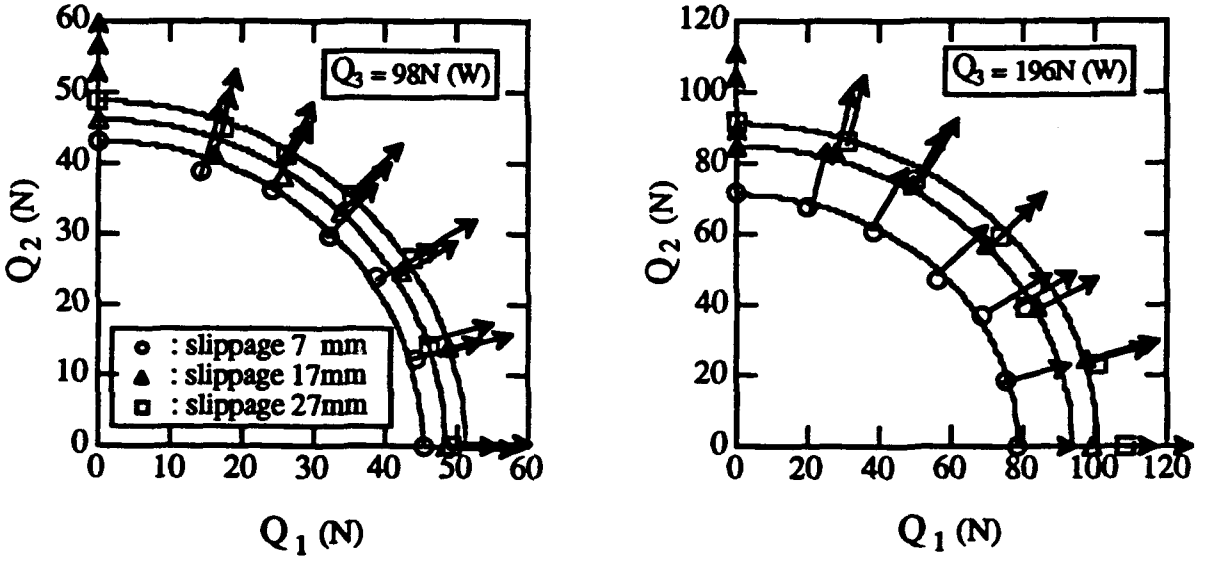

Figs. 3 Loading Surfaces for the loading plate with grousers under Q_3=98N and 196 N

Figures 3 show the loading surfaces, at plastic slippage 7 mm, 17 mm, and 27 mm, in the shear force plane for the plate with grousers, for the normal force Q_3 = 98N and 196 N. The experimental data for both Q_3 = 98N and 196 N show that loading surfaces in the Q_1 and Q_2 plane can be described by ellipses. The arrows of plastic slip velocity plotted on the loading surface show that plastic slip velocity is normal to the loading surface.

Generalized Janosi's Shear Force-Slippage Relation

For an arbitrary plane slippage, the effective shear force Q_{eff} is introduced:

$$Q_{eff} = \sqrt{(Q_1)^2 + (\kappa Q_2)^2} \ , \tag{2}$$

where κ represents the ratio between the longitudinal critical shear force and the lateral critical shear force. Equation (2) describes an elliptical loading surface in the interaction shear force plane.

In order to account for irreversible slippage observed after unloading, the slip velocity is decomposed into elastic and plastic parts denoted by $[V_i]^{el}$ and $[V_i]^{pl}$. From the normality of the slip velocity to each loading surface the following effective slip velocity is employed:

$$[\dot{u}_{eff}] = \sqrt{([V_1]^{pl})^2 + (\frac{1}{\kappa}[V_2]^{pl})^2} \ . \tag{3}$$

Figures 4 show the data in Figs. 2 expressed with respect to the above effective quantities. The effective shear stress is defined as $\tau_{eff} = Q_{eff}/A$ where A is the contact area of the loading plate. The results show that all the curves in Figs. 2 collapse nicely with the effective shear force and slippage, and the collapsed loading curves are described by Janosi's monotonic loading curve (1).

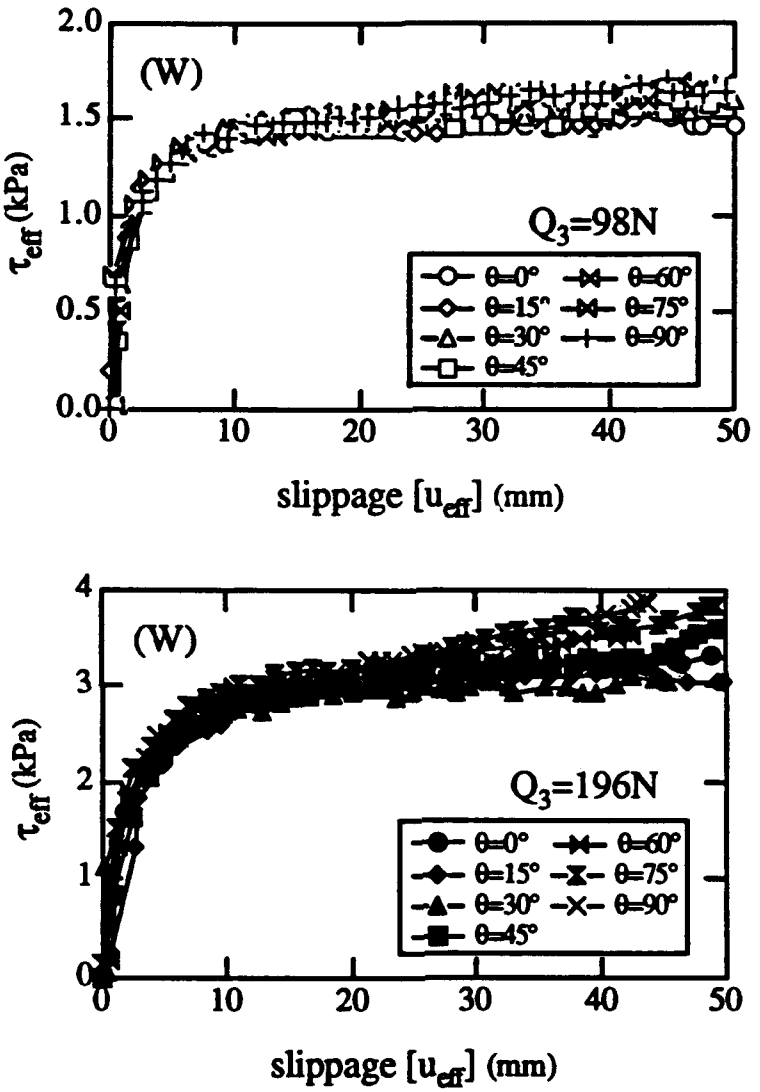

Figs. 4 The effective shear force-slippage relation for the loading plate with grousers under Q_3=98N and 196 N

REFERENCES

Janosi, Z., and B. Hanamoto, The analytical determination of drawbar pull as a function of slip for tracked vehicles in deformable soils, Proc. of the 1st International Conference on the Mechanics of Soil-Vehicle Systems, Torino, Italy, p. 707 (1961).

Modeling The Mechanics Of Off-Road Mobility Workshop

Technical Notes

Submitted By

Mark D. Osborne
Keweenaw Research Center
Michigan Technological University

Introduction

At KRC our main area of mobility research and development has been in off-road terrains in cold climates which includes shallow snow, deep snow, thawing soils, compacted snow and ice. We have done some modeling, field validation and development of devices for characterizing the different terrain materials. The following is a brief summary of the areas that we have been involved with in the past.

Modeling - KRC has run the NRMM for several clients over the past several years and have worked with CRREL and WES in the development and validation of the Shallow Snow Model for the NRMM.. We have developed a simple vehicle countermobility model in snow. KRC also has a group that has developed a sophisticated thermal signature model of the terrain and vehicles which has been widely distributed among Army and Air Force users. Overall, KRC has had a minimal amount of experience in developing new mobility models.

Field Validation and Evaluation - KRC has a tremendous amount of experience in evaluating vehicles for mobility performance in winter terrains (and validating model predictions). We have tested many military tracked vehicles ranging from a snowmobile up to the M1A1 tank. KRC has also evaluated several wheeled vehicles ranging in size from small jeeps up to 5 ton trucks. We jointly participated in the "Wheels vs Tracks" project with CRREL and WES. KRC has been involved in unique projects such as a comparison between a standard wheeled MK48 and a prototype version utilizing the Caterpillar Mobil Trac System. We have tested vehicles with anti-lock brakes, various traction systems and CTIS. Types of tests conducted in the past have included drawbar pull, motion resistance, mobility evaluations, slope climbing, side slope evaluation, acceleration, braking and handling. Although the majority of our testing experience has been in winter terrains, especially snow and ice, the multi season/ terrain capability of several vehicles has been evaluated. The wide range of vehicles, terrains, and tests has resulted in KRC developing expertise in instrumentation, data acquisition, data processing and validation. Current equipment includes a wide range of sensors and transducers, portable computerized data acquisition systems and telemetry systems. Finally, our work in the winter mobility area has resulted in the design, development and testing of ice cleats for the Marine Corps LTV-P7 and the M1A1 Abrams tank.

Terrain Characterization - KRC has performed various soil property measurements including use of the cone penetrometer but mobility in soils has not been our main area of interest. Snow is another story. KRC was one of the first to build a bevameter including both the shear and compaction device. We have used several snow density kits and developed one of our own. We have also used the Ramsonde, Canadian snow hardness gauges, several types of free water content methods and coefficient of friction or traction devices for characterization of snow. KRC has designed and built a portable bevameter as well. Currently, KRC is testing a CRREL developed load frame device for characterizing snow. On ice, we have used a friction tester for measuring the coefficient of friction of the ice. KRC has also conceptualized a design for an ice strength measurement device but has never fully designed or fabricated one. Thus far, we have not been able to find any other organization interested in measuring the strength of ice. As far as KRC is concerned, when we develop a traction aid for a tracked vehicle and test two or more designs on two or more different days we need to know the characteristics of the ice. Ice tends to change and coefficient of friction is not useful because the ice cleats dig in to the ice. Penetration and shear strength are the important parameters with traction devices for ice.

Future Areas Of Interest

We are currently working with vehicles that have anti-lock brakes, various traction control systems, central tire inflation systems and independent suspensions. It has always appeared that people have considered vehicle dynamics modeling separate from vehicle mobility modeling. At KRC, we would like to bring the vehicle dynamics closer to mobility modeling for modeling ABS and TC systems in off-road winter terrains. This will require being able to input deformable terrains into a dynamics model. A better tire model is also required. Some tire models are known but most are not considered ideal. We know that some companies, i.e., tire companies and some of the ABS and auto companies have better tire models but they don't want to release them because they have put all their resources into it and consider them proprietary information. "Good" tire models for hard pavement may be insufficient for off-road modeling. Our future efforts will include attempting to use the models of deformable terrain in the dynamics models.

USING THE FINITE ELEMENT METHOD TO PREDICT SOIL STRESSES BENEATH A RIGID WHEEL

R.L. Raper[1], C.E. Johnson[2], A.C. Bailey[1], and E.C. Burt[1]

Introduction

The objective of this experiment was to investigate the ability of the finite element method to predict soil stresses beneath a rigid wheel in two soils and in two soil conditions. An experiment was conducted in the soil bins at the National Soil Dynamics Laboratory (NSDL) during which the transducers were used to measure soil stress beneath the rigid wheel. Two different constitutive relationships for soil were compared to determine which modeled actual soil behavior the closest. Soil stress measurements were then compared to results predicted with the finite element method.

Procedure

The plane strain assumption was used to model the rigid wheel. The rigid wheel must be visualized as infinitely wide to understand this assumption. This of course is not true, but the stresses beneath the center of the rigid wheel should not differ greatly from those beneath an infinitely wide cylinder.

Modeling the soil matrix is the most difficult problem being confronted by soil compaction researchers. This non-homogeneous, non-linear, elastic-plastic, particulate medium makes exact solutions impossible. Assumptions must be made about its previous history, the existence of clods, and the location of hard pans. Neglecting these problems and treating the soil as a homogeneous medium has allowed some limited successes in soil compaction modeling. A model has been developed that relates the volumetric strain to the applied hydrostatic stress (Bailey *et al.*, 1984).

$$\epsilon_v = (A+B\sigma_{hyd})*(1-e^{(-C\sigma_{hyd})}) \quad (1)$$

where ϵ_v = volumetric strain, (change in volume / original volume)
σ_{hyd} = hydrostatic stress, kPa
A, B, and C = compactibility coefficients established by fitting data to equation.

---

[1]USDA, ARS, National Soil Dynamics Laboratory, Auburn, AL 36831, U.S.A.

[2]Agricultural Engineering Department, Alabama Agricultural Experiment Station, Auburn University, AL 36849 U.S.A.

The hydrostatic soil compaction model assumes that all stresses surrounding a soil particle exerted equal forces on this particle. Of course this assumption does not allow for the development of unequal directional stresses which create shear. These shear stresses have been shown to increase the magnitude of soil compaction. A model has been developed that improves on the hydrostatic soil compaction model to include the effects of shear stress (Bailey and Johnson, 1990).

$$\bar{\epsilon}_v = (A+B\sigma_{oct})*(1-e^{(-C\sigma_{oct})})+D(\frac{\tau_{oct}}{\sigma_{oct}}) \quad (2)$$

where $\bar{\epsilon}_v$ = natural volumetric strain, ln (change in volume / original volume)
σ_{oct} = octahedral normal stress, kPa
τ_{oct} = octahedral shearing stress, kPa
D = another compactibility coefficient

This model is similar to Equation 1 except for the addition of the shearing stress component and the use of the natural strain definition. Limitations were placed on the shearing stress component in the above model to indicate maximum density at plastic flow. The restricting relationship is:

$$\tau_{oct_y} = K\sigma_{oct} \quad (3)$$

where τ_{oct_y} = ultimate shearing stress at maximum density
K = coefficient representing soil plastic flow yield

Although the soil constitutive equations have been given, much more must be accomplished before they are useable in a finite element model. These equations must be used to predict the linear-elastic parameters, Young's Modulus (E) and Poisson's ratio (ν). Each of these parameters varies with different stress and strain levels in the soil (Duncan and Chang, 1970). For further information regarding the prediction of these parameters using triaxial data see Raper et al. (1992)

The mesh designed to model the soil beneath the rigid wheel is shown in Figure 1 along with a deformed grid overlaid. The exact shape of the rigid wheel was maintained as it came in contact with the soil until it applied the maximum load. Twenty load steps were found to be adequate to allow the model to incorporate the non-linear behavior of soil.

An experiment was performed using the rigid wheel in the soil bins at the NSDL. This wheel (30.5 cm wide and 137.2 cm in diameter) was used in two different soil types, a Norfolk sandy loam soil and a Decatur clay loam soil. The soils were prepared in a uniformly loose state and also with a hard pan. The experiment as reported here involved dynamic loads on the rigid wheel of 5.8 and 11.6 kN. Four replications were performed of each treatment.

Stress State Transducers (SST's) (Nichols *et al.*, 1987) were buried beneath the center of the rigid wheel at a 30 cm depth in the loose soil and on the hard pan in the other treatment. The final depths of the SST's were used to establish the depth that the finite element results would be analyzed.

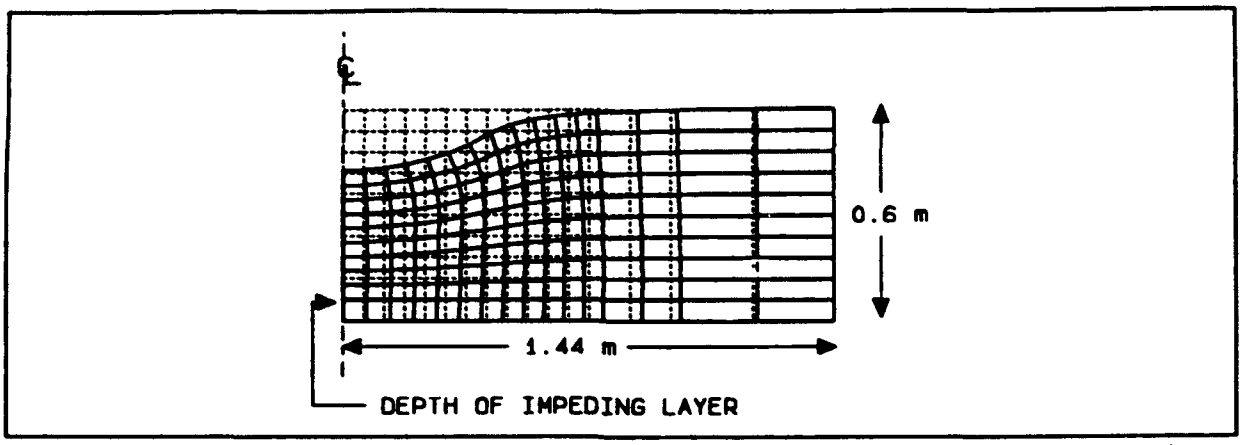

Figure 1. Original finite element mesh and final displaced mesh showing location of impeding layer in Decatur clay loam soil when loosely tilled. Only one half of the soil was modeled beneath the rigid wheel because of symmetry.

Displacements of the soil surface and the transducers were measured at the conclusion of each experimental run. The surface displacement depths were used to load the finite element model in the vertical direction. An average depth of surface displacement was obtained for each treatment and a 95% confidence interval established. Three finite element models were then run; one at the mean value, and one each at the upper and lower 95% confidence intervals.

Penetrometer measurements were made in the soil bins to determine the depth of any impeding layers. In the hard pan treatments, this layer was found at a depth of approximately 36 cm in both the Norfolk sandy loam soil and the Decatur clay loam soil. When the loose soil treatment was used, a root impeding layer was found at a depth of 48 cm in the Norfolk soil and at 54 cm in the Decatur soil. These depths were used to fix the nodes of the finite element mesh to prevent soil movement past this depth.

Results and Discussion

The peak octahedral normal stress and peak major principal stress were investigated to determine if they fit within 95% confidence intervals of stress determined from the SST's. When examining the octahedral normal stresses (Figure 2), the hydrostatic model seems to be the better model if only the lower loads are considered. This result may be reasonable because of the lack of shear stress that is developed at the low load levels, which the hydrostatic model does not account for. When considering the high load treatment, however, neither model was able to predict the stresses with much certainty, especially in the Norfolk soil.

Major principal stress was predicted with slightly more accuracy (Figure 2). Again at the low load levels, the hydrostatic model fit across both soil types and both soil conditions. At the high loads, the shear stress model fit all of the measured data except the high load treatment in the Norfolk soil. The shear stress model managed to fit all of the data in the Decatur soil, both low and high loads.

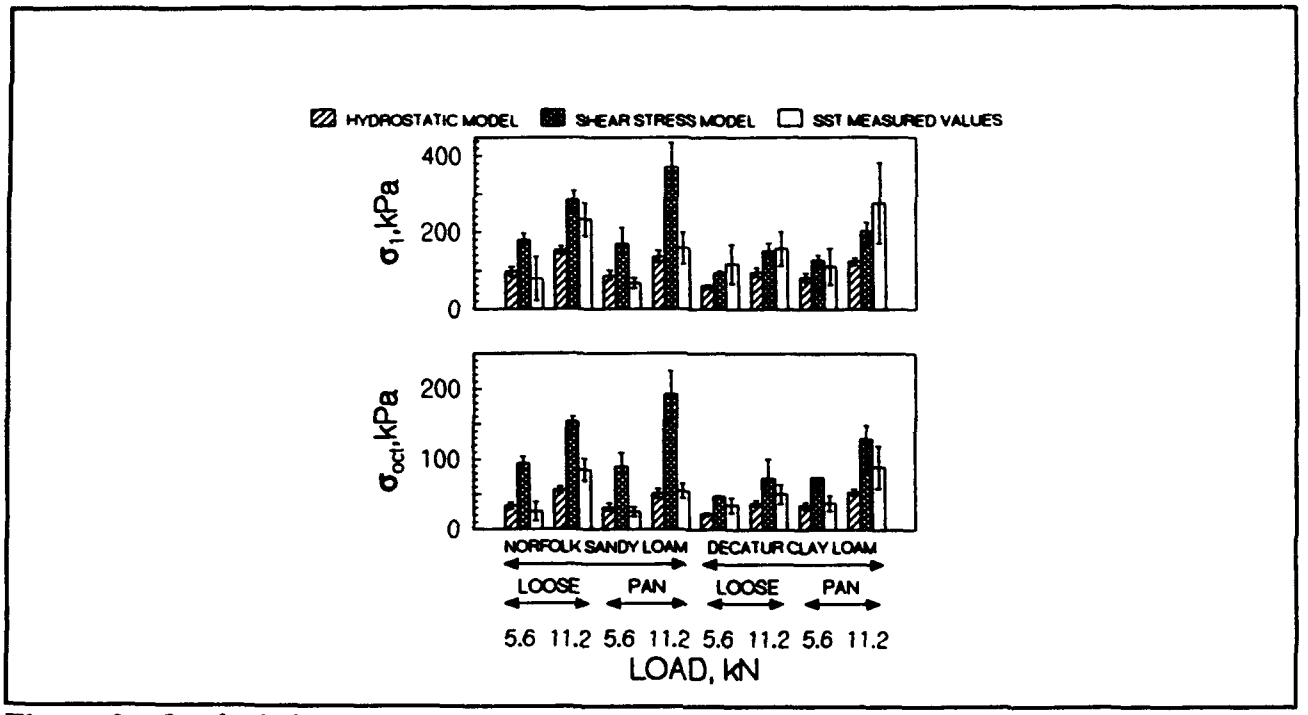

Figure 2. Octahedral normal stress, σ_{oct}, major principal stress, σ_1, and their 95% confidence intervals measured with the SST's plotted against the finite element results.

Continued development of the finite element model is warranted to allow better predictions of soil stress to be accomplished. A true three-dimensional finite element model could enable better predictions to be made. Excessive stress predictions of the shear stress model could be the result of the plane strain assumption. These large stresses could be due to the effect of confining stresses that develop from the rigid wheel being modeled as an infinitely long roller.

References

Bailey, A.C., C.E. Johnson, and R.L. Schafer. (1984) "Hydrostatic compaction of agricultural soils", *Trans. ASAE*, 27(4):952-95.

Bailey, A.C., and C.E. Johnson. (1989) "A soil compaction model for cylindrical stress states", *Trans. ASAE*, 32(3):822-825.

Duncan, J.M., and C.Y. Chang. (1970) "Nonlinear analysis of stress and strain in soils", *J. Soil Mechanics na Foundations Div., Proc. of Am. Soc. Civil Eng.*, 96(5):1629-1653.

Nichols, T.A., A.C. Bailey, C. E. Johnson, and R.D. Grisso. (1987) "A stress state transducer for soil", *Trans. ASAE*, 30(5):1237-1241.

Raper, R.L., C.E. Johnson, A.C. Bailey, E.C. Burt, and W.A. Block. (1992) "Using the finite element method to predict soil stresses beneath .gid wheel", *Proceedings of the 4th North American Regional Meeting of ISTVS*, pp. 144-151.

A Contact Mechanics Approach to the Modeling of Dynamic Soil-Vehicle Interaction

Dr. Antoinette Tordesillas[1]

Introduction

A new approach to the modeling of soil-vehicle interaction is introduced. The interaction at the interface between vehicle and soil is formulated as a dynamic contact problem and is solved using the principles and methodologies of the theory of Contact Mechanics. This approach has two important advantages over existing analytical soil-vehicle interaction models. First, a contact mechanics formulation obviates the need to know *a priori* the stresses or deformations at the soil-vehicle interface. Instead, these interfacial properties are determined using directly and precisely measurable quantities. Second, this formulation avails the analysis of the interfacial phenomena to the comprehensive theories of contact mechanics and tribology, with their proven economic and reliable techniques for establishing detailed information on contact properties. The scope of the field of contact mechanics is extensive. Material models which have been commonly studied span the range from elastic, viscoelastic, elastoplastic, to viscoplastic. In such analyses, various geometric properties and contact configurations of the bodies have been considered, in conjunction with both non-classical and classical Coulomb friction laws. We are conducting a preliminary study on the soil-tire interaction system. In accordance with the studies of Pi (1988), the basic soil behavior under dynamic vehicle passage is considered to be viscoelastic and is represented by a Maxwell-Kelvin 3-parameter model. A new model for the tire is introduced which consist of a three-dimensional circular elastic cylinder, and is based on recently derived stress-displacement constitutive relations unique to the cylindrical geometry. This is a significant improvement to the previously adopted Hertz theory in which the cylinder is idealized and assumed to deform as an elastic half-space. Thus, this new tire model incorporates the pertinent tire curvature and edge effects into the overall soil-tire interaction model.

The Theory of Two-Body Contact Mechanics

The theory of contact mechanics concerns itself entirely with the local interaction phenomena arising at the interface between two bodies which are brought into contact. This emphasis on the contact interface rests on the premise that the conditions therein determine the internal states of each body. Specifically, if the fundamental properties consisting of the contact stresses and deformations, as well as the size and shape of the contact area are known, then the stresses and displacements at any point inside each body can, in principle, be found. The general laws of contact mechanics are summarized below and are illustrated in Figure 1:

1) Compatibility condition: no interpenetration exist between the contacting surfaces, i.e.

$$u_{z1} + u_{z2} + h(x,y) - \delta \begin{cases} = 0, \text{ inside } \Omega, \\ > 0, \text{ outside } \Omega. \end{cases} \qquad (1)$$

where δ is the relative approach of the bodies, Ω is the contact area, $h(x,y)$ is the initial separation of surface points, and u_{zi}(body i=1,2) denote the displacements.

2) No tensile tractions are allowed on contacting boundaries. The normal stress p is compressive and vanishes outside the contact area Ω,

$$p > 0, \text{ inside } \Omega; \quad p = 0, \text{ outside } \Omega. \qquad (2)$$

[1] Department of Mechanical Engineering, Kansas State University

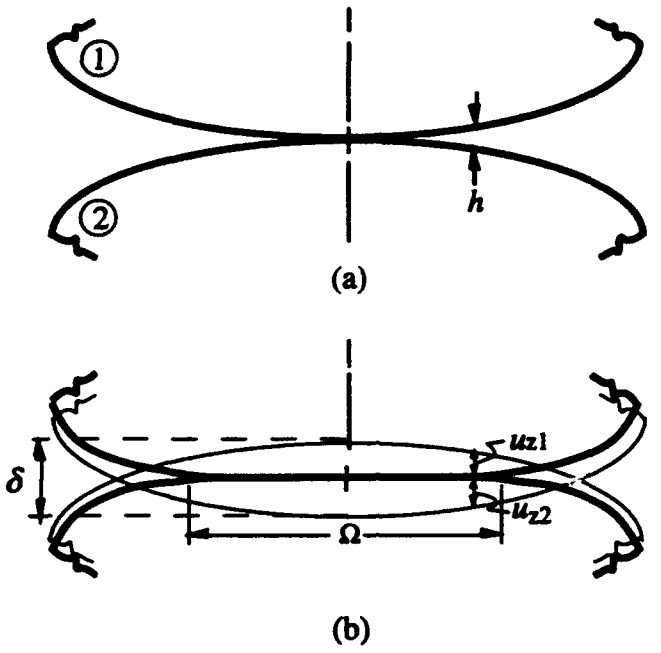

Figure 1. The contact of two deformable bodies: (a) unloaded, (b) loaded.

The tangential stresses q are related to the normal stresses by the appropriate friction law depending on the nature of the contact surfaces. If Coulomb's law is assumed, then two zones of adhesion and slip within the contact area result, viz. Ω_A and Ω_S, respectively, and

$$|q| < \mu p, \text{ adhesion zone } \Omega_A; \quad q = \pm \mu p, \text{ slip zone } \Omega_S; \quad \Omega_A + \Omega_S = \Omega. \tag{3}$$

Solution techniques for various classes of contact problems have been developed which incorporate either finite element or boundary element methods. The finite element, in conjunction with a variational formulation of the contact system, has proved to be the most powerful methodology for solving the more difficult classes of contact problems such as three-dimensional frictional contact. The premise of the variational theory for solid body contact is that the true contact area and the stresses which act therein are those which minimize an appropriate energy function. On this basis, a set of variational inequalities which constitute a minimization problem of functionals can be derived. Specifically, the contact problem can be reduced to a single relation in which the total complementary energy $U^* = f(u_i, p, q, \Omega)$ is minimized subject to the conditions of equations (2) and (3). In a numerical implementation the resulting minimization problem are discretized to yield a system of equations which can be solved using any of the existing mathematical programming techniques of optimization. Clearly, the distinct advantage of this type of formulation is that all boundary conditions, including the contact conditions, are incorporated into a single variational inequality and available minimization routines can be used to solve the problem. Expected results from a contact mechanics model include: size and shape of the contact area, complete surface and subsurface stresses and displacements, boundary bordering regions of slip and adhesion at the contact interface, and the relative approach of the bodies (i.e. sinkage).

Constitutive Stress-Displacement Relations

Of prime importance in a contact mechanics formulation are the body displacements u_z which result from the surface tractions at the contact interface, as called for in the compatibil. y relation of equation (1). It is therefore important that the stress-displacement relation accurately represent the body's response to surface tractions, from the point of view of both its material and geometric properties.

SOIL MASS. The stress-strain behavior of soil is simulated by a standard three-parameter model as in Pi (1988), consisting of a Maxwell spring and a Kelvin element in series as illustrated in Figure 2. It has been shown that an equivalent of the Boussinesq-Cerruti linear elastic relation can be derived for the viscoelastic half-space using the correspondence principle of elasticity (Kalker 1990). This facilitates the calculation of the entire elastic field, viz. the stresses and deformations both on the surface and in the interior of a viscoelastic half-space.

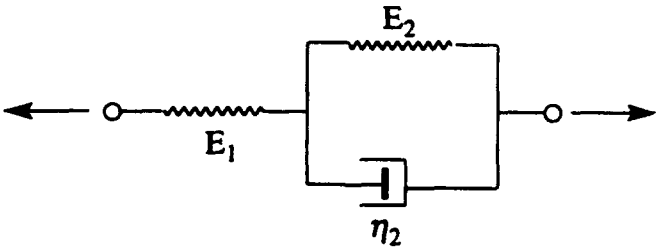

Figure 2. Viscoelastic model for soil; elastic moduli E_1 and E_2, and coefficient of viscosity η_2.

TIRE. For the tire model, we introduce a three-dimensional circular elastic cylinder with diameter and width equal to that of the pneumatic tire to be analyzed. The constitutive stress-displacement relation accounts for both its sectional and longitudinal curvature and dimensions. A recently derived solution for the stress-displacement relation unique to a circular elastic cylinder in a two-body contact system is adopted (Tordesillas and England 1994). This should provide an improvement on models which are based on the Hertz theory in which the curvature of the bodies are ignored. Prior to our work in Hill and Tordesillas (1989, 1992), various simplifications of this type were adopted to the study of cylindrical contact since the important solution for a point force(s) acting on the boundary of a circular elastic cylinder had not been established. Such stress-displacement solutions relating to specific point force systems, as shown in Figure 3(b), yield the constitutive stress-displacement relation for the body under a distributed loading as depicted in Figure 3(a). The procedure is based on the classical superposition principle of linear elasticity, and involves the summation of the point force solutions over the contact area to obtain the corresponding stress-displacement relation for the body subject to a distribution of forces at its boundary. In Hill and Tordesillas (1989), we developed a novel technique to derive exact solutions for various point force systems relating to cylindrical three-body contact problems. The technique is based on complex variable theory and is one that has been recently used to establish the basic solution corresponding to the two-body contact problem. The empirical input parameters for the tire model are: Diameter, Width, Poisson's ratio, ν_{tire} , Young's elastic modulus, E_{tire}. Specifically, the Young's elastic modulus for the tire must be as close as possible to that for the given pneumatic tire, and reflect its particular inflation pressure and carcass stiffness or strength.

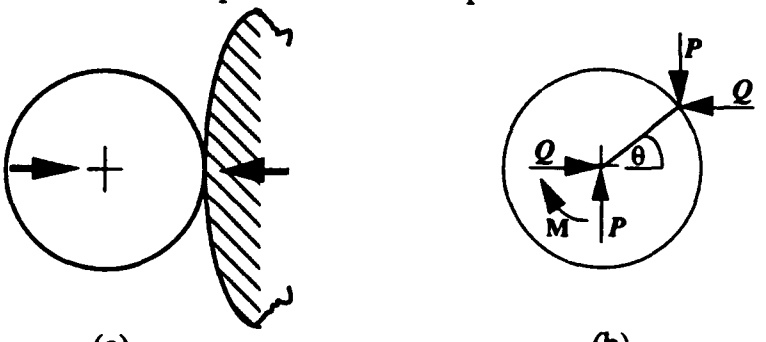

Figure 3. (a) Two-body contact involving a circular elastic cylinder, (b) Basic point-force system.

The phenomenon of stress concentrations arising from 'edge contact' is being studied for the case of a viscoelastic media. Contact stress concentrations which arise from any discontinuities

or significant changes in body profiles manifest themselves as stress singularities when studied within the framework of linear elasticity. A thorough evaluation of the precise structure and order of these singularities was carried out by Comninou (1976) for frictional contact of bodies of various elastic and geometric properties. In certain cases, the appropriate stress concentrations at the edges of a cylinder can be incorporated using the technique employed in Tordesillas and Hill (1991). This technique essentially involves scaling the discretized stresses at each element i, p_i, by the appropriate order of singularity. This procedure has been successfully applied in the design analysis of roller bearings whose edges have been partially rounded at the ends so as to relieve stress concentrations (Ahmadi et al. 1983). We successfully applied it to the analysis of cylindrical steel and rubber-covered steel contact systems (Tordesillas 1991).

References

Ahmadi, N, Keer, L.M. and Mura, T. (1983) "Non-Hertzian contact stress analysis for an elastic half-space-normal and sliding contact", *International Journal of Solids and Structures*, 19, 357-373.

Comninou, M. (1976) "Stress singularity at a sharp edge in contact problems with friction", *Journal of Applied Mathematics and Physics*, 27, 493-499.

Hill, J.M. and Tordesillas, A. (1989) "The pressure distribution for symmetrical contact of circular elastic cylinders", *Quarterly Journal of Mechanics and Applied Mathematics*, 42, 581-604.

Hill, J.M. and Tordesillas, A. (1992) "The symmetrical adhesive contact problem for circular elastic cylinders", *Journal of Elasticity*, 27, 1-36.

Hiroma, T. and Ota, Y. (1990) "Analysis of normal stress distribution under a wheel using a viscoelastic model of soils", Proceedings of the 10th International Conference of the ISTVS, Kobe, Japan.

Kalker, J.J. (1990) Three-Dimensional Elastic Bodies in Rolling Contact, Kluwer Academic Publishers, The Netherlands.

Karafiath, L.L. and Nowatzki, E.A. (1978) Soil Mechanics for Off-Road Vehicle Engineering, Trans Tech Publications, Clausthal, Germany.

Panek, C. and Kalker, J.J. (1980) "Three-dimensional contact of a rigid roller traversing a viscoelastic half-space", *Journal of the Institute of Mathematics and its Applications*, 26, 299-313.

Pi, W. S. (1988) "Dynamic tire/soil contact surface interaction model for aircraft ground operations", *Journal of Aircraft*, 25, 1038-1044.

Tordesillas, A. and Hill, J.M. (1991) "Three-dimensional frictionless contact between layered elastic bodies and incorporating sharp edges", *Journal of Computational Mechanics*, 8, 257-268.

Tordesillas, A. (1991) "A numerical analysis of three-dimensional non-Hertzian contact problems and its application to roller coating", *Australian Mathematical Society Gazette*, 18, 145-150.

Tordesillas, A. and England, A.H. (1994) "The complete stress and displacement field for a linear elastic cylinder subject to a concentrated force at the boundary", to be published.

Tordesillas, A. and Hill, J.M. (1989) "Numerical comparison of pressure distributions for non-conforming line contact between circular elastic cylinders", *Computational Techniques and Applications - 89' Proceedings*, 525-532.

Wong, J.Y. (1989) Terramechanics and Off-Road Vehicles, Elsevier

Wong, J.Y. (1991) "Some recent developments in vehicle-terrain interaction studies", *Journal of Terramechanics*, 28, 269-288.

Tire-Terrain Modeling for Deformable Terrain

S. Shoop, CRREL

Objective: To develop a numerical model simulating the interaction between a tire and highly deformable terrain material. Vehicle movement on typical cold regions surfaces may result in large deformation from both compaction and mass movement. The model will be of assistance in predicting vehicle/tire performance, designing off-road tires, and estimating terrain damage due to compaction and rutting.

Approach: Current tire design technology does not consider the interaction of the tire and various deformable materials such as soil or snow, focusing primarily on tire/pavement interactions. This project is designed to integrate research being conducted in two very different areas; experimental and numerical simulation of tractive loading on deformable terrain, and numerical models of tire deformation.

Two-dimensional simulations will be used to study the kinematics of the problem. Three-dimensional simulations will concentrate initially on the terrain deformation, and finally the full tire-terrain system.

Much preliminary work has been completed that relates directly to the modeling effort including constitutive models of cold regions terrain (snow, freezing ground, thawing ground), detailed measurement of terrain deformations including melting, and numerous measurements of the forces generated at the tire-surface interface for off-road, unsurfaced roads, freezing and thawing soils, snow and ice.

Applications:

- Parametric study of effects of tire configuration and snow/soil properties on tire performance and terrain deformation/damage.
- Effects of strong soil layering (such as produced by freeze/thaw) on tire/vehicle performance
- Damage prediction on unpaved surfaces
- Off-road and all-season tire design

Results will be of interest to construction, mining, agriculture, forestry, recreation, military, tire and auto companies.

Collaboration: Auburn, UC Davis, Goodyear

S. Shoop
Cold Regions Research and Engineering Laboratory (CRREL)
Hanover, NH 03755-1290
Phone: (603)646-4321
Fax: (603)646-4640
e-mail: sallys@hanover-crrel.army.mil

The Role of High Resolution Simulations in Vehicle Performance Assessment

Roger A. Wehage[1]

Introduction

This technical note summarizes a proposal previously submitted to the Marine Corps for developing an interactive, high resolution vehicle modeling and simulation methodology to support the acquisition and evaluation of a future Medium Tactical Vehicle Replacement (MTVR) system. The discussion gives an idea of the many critical subsystems which contribute to a vehicle's mobility, ride quality and dynamic stability, and the level of effort required to implement and validate such a system.

Motivation for High Resolution Interactive Models

A Real-Time Operator-In-The-Loop Concept

The System Simulation & Technology Division (SSTD) at the Tank-Automotive Research & Development Engineering Center (TARDEC) and the Nevada Automotive Test Center (NATC) proposed to cooperate in the development of an advanced high resolution vehicle dynamic performance evaluation methodology. The methodology would develop and implement procedures to generate vehicle models capable of running at or near real time on moderate to large scale computers. The real-time simulation models would provide rapid and accurate dynamic performance evaluations because the critical human decision making and response processes, which are impossible to characterize and model, would be input directly to the models by a user through a graphics-based vehicle simulation workstation. The optimized vehicle equations and computer algorithms would be generated by a new modeling and simulation methodology under development at TARDEC, called Symbolically Optimized Vehicle Analysis System (SOVAS). SOVAS-generated equations would be executed under control of an interactive graphics-based program called Dynamic Response—Interactive Vehicle Emulator (DRIVE). DRIVE would provide a continuous display of the driver's view of the surrounding vehicle and terrain operating scenarios and would allow him to input control commands from a workstation interface, similar to those in the vehicle. All vehicle subsystems, and vehicle/terrain interactions would be modeled as accurately as feasible to achieve the maximum possible resolutions while still retaining real-time simulation capability. SOVAS and DRIVE-based vehicle models would provide performance discrimination capabilities which, until now, could only be obtained through expensive, time consuming, and possibly dangerous field and laboratory tests. A second main feature was that the methodology would also allow application of the same high resolution performance assessments to concepts and prototypes that may only exist on paper or that may be unavailable for extensive field and laboratory testing.

Many Subsystems are Critical to Vehicle Performance Predictions

A high performance tactical wheeled vehicle contains many unique subsystems, of which a good number are critical to its successful performance. Many of these subsystems significantly influence a vehicle's dynamic performance, and an operator's ability to control it. Various

[1]Tank-Automotive Research, Development and Engineering Center, AMSTA-RYA, Warren, MI 48397-5000

subsystems are more critical than others for a given performance aspect, and it is generally impossible to specify their relative degree of importance. Thus, the best that can be done in lieu of a time consuming and expensive sensitivity study, is to model each subsystem to the highest degree of resolution commensurate with the modeling and simulation capabilities. Validation studies which encompass the important dynamic performance aspects are necessary to insure that each subsystem model is correct and has the necessary resolution.

Successful vehicle performance is becoming more and more dependent on the application of on-board sensors and computer algorithms to carry out many of the critical tasks. Successful performance prediction models must also include accurate representation of the sensor and controller dynamics, as well as the onboard computer algorithms. Thus the next generation modeling and simulation methodologies must place heavy emphasis on accurate characterization of these subsystems, and modeling and simulating them.

A vehicle's chassis and the driver/passenger compartment are the framework of its operating system. The vehicle interacts with its surrounding environment and the operators through a number of intricate subsystems. Likewise the operators interact with the vehicle and the environment by sensing and controlling many of these subsystems. While it is feasible to accurately model the subsystems in a graphics-based workstation, it is impossible to model the operators. The most cost effective alternative is to allow the operator to control a vehicle model directly from a workstation. Graphical feedback would allow the driver to "see" and "experience" what is happening, both inside and outside the vehicle. Various controls such as joysticks, switches and on-screen touch sensitive devices would allow the driver to control the vehicle. Since a vehicle model's 'driver' would not be in the physical environment, he would not get many of the normal visual, audio and touch sensory feedback signals. Thus the DRIVE methodology would have to be designed to augment the graphical system with additional visual and audio signals. Experience with ground and flight simulators has shown that operators can effectively control systems with a reduced set of sensory inputs.

Critical Elements of a Vehicle Model

The following discussion gives a brief description of the most important MTVR subsystems. This discussion gives a general indication of the critical interaction dynamics which goes on between these systems, the operator, the vehicle, and its surrounding environment. The subsystems have not been arranged in any particular order of importance. In fact, it is impossible to rank them because it is only their overall synergistic performance that can be evaluated. It is also impossible to test each subsystem separately because they are so tightly coupled together and interdependent.

Role of the Drive Train

The engine model is discussed first because it provides the driving energy source for the vehicle. It is partially controlled by the driver through a number of inputs, and by other subsystems that may be partially under computer control. The primary control is through the throttle which may be indirectly affected by a governor and other electronic control devices. Computer algorithms may directly or indirectly control a number of engine parameters based on various sensed vehicle states. The driver may also select various levels of engine braking involving jake brakes or other types of installed engine braking devices. Engine braking may also be influenced by the state of operator applied brakes and the antilock braking system (ABS). It is not feasible to develop and incorporate high resolution dynamic engine models into a real-time simulation methodology, so engine torque output should be based on empirically measured data curves which depend on a number of controller and vehicle state variables.

Most of the systems in a vehicle rely on hydraulic, air and electrical supply systems to function properly. These systems must be characterized and modeled to insure they are capable of providing the necessary energy to drive all of the actuators. The power supply models will determine the power drain on the engine.

A rotating inertia would be used to represent the engine crankshaft and flywheel which is connected to the transmission torque converter. A typical torque converter assembly consists of a rotary impeller, turbine and stator designed to smooth out transient motions in the drive train and provide the torque gains necessary to rapidly bring a vehicle up to speed when accelerating, or to slow it down during engine braking. An electro-hydraulically controlled clutch is used to lock out the torque converter when it saturates, to improve engine efficiency. As noted above for the engine, it is not feasible to develop and incorporate high resolution dynamic torque converter models into a real-time simulation methodology, so the turbine and clutch output torque relationships are best determined empirically and incorporated into the model as functions of various controller and system states.

The torque converter output is coupled into the vehicle's transmission gear box. A number of user-selectable or computer controlled gear reduction systems, which are activated or deactivated by computer controlled electro-hydraulic clutches, work to give the vehicle a suitable speed and power range. Again, it is not feasible to develop and incorporate high resolution clutch torque models into a real-time simulation methodology, so these outputs are best empirically determined and included in the model along with models of the control computer algorithms (or the actual control computer code from the vehicle) and other measured system states.

The MTVR has an intricate arrangement of inter and intra axle differentials to give a wide range of possible axle drive configurations. The differentials are electro-pneumatically activated and deactivated through manual switches located in the cab. Time constants for the actuators would be determined empirically. The driver would be able to control the state of these systems according to his observance of the surrounding environment and the vehicle's dynamic states.

The MTVR has a unique suspension system, as do other high mobility vehicles. They represent intricate interactions between axles, springing devices, dampers, wheels, travel limiters, tires and the terrain. In fact, the suspension must be considered an integral part of the power train from the engine all the way to the tires and ground. Poorly designed suspension systems (and models) could cause internal oscillations resulting in loss of traction control, poor ride quality, excessive wear, etc. Thus it is important to accurately model the suspensions, as well as the other interconnected systems, to insure that the model, itself, does not inadvertently degrade or improve a vehicle's predicted performance.

The steering system also affects a vehicle's dynamic performance. It is necessary to accurately represent the steering kinematics all the way from the steering wheel to the wheel hubs. Incorrect steering kinematics and compliance can result in over steering, under steering or incorrect load transfer to the suspensions and tires. This can cause vehicle instabilities, loss of traction and other problems. The time response characteristics of hydraulically power assisted units will also affect steering performance.

Between the Vehicle and the Road

The MTVR central tire inflation system (CTIS) has been designed to provide a means for automatically adjusting tire pressures in response to current terrain and operating conditions. Depending on the system design, the CTIS states may be manually controlled from the cab, or they may be directly or indirectly controlled by one of the on-board computers used for other

purposes. The response characteristics of the CTIS control valves would be determined empirically.

On the MTVR, ABS is designed to control wheel slip during manual braking. It senses wheel rotational speeds and brake pad temperatures, and uses this information to control the pneumatically actuated brakes. Some systems may also use ABS-type control algorithms to improve traction control while accelerating or towing loads. ABS requires a sophisticated computer program to perform its functions, and this program would have to be included in the vehicle model as well.

A tire is one of the most complex and critical subsystems in a vehicle and a comprehensive representation of its interaction dynamics with irregular nondeforming or deforming surfaces has not been obtained, even through extensive research efforts. Thus the most feasible solution is to use models based on empirically determined data. A dynamic enveloping tire model could be used to obtain a set of tire state variables which would then be inserted into an empirical tire/soil interaction model. This model would return a set of interaction forces and moments which would then be applied back to the dynamic enveloping tire model. An iterative procedure would be used to converge the two models to a common solution. This approach would require very low order models to obtain accurate results so real-time simulations would still be possible.

Accurate representation of tire/soil interaction dynamics is very crucial to many of the dynamic vehicle performance analyses. Mobility is likely the most important vehicle performance aspect and many of the major vehicle subsystems were designed with this in mind. Dynamic stability and ride quality are two other important performance aspects which depend on many of the subsystems, and tire/soil interaction dynamics. Thus it is clear that if computer-based analysis is to be a useful tool for studying these phenomena, the corresponding models must be accurate enough to emulate the critical subsystems' dynamic response characteristics.

Empirical characterization of tire/soil/terrain interaction dynamics is encumbered by the wide range of tire, soil and terrain configurations. A program to accomplish such a task would require identification of the most important tire, soil and terrain parameters and elimination of all others. Then a comprehensive parameter identification and measurement procedure would have to be established.

Interfacing a Vehicle Model, the Driver and the Environment

The Role of a Vehicle Operator in Performance Prediction

This discussion has emphasized the importance of accurate representation of the various vehicle subsystem models. However, the most important vehicle subsystem which is impossible to characterize or model is the driver. The best driver model which might possibly be defined could severely compromise a vehicle's performance because it simply could not come close to emulating a human's thought and response processes. The most feasible solution, which would allow a vehicle model to be accurately exercised through the widest range of highly nonlinear displacements that a corresponding vehicle in the field might experience, is to allow an operator to perform these functions, in real time, at a graphics workstation or in some other physical simulation environment.

Interfacing the Operator With the Vehicle

Two major efforts would be required for interfacing the driver to the vehicle simulation model. First, adequate controls would have to be provided to allow him to comfortably and accurately input the necessary commands to the vehicle. Second, sufficient graphical and audio

feedback signals would have to be provided so he could continuously determine what the vehicle is doing. Numerous ground vehicle and flight simulators have demonstrated that it is possible to provide sufficient controls and sensory inputs, and that a user can adequately control such systems in an emulated environment. A number of field and laboratory tests with actual vehicles would have to be performed to learn what controls and sensory inputs are necessary for adequate vehicle control.

Interfacing the Operator With the Environment

In a realistic operational environment, it would also be necessary to account for other types of vehicle and operator interactions with the surrounding environment. The most important interaction would be chassis interference with the terrain and surrounding vegetation. An extensive amount of empirical data has been collected for the NATO Reference Mobility Model (NRMM) which could be used to support such a modeling and simulation effort. In addition, some commercial software programs could be used to incorporate Defense Mapping Agency Digital Terrain Elevation Data (DMA-DTED) and Digital Feature Analysis Data (DMA-DFAD) directly into MTVR models. NATC has access to world-wide DTED and DFAD data bases and procedures could be developed to extend their resolutions down to any degree of accuracy necessary to carry out the corresponding analyses. DTED data files give the terrain elevation data for many locations in the world and any number of surface and material properties could be associated with each piece of the terrain. DFAD data files define the types of features on the terrain profiles and their properties. For example, DFAD files have attributes defining feature type, height, orientation, identification, surface material code, etc., and any number of additional feature properties could be added as necessary to extend this data base. A number of dynamic form drag and interference models have been reported in the literature. These models could be investigated and incorporated into the DRIVE methodology to obtain representative vehicle/obstacle/vegetation interference models. This data would be important for providing the necessary vision impairments to vehicle operators as well.

Importance of Trailer and Wagon Models

Equal emphasis must be placed on the characterization of trailers and wagons, and the development of high resolution models for these systems. Trailer dynamics can adversely affect a truck's mobility, ride quality and dynamic stability. In fact, any truck/trailer combination must be considered as a single integrated system with its own mobility, ride quality and dynamic stability properties. Failure of the trailer generally means failure of the system as well. If a given trailer uses the truck's hydraulic, air or electrical supply systems, then these extra loads must also be accounted for in the truck models. If any trailer functions are influenced or controlled by the truck's on board computers, such as ABS functions, procedures must be established to incorporate them into the models as well. Finally, procedures must be established to give the driver adequate visual and sensory feedback on the trailer's dynamic state so he can respond accordingly.

System Characterization and Model Validation

System characterization and model validation is considered an extremely important and integral part of every subsystem model development effort. TARDEC engineers have an extensive background in defining the supporting mathematical equations, developing the computer algorithms, obtaining the system states and interpreting the results. However, they have very limited, or no knowledge of the functional operation of most of the MTVR's complex subsystems. On the other hand, NATC engineers have an extensive knowledge of the intricate operation of every major subsystem because they were either responsible for the system performance specifications to other developers, or they developed the systems themselves. They also have close working relationships with many of the vendors and system developers. For a

proposed program to be successful, TARDEC engineers would have to learn the functional operation of these subsystems and NATC engineers would have to learn the basics of computer-based vehicle modeling and simulation so the two groups could create the best possible vehicle models and analysis tools. Thus TARDEC and NATC engineers would have to work closely at each step of a cooperative project to insure that the operational performance of every major subsystem is thoroughly understood by everyone involved. In addition, the participants would have to insure that all necessary subsystem characterization and model validation tests were carefully defined and performed so the models could be accurately defined and validated. TARDEC and NATC engineers would have to learn from each other in such a project so they would be in a good position to apply this gained knowledge and experience to follow-on efforts.

Motivation for Support of the Acquisition Process

It was expected that such an effort would result in a comprehensive performance specification which would go into a subsequent Request For Proposal (RFP) and that the RFP would require each prospective bidder to extensively evaluate his concepts using high resolution computer-based vehicle models. It was further expected that this effort would give NATC engineers the ability to define and execute these high resolution models (with some assistance from TARDEC engineers), and that most serious contractors would seek help from NATC. It was also expected that TARDEC engineers would be tasked to model, simulate and evaluate the proposed systems following receipt of the proposals, and during further down-select phases. The critical issue for TARDEC's evaluation efforts has always been the lead time and manpower required to develop and validate comprehensive models in order to give reasonable proposal evaluation response times. If contractors were encouraged to use such a methodology in the initial development phases, and if NATC engineers were to use their gained knowledge to insure that the contractors carefully obtained the necessary data for the models, then they would be in an excellent position to supply accurate model data or entire models to TARDEC in a timely manner. This would have the added advantage of forcing the contractors to create better prototype designs. In addition, it would allow TARDEC engineers to evaluate the proposals in a more timely manner, thereby increasing the probability the Marine Corps would get the best possible product.

Development and Validation of the Methodology—A Cooperative Effort

The second major task would concentrate on the development and validation of a comprehensive high resolution model of the MTVR and trailers. In this process, the methodologies to support high resolution, real-time, man-in-the-loop simulations in a graphics-based workstation environment would be perfected. The first effort would concentrate on expanding the modeling and simulation methodology in preparation for defining the performance specifications and evaluation criteria which would go into the Request For Proposal. Six major research areas were anticipated to complete this effort:

1. Validate derivability of the methodology against extensive MTVR field test data.

2. Expand the methodology to assess MTVR performance in the Marine Corps world-wide operational scenarios.

3. Define and develop a unique set of computer-based vehicle simulations which must be carried out to quantify and discriminate between new concept and prototype vehicle performance parameters.

4. Develop advanced subsystem characterization, model development and validation procedures necessary to minimize the time between receipt of vehicle data and completion of performance analyses.

5. Develop comprehensive vehicle performance specifications, data requirements and evaluation procedures Data Item Descriptions (DIDS) which must be incorporated into the RFP's to insure that sufficient and accurate information is provided to and by contractors.

6. Design flexibility into the modeling and simulation methodology to simplify the definition and incorporation of all unique design features of each proposed concept or prototype into the models, thus minimizing the possibility of compromising promising new design features.

Field Tests for Model Validation

The above discussion clearly indicates that the SOVAS-generated MTVR and trailer models would have to be quite extensive and sophisticated in order to address all of the critical dynamic operational performance aspects of a system of this magnitude. Furthermore, the DRIVE-based man-in-the-loop methodology would have to be capable of insuring that the models can be accurately exercised to answer the critical design and evaluation questions. Thus the first and most critical step of this effort would be to define and carry out a battery of comprehensive and carefully controlled field tests to generate SOVAS and DRIVE validation data. The scope of these tests would be determined in conjunction with the actual model development efforts. In general, it would be impossible to predict the type and detail of model validation tests required until the subsystem characterization and model development efforts were underway or completed. Thus part of the effort would be to identify and define the validation procedures that would have to be conducted. The confidence gained in the subsystem characterization and model development procedures from these validation efforts would allow TARDEC and NATC engineers to reliably extend the methodologies to new concepts and prototypes, and to new operational scenarios as described above.

The Marine Corps world-wide MTVR operational performance requirements involve a large number of terrain, soil, vegetation and obstacle types. NATC and TARDEC would create extensive DTED and DFAD data bases for these regions. MTVR operational performance on these data bases would be validated against test data within these regions or test data taken from other areas with similar types of terrain, soil, vegetation and obstacles. The validated model and data bases would then be available for future concept and prototype evaluations.

NATC and other Government agencies perform a broad spectrum of carefully controlled field tests in order to quantify a vehicle's dynamic operational performance capabilities. These tests are run on many types of terrain profiles, conditions and operating environments. All field tests which could be augmented or replaced by SOVAS and DRIVE-based vehicle emulations should be defined and validated. Test procedures would have to be identified and installed into the DRIVE workstation environment. It would be best if all such procedures were in place prior to receipt of proposals and prototypes in order to achieve the necessary evaluation response times.

System Characterization, Model Development and Validation

Another critical area that would have to be addressed by TARDEC and NATC engineers is the definition and development of advanced subsystem characterization, model development and validation procedures to minimize the time between receipt of vehicle data and completion of performance analyses. It would be ideal if every contractor provided data or subsystem models which could be entered directly into the SOVAS and DRIVE methodologies. However, TARDEC's experience is that many contractors either lack the ability or desire to provide data or models, and when such information and models are supplied, their accuracy and resolution is often questionable. Also, contractors often consider their on-board control algorithms and systems to be proprietary and would refuse to release information to TARDEC or NATC. If high

resolution vehicle simulations are to be useful evaluation tools, the RFP's must be very specific in what the contractors must supply and how the information would be used in the evaluation process. TARDEC and NATC engineers would have to clearly define what is required to support these modeling and simulation efforts and what the contractors' responsibilities would be.

Development for Support of the Acquisition Process

Defining the Performance Specifications

TARDEC and NATC engineers would also have to develop comprehensive vehicle performance specifications, data requirements and evaluation procedures DIDS which must be incorporated into the RFP's to insure that sufficient and accurate information is provided to the contractors. An important goal of this proposed program would be to quantify unique vehicle design features that contribute to improved mobility, stability and ride quality, and to develop computer-based modeling and simulation methodologies that would allow rapid evaluation of new concepts and prototypes to determine how well the contractors' proposals have met these criteria. The challenge would be the wording of these specifications so the Government would not be telling the contractors how to design their vehicles, yet would have a good probability that the proposals would meet the Marine Corps needs. The DIDS would have to be very specific on what data the contractors must supply and in what forms it must be supplied. Furthermore, it should be made very clear that incomplete or inaccurate data could lead to incorrect evaluation of their proposals, and possible rejection.

Model Adaptability to Unique Vehicle Designs

The proposed effort would also design the SOVAS and DRIVE methodologies to accept a wide range of subsystem models. This would be necessary in order to simplify the definition and incorporation of all unique design features of each proposed concept or prototype into the models, thus minimizing the possibility of compromising promising new design features. No features of the MTVR or trailer models would be hard coded into the SOVAS and DRIVE methodologies. Each of the major subsystems which the MTVR, and nearly every concept or prototype must have, would be defined as stand-alone modules which could be tailored and optimized for each vehicle model. That is, each major subsystem would have a generic module with the main functional requirements which could be tailored and optimized as necessary. A major goal of this project would be to gain experience with the subsystem characterization, model development and validation efforts using the MTVR so it would become more of a routine procedure to tailor and optimize the generic modules in the follow-on evaluation efforts.

Soil Plowing Using the Discrete Element Method

David A. Horner

U.S. Army Engineer Waterways Experiment Station
Vicksburg, Mississippi 39180-6199

BACKGROUND

Many vehicle-soil interaction problems involve large discontinuous deformations. Such problems include sinkage of vehicle tracks and tires in soft soils and vehicle plowing problems. The traditional use of continuum mechanics is limited to large strains with continuous deformation. The principal difficulty comes from the mathematical description of the kinematics that describes the movement of material "particles" within the continuum. In a continuum, movement must obey compatibility relationships that preclude formation of slip planes and separations. However, in real materials, large deformations can occur that violate compatibility in the strict sense imposed by continuum formulations. To model discontinuous deformations, as done in finite element analysis of fracture propagation or at interfaces in the soil-structure interaction problems, special joint elements are often introduced to model slip or separation (Wong and Hanna, 1977). Use of these elements complicate analyses for small deformation problems and become excessively complicated for large deformation problems. The joint elements also require assumptions to be made on the location of the discontinuities.

An alternative to the continuum description for soil and rock mechanics problems is the Discrete Element Method (DEM) which models the material as a collection of individual unconnected particles. The motion of the particles is controlled by Newton's laws of motion and is only restricted kinematically by the requirement that particles cannot penetrate each other. Several authors have used DEM to model granular assemblies (Cundall and Strack, 1979, Christoffersen, et. Al., 1981, Bathurst and Rothenburg, 1988). Ng and Dobry (1991) used DEM to model small strain cyclic loading. Their simulation results agreed closely with trends found in laboratory tests of sands. Shukla and Sadd (1990) used DEM to investigate how mechanical stress waves propagate in granular material and how they are influenced by media microstructure. DEM has been used to model the results of tunnel failure resulting of a nuclear explosion (Heuze, et. Al., 1991). Sophisticated algorithms have been developed to describe the evolution of the

particulate system including the formation and breaking of inter-element contacts (Ting, et. Al., 1989). Computing forces between elements requires relationships to describe normal and shear interaction at the contacts. In some models the individual particles can "break" when stress conditions within the particle reach some critical level (Cundall and Hart, 1985). Typically soil particles have been modeled as two-dimensional circular rigid disks. Ting (1991) has developed an ellipse-based two-dimensional particle to represent contact flatness and particle angularity. Six-sided solid shapes have been used to model granular material (Ghaboussi and Barbosa, 1990). The predominant disadvantage of DEM is the enormous computational requirement, which is a result of keeping track of all particle contact locations.

PARTICLE PLOW SIMULATION

A 1,200 particle simulation was performed to illustrate the potential use of the DEM for investigating the response of the particles to a rigid plow moving through the particulate mass . The simulation consisted of dropping the particle into the test chamber, allowing the particle come to rest, and then moving the plow through the test specimen at a constant rate. The plow blade angle was set to 45°. Figure 1 plots the force magnitude of the particles prior to plowing. The lighter the color the more force acting on the particle. Figure 2 plots the force magnitude of the particles after plowing. Particles near the plow tip show an build up of force concentration.

Figure 3 shows only those particles that have horizontal motion at the end of the plowing test. The lighter color represents those particles with horizontal velocity. Using scientific visualization to animate the results of the simulation allows for the observation of soil deformation patterns forming and identify formation of failure surfaces.

CONCLUSIONS

The Distinct Element Method is an analytical tool for fundamental research into the behavior of granular material. The DEM allows the simulation of complex nonlinear interaction problems in terramechanics. The major drawback to the DEM is the enormous computional requirement. Future research in the use of scaling principle for full scale modeling and the use massively scalable parallel computer systems will be attempts to address this problem. The advantage of the DEM is that slip planes and separations can form between groups of particles thus capturing evolving failure mechanisms in a simpler and more realistic way than models based on a continuum description of the soil mass.

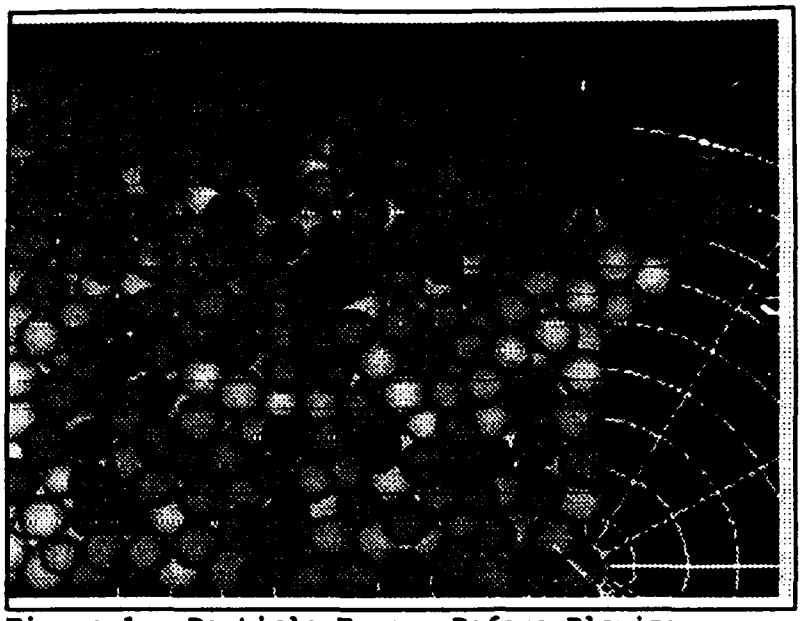

Figure 1. Particle Force Before Plowing

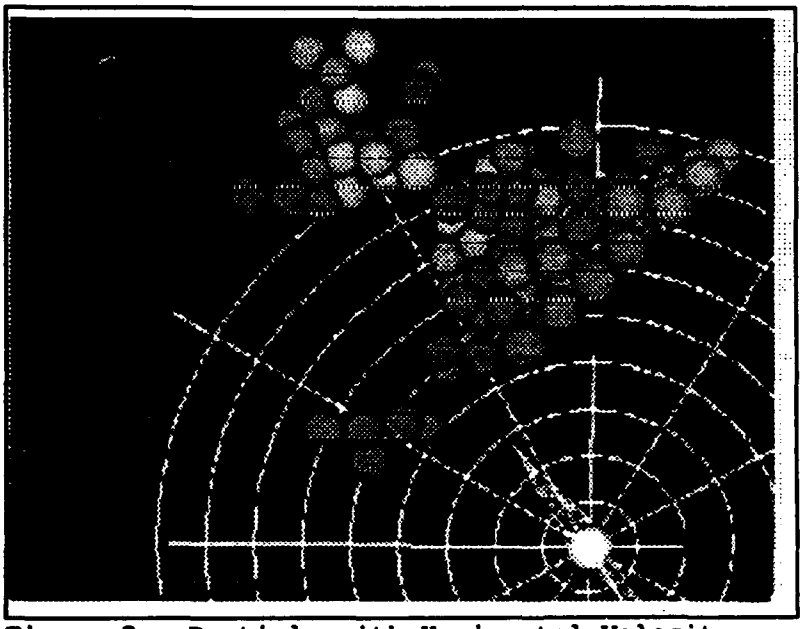

Figure 2. Particle with Horizontal Velocity

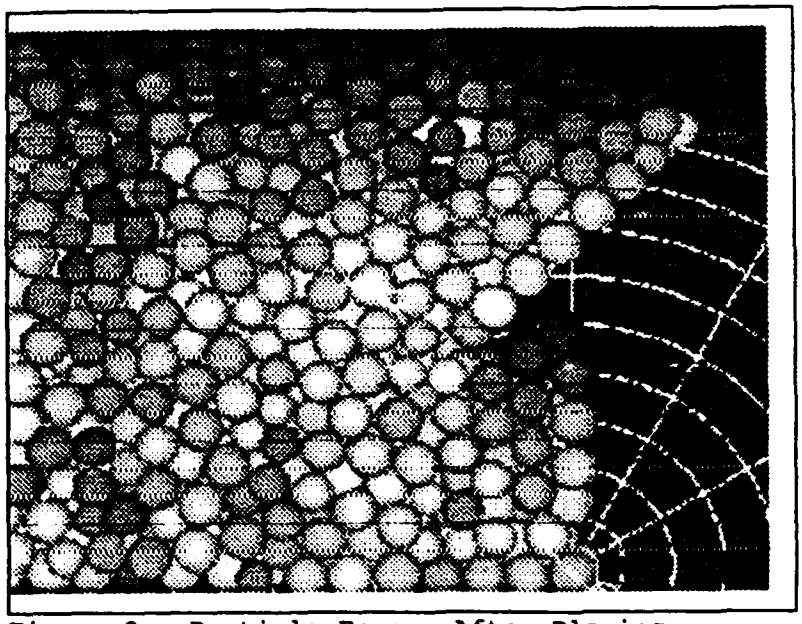

Figure 3. Particle Forces After Plowing

REFERENCES

Bathurst, R. J., and Rothenburg, L., (1988), "Micromechanical Aspects of Isotropic Granular Assemblies with Linear Contact Interactions," Journal of Applied Mechanics, Vol. 55, March, pp. 17-23.

Christoffersen, J., Mehrabadi, M., and Nemai-Nasser, S., (1981), "A Micromechanical Description of Granular Material Behavior," Journal of Applied Mechanics, Vol. 48, June, pp. 339-344.

Cundall, P. A., and Strack, O. D. L., (1979), "A Discrete Numerical Model for Granular Assemblies," Geotechnique, Vol. 29, No. 1, pp. 47-65.

Cundall, P.A., and Hart, R.D., (1985), "Development of Generalized 2-D and 3-D Distinct Element Programs for modeling Jointed Rock," Miscellaneous Paper SL-85-1, U.S Army Engineer Waterways Experiment Station, Jan.

Ghaboussi, J., and Barbosa, R, (1990), "Three-Dimensional Discrete Element Method for Granular Materials," International Journal for Numerical and Analytical Methods in Geomechanics, Vol. 14, pp. 451-472.

Heuze, F., Walton, O., Maddix, D., Schaffer, R., and Butkovich, T.,"Models for Rock Mass Dynamics," Proceedings of Mechanics Computing in 1990's and Beyond, American Society of Civil Engineers, Columbus, Ohio, May 20-22,

(1991), Vol. 2, pp.1169-1173.

Hockney, R. W., and Eastwood, J. W., (1988), "Computer Simulation using Particles," Adam Hilger Book Co.

Ng, T., and Dobry, R., "Numerical Undrained Cyclic Loading Simulations using the Discrete Element Method," Proceedings of Mechanics Computing in 1990's and Beyond, American Society of Civil Engineers, Columbus, Ohio, May 20-22, (1991), Vol. 2, pp.1234-1238..

Russo, Giovanni, (1990) "Deterministic Diffusion of Particles," Communications on Pure and Applied Mathematics, Vol. XLIII, No. 6, Sept., pp. 687-733.

Shukla, A., and Sadd, M., (1990), "Wave Propagation and Dynamic Load Transfer due to Explosive Loading in Heterogenous Granular Media wtih Microstructure," Prepared for U.S. Air Force Office of Scientific Reseach Under Contract No. F49620-89-C-0091, Bolling Air Force Base.

Ting, J. M., Corkum, B. T., Kauffman, C. R., and Greco, C., (1989), "Discrete Numerical model for Soil Mechanics," Journal of Geotechnical Engineering, American Society of Civil Engineers, Vol. 115, No. 3, Mar., pp. 379-398.

Wong, R. N., and Hanna, A. W., (1977), "Finite Element Analysis of Plane Soil Cutting," Journal of Terramechanics, Vol. 14, No. 3, pp. 103-125.

Appendix C
List of Participants

Mr. Colin Ashmore
Nevada Automotive Test Center
P.O. Box 234
Carson City, NV 89702

Dr. Alvin Bailey
U.S.D.A. National Soil Dynamics Laboratory
P.O. Box 3439
Auburn, AL 36831-3439

Mr. Michael Belczynski
U.S. Army Tank Automotive Command
AMSTA-RYA
Warren, MI 48397-5000

Mr. Paul Corcoran
Caterpillar, Inc.
P.O. Box 1895
Peoria, IL 61656-1895

Mr. Dan Creighton
U.S.A.E. Waterways Experiment Station
CEWES-GM-L
3909 Halls Ferry Road
Vicksburg, MS 39180-6199

Dr. Dean Freitag
312 Parragon Road
Cookeville, TN 38505

Mr. David Gunter
U.S. Army Tank Automotive Command
AMSTA-RYA
Warren, MI 48397-5000

Dr. Peter Haff
Department of Geology
Duke University
Box 90230
Durham, NC 27708-0230

Dr. Russell Harmon
Engineering and Environmental Sciences Division
U.S. Army Research Office
P.O. Box 12211
Research Triangle Park, NC 27709-2211

Mr. David Horner
U.S.A.E. Waterways Experiment Station
CEWES-GM-L
3909 Halls Ferry Road
Vicksburg, MS 39180-6199

Dr. Frank Huck
Caterpillar, Inc.
P.O. Box 1875
Peoria, IL 61656-1875

Dr. Clarence Johnson
Department of Agricultural Engineering
Auburn University
Auburn, AL 36849-5417

Mr. Roger Meier
U.S.A.E. Waterways Experiment Station
CEWES-GM-L
3909 Halls Ferry Road
Vicksburg, MS 39180-6199

Dr. Hidenori Murikami
Department of Applied Mechanics and Engineering Sciences
University of California, San Diego
9500 Gilman Drive
La Jolla, CA 92093-0411

Mr. Mark Osborne
Keweenaw Research Center
Michigan Technological University
1400 Townsend Drive
Houghton, MI 49931

Dr. Randy Raper
U.S.D.A. National Soil Dynamics Laboratory
P.O. Box 792
Auburn, AL 36831

Ms. Sally Shoop
U.S. Army Cold Regions Research and Engineering Laboratory
72 Lyme Road
Hanover, NH 03755-1290

Dr. Antoinette Tordesillas
Department of Mechanical Engineering
Kansas State University
Manhattan, KS 66506-5106

Dr. Michael Trinko
Goodyear Tire and Rubber Company
D/431A Technical Center
P.O. Box 3531
Akron, OH 44309-3531

Dr. Shrini Upadhyaya
Biological and Agricultural Engineering Department
University of California
Davis, CA 95616

Dr. Roger Wehage
U.S. Army Tank Automotive Command
AMSTA-RYA
Warren, MI 48397-5000

Prof. J. Y. Wong
Vehicle Systems Development Corporation
49 Fifeshire Crescent
Nepean, Ontario, Canada K2E 7J7

REPORT DOCUMENTATION PAGE

Form Approved
OMB No. 0704-0188

1. AGENCY USE ONLY (Leave blank)	2. REPORT DATE	3. REPORT TYPE AND DATES COVERED
	August 1994	Final report

4. TITLE AND SUBTITLE
Proceedings, First North American Workshop on Modeling the Mechanics of Off-Road Mobility

5. FUNDING NUMBERS

6. AUTHOR(S)
Roger W. Meier, David A. Horner

7. PERFORMING ORGANIZATION NAME(S) AND ADDRESS(ES)
U.S. Army Engineer Waterways Experiment Station
3909 Halls Ferry Road
Vicksburg, MS 39180-6199

8. PERFORMING ORGANIZATION REPORT NUMBER
Miscellaneous Paper
GL-94-30

9. SPONSORING/MONITORING AGENCY NAME(S) AND ADDRESS(ES)
U.S. Army Research Office
P.O. Box 12211
Research Triangle Park, NC 27709-2211

10. SPONSORING/MONITORING AGENCY REPORT NUMBER

11. SUPPLEMENTARY NOTES
Available from the National Technical Information Service, 5285 Port Royal Road, Springfield, VA 22161.

12a. DISTRIBUTION/AVAILABILITY STATEMENT
Approved for public release; distribution is unlimited.

12b. DISTRIBUTION CODE

13. ABSTRACT (Maximum 200 words)

In order to (1) assess the current state of the art in vehicle mobility modeling, (2) identify the most promising areas of current research, and (3) determine the most profitable directions for future research, the Mobility Systems Division of the U.S. Army Engineer Waterways Experiment Station (WES) invited recognized leaders in the field of vehicle mobility modeling from throughout the United States and Canada to participate in a two-day workshop on "Modeling the Mechanics of Off-Road Mobility." This report documents the proceedings of that workshop.

14. SUBJECT TERMS
Mobility performance
Off-road vehicles
Soft soil
Vehicle-terrain interaction

15. NUMBER OF PAGES
151

16. PRICE CODE

17. SECURITY CLASSIFICATION OF REPORT	18. SECURITY CLASSIFICATION OF THIS PAGE	19. SECURITY CLASSIFICATION OF ABSTRACT	20. LIMITATION OF ABSTRACT
UNCLASSIFIED	UNCLASSIFIED		